

# PHYSICO-CHEMICAL STUDY OF POLYANILINE/FLYASH COMPOSITES

A Major Dissertation Submitted To Faculty of Technology  
of

University of Delhi

Towards The Partial Fulfillment of the Requirement

For

The Award of the Degree

MASTER OF ENGINEERING

IN

POLYMER TECHNOLOGY

*Submitted by*

**SURENDRA KUMAR**

**Roll No: 9006**



**DEPARTMENT OF APPLIED CHEMISTRY AND POLYMER TECHNOLOGY**

**DELHI COLLEGE OF ENGINEERING,  
NEW DELHI -110042**

**DEPARTMENT OF APPLIED CHEMISTRY AND POLYMER TECHNOLOGY  
DELHI COLLEGE OF ENGINEERING**

**UNIVERSITY OF DELHI**

**BAWANA ROAD, NEW DELHI -110042**



**CERTIFICATE**

This is to certify that the dissertation entitled “Physico-Chemical Study Of Polyaniline/flyash Composites” submitted by Mr. Surendra Kumar to Delhi College of Engineering in Applied Chemistry and Polymer Technology is a record of bonafide work carried out by him. Mr.Surendra Kumar has worked under our guidance and supervision for fulfilled the requirement for the submission of this dissertation. The work has been carried out during 9th August 2010 to 30<sup>th</sup> June 2011.

**Supervisor**

**Prof.R.C.Sharma**

**Department of Applied Chemistry  
Laboratory**

**And Polymer Technology**

**Delhi College of Engineering**

**New Delhi**

**Co-Supervisor**

**Dr.S.K.Dhawan**

**National Physical**

**New Delhi**

**Prof.G.L.Verma**

**Head, Department of Applied Chemistry**

## ACKNOWLEDGEMENTS

Taking the opportunity of this column, I would like to express my sincere gratitude to all those who directly or indirectly helped me in successful completion of my Project work.

My heartfelt thanks to my mentor and guide **Professor R.C. Sharma**, Department of Applied Chemistry & Polymer Technology, Delhi College of Engineering, who provided me an opportunity to work under his able guidance. His valuable guidance and motivation has helped me to complete my project successfully.

I would like to convey my heartiest thanks my Co- Supervisor **Dr. S. K. Dhawan** who introduced me to the field of conducting polymers, offered his vision and guidance in planning experiments, and led me to a proper understanding of the experimental results.

I express my grateful thanks to **Professor G.L.Verma**, Head, Department of Applied Chemistry & Polymer Technology, Delhi College of Engineering and all the faculty members of the departments for their valuable suggestions and help.

I am extremely grateful to all members of Conducting Polymer Research Group where I conducted most of my research work of the project. I would also like to thank **Er. Parveen Saini, Mr. Taukeer Khan, Mrs. Hema Bhandri, Mr. Anoop Kumar, Miss. Ranoo, Mr. Firoz Alam, Mr. Tiklal Rana, Mrs. Seema Joon, Miss Chandrika**, Thanks is too small a word to acknowledge the contribution of my friends, **Devendra Pratap, Rohit, Prabhat, Preeti Yadav** in my dissertation.

I am highly thankful to **Mr. Brijesh Sharma, Mr. Devraj Joshi** and **Mrs. Barkha** for their technical help during my work.

Last, but not the least, my parents, my brothers and sisters and my well-wishers have been with me at every step of this exciting journey. I thank them for all their prayers, encouragements and best wishes.

Thank you all

SURENDRA KUMAR

### Abstract

In situ polymerization of aniline with chemical was carried out in presence of Fly ash (FA) to synthesize polyaniline/fly ash composites (PANI/FA) doped with  $H_3PO_4$  1:1,1:2 composition of FA in PANI, and after that undoped these composites with ammonia. The composites thus synthesized have been characterized by Ultraviolet-Visible spectroscopy, FTIR, X-ray diffraction, TGA, conductivity have been measured by four probe method. The morphology of samples was studied by scanning electron microscopy. Corrosion-inhibition performance of Polyaniline and its composites with Flyash carried by Tafel method, Sample was prepared by make blends with 5% loading of Polyaniline and Polyaniline/Flyash composites with epoxy resin, after these powder is coated on iron electrode of dimension of 1 cm x 1cm by powder coating instrument. Check corrosion inhibition performance at room temperature in aqueous solution of 1.0 M HCl by using potentiodynamic polarization technique. Corrosion efficiency increases as flyash concentration increases.

## Contents

### Chapter1 Introduction

<b>1.1.1 Introduction of Conducting Polymers</b>	<b>2</b>
<b>1.1.2 Discovery of Conducting Polymers</b>	<b>3</b>
<b>1.1.3 Structural Characteristics and Doping Concept</b>	<b>5</b>
<b>1.1.4 Charge Storage</b>	<b>9</b>
<b>1.1.5 Charge Transport</b>	<b>13</b>
<b>1.1.6 Stability</b>	<b>13</b>
<b>1.1.7 Processibility</b>	<b>14</b>
<b>1.2.1 Polyaniline</b>	<b>16</b>
<b>1.2.2 Molecular Structure and Proton Doping</b>	<b>17</b>
<b>1.2.3 Synthesis Method</b>	<b>19</b>
<b>1.2.3(a) Chemical Method</b>	<b>19</b>
<b>1.2.3(b) Electro-Chemical Method</b>	<b>21</b>
<b>1.2.3(c) Mechano-Chemical Route</b>	<b>22</b>
<b>1.2.4 Physical Properties</b>	<b>23</b>
<b>1.2.4(a) Nonlinear Optical (NLO)</b>	<b>23</b>
<b>1.2.4(b) Electrical and Charge Transport Properties</b>	<b>24</b>
<b>1.2.4(c) Magnetic Properties</b>	<b>25</b>
<b>1.2.4(d) Other Properties</b>	<b>25</b>
<b>1.2.4(e) Solubility and Processability</b>	<b>27</b>

<b>1.2.4(f) Solubility</b>	<b>27</b>
<b>1.2.4(f<sub>1</sub>) Substitution onto Backbone</b>	<b>27</b>
<b>1.2.4(f<sub>2</sub>) Self-Doping PANI (SPAN)</b>	<b>28</b>
<b>1.2.4(f<sub>3</sub>) Water soluble PANI</b>	<b>30</b>
<b>1.2.5 Processability</b>	<b>32</b>
<b>1.2.5(a) Adsorption Polymerization</b>	<b>33</b>
<b>1.2.5(b) Layer-By-Layer</b>	<b>33</b>
<b>1.2.5(c) Photolithography Technique Associated with Photo-Acid Generation Process</b>	<b>34</b>
<b>1.3 Present And Future Potential Application</b>	<b>35</b>
<b>1.3.1 Corrosion Protection</b>	<b>35</b>
<b>1.3.2 Sensors and Electromechanical Device</b>	<b>36</b>
<b>1.3.3 Electrochromic cell</b>	<b>38</b>
<b>1.3.4 Controlled-released Application</b>	<b>40</b>
<b>1.3.5 Radar Application</b>	<b>41</b>
<b>1.3.6 LEDs</b>	<b>42</b>
<b>1.3.7 Conducting Polymers for EMI/ESD Shielding</b>	<b>44</b>
<b>1.3.8 Conducting polymer coated Fabrics for EMI Shielding</b>	<b>44</b>
<b>1.4 Fly ash</b>	<b>45</b>
<b>1.4.1 Composition and Property of Flyash</b>	<b>45</b>
<b>1.4.2 Application of Fly ash</b>	<b>48</b>
<b>1.5 Corrosion Study</b>	<b>48</b>

<b>1.5.1 Electrochemical Basis of Corrosi</b>	<b>48</b>
<b>1.5.2 Quantitative Corrosion Theory</b>	<b>51</b>
<b>1.5.3 Polarization Resistance</b>	<b>53</b>
<b>References</b>	<b>56</b>
 <b>Chapter 2 Characterization Techniques</b>	
<b>2.1: Ultraviolet-visible (UV-Vis.) Spectromete</b>	<b>70</b>
<b>2.2: Fourier Transform Infrared (FTIR) Spectrometer</b>	<b>72</b>
<b>2.3: X-ray Diffractometer (XRD)</b>	<b>74</b>
<b>2.4: Scanning Electron Microscope (SEM)</b>	<b>75</b>
<b>2.5: Thermo Gravimetric Analysis (TGA)</b>	<b>77</b>
<b>2.6: Four Probe Method</b>	<b>78</b>
<b>2.7 Cyclic Voltametry</b>	<b>79</b>
<b>References</b>	<b>81</b>
 <b>Chapter 3 Experiments</b>	
<b>3.1: Synthesis of Polyaniline (PANI)</b>	<b>83</b>
<b>3.2: Cleaning of Flyash</b>	<b>83</b>
<b>3.3: Synthesis of Polyaniline/ Flyash Composite(1:1)</b>	<b>83</b>
<b>3.4: Synthesis of Polyaniline/ Flyash Composite (1:2)</b>	<b>84</b>
<b>3.5: Undoping of Polyaniline/Flyash Composites</b>	<b>85</b>

## **Chapter 4 Results and Discussion**

<b>4.1 UV-Visible Spectral Analysis</b>	<b>87</b>
<b>4.2 Conductivity Measurement of PANI and its composites</b>	<b>88</b>
<b>4.3 Scanning Electron Microscope (SEM)</b>	<b>89</b>
<b>4.4 X-ray diffraction</b>	<b>93</b>
<b>4.5 FTIR Spectra</b>	<b>96</b>
<b>4.6 Thermogravimetric analysis</b>	<b>97</b>
<b>4.7 Study of the corrosion- inhibition performance of inhibitors</b>	<b>98</b>
<b>References</b>	<b>102</b>
<b>Conclusion</b>	<b>103</b>



# Chapter 1

## INTRODUCTION

### Introduction

Polymer are high molecular weight organic/ inorganic compound formed by chemical reaction (polymerization) of monomers or the continued reaction between lower molecular weight polymers or oligomers . Polymers may be natural or synthetic. Natural polymers include proteins (polymer of amino acids) carbohydrate, fat lipids and cellulose (polymer of sugar molecules) while polyvinyl chloride (PVC), polytetrafluoroethylene (PTFE or Teflon), polyacetylene (PA), polyaniline (PANI), and Bakelite etc., are synthetic polymers. A key property of the polymers that distinguishes them from metals is their inability to carry electricity. It is a general view that plastic and electrical conductance is mutually exclusive. However with time the possibilities have changed, plastic can indeed, under certain circumstances, be made to behave very like a metal - a discovery for which Prof. Alan J. Heeger, Prof. Alan G. MacDiarmid and Prof. Hideki Shirakawa received the Nobel Prize in Chemistry 2000.

#### 1.1.1: Introduction of Conducting Polymers

According to electrical properties, materials can be divided into four-types: insulator, semiconductor, conductor and superconductor. In general, a material with a conductivity less than  $10^{-7}$  S/cm is regarded as an insulator. A material with conductivity larger than  $10^{-3}$  S/cm is called as a metal whereas the conductivity of a semiconductor is in a range of  $10^{-4}$  -  $10$  S/cm depending upon doping degree.

Plastics are typical organic polymers with saturated macromolecules and are generally used as excellent electrical insulators. Since discovery of conductive polyacelene (PA) doped with iodine [1], a new field of conducting polymers, which is also called as “synthetic metals”, has been established and earned the Nobel Prize in Chemistry in 2000 [2]. Nowadays, conducting polymers as functionalized materials hold a special and an important position in the field of material sciences. In this Chapter, discovery, doping concept, structural characteristics, charge transport and conducting mechanism for the conducting polymers will be brief discussed.

## 1.1.2: Discovery of Conducting Polymers

In the 1960s—1970s, a breakthrough, polymer becoming electrically conductive, was coming-out. The breakthrough implied that a polymer has to imitate a metal, which means that electrons in polymers need to be free to move and not bound to the atoms. In principle, an oxidation or reduction process is often accompanied with adding or withdrawing of electrons, suggesting an electron can be removed from a material through oxidation or introduced into a material through reduction. Above idea implies that a polymer might be electrically conductive by withdrawing electron through oxidation (i.e. a “hole”) or by adding electron through reduction, which process was latterly described by an item of “doping”. The breakthrough was realized by three awarders of Chemistry Nobel Prize in 2000, who were Alan J. Heeger at the University of California at Santa Barbara, USA, Alan G. MacDiarmid at the University of Pennsylvania, Philadelphia, USA, and Hideki Shirakawa at the University of Tsukuba, Japan [2].

The unexpected discovery not only broken a traditional concept, which organic polymers were only regarded as the insulators, but also establishing a new filed of conducting polymers, which also called as “Synthetic Metals”. PA could be regarded as an excellent candidate of polymers to be imitating a metal, because it has alternating double and single bonds, as called conjugated double bonds.

From Fig. 1.1, PA is a flat molecule with an angle of  $120^\circ$  between the bonds and hence exists in two different forms, the isomers cis-polyacetylene and trans-polyacetylene [2].

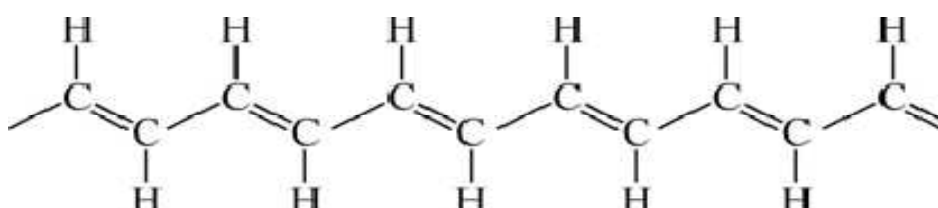


Figure 1.1 Molecular structure of polyacetylene [1, 2]

Thereby, synthesis of PA received great of attention at that time. At the beginning of the 1970s, Hedeki Shirakawa at Tokyo Institute of Technology, Japan, was studying the polymerization of acetylene into plastics by using catalyst created by Ziegler-Natta. PA was

affected by reaction temperature, for instance, the silvery film was trans-polyacetylene whereas copper-colored film was almost pure cis-polyacetylene.

Miracle took place on November 23, 1976! At that day, Dr. C.K. Chiang, a postdoctoral fellow under Professor Heeger, for measuring the electrical conductivity of PA by a four-probe method. Surprise to them, the conductivity of PA was ten million times higher than before adding bromine. This day was marked as the first time observed the “doping” effect in conducting polymers. In the summer of 1977, Heeger, MacDiarmid, and Shirakawa co-published their discovery in the article entitled “Synthesis of electrically conducting organic polymers: Halogen derivatives of polyacetylene  $(CH)_n$ ” in The Journal of Chemical Society, Chemical Communications [1]. After discovery of the conductive PA, fundamental researches dealing with synthesis of new materials, structural characterization, solubility and processability, structure-properties relationship and conducting mechanism of conducting polymers as well as their applications in technology have been widely studied and significant progress have been achieved.

After 23 years, The Royal Swedish Academy of Sciences has decided to award the Nobel Prize in Chemistry for 2000 jointly to Alan J. Heeger at University of California at Santa Barbara, USA, Alan G. MacDiarmid at University of Pennsylvania, Philadelphia, USA, and Hideki Shirakawa at University of Tsukuba, Japan “for the discovery and development of conductive polymers” [2].



**Alan Heeger**  
University of California  
at Santa Barbara



**Hideki Shirakawa**  
University of Tsukuba



**Alan MacDiarmid**  
University of  
Pennsylvania

### 1.1.3 Structural Characteristics and Doping Concept

$\pi$ -conjugated polymer chain is a basic requirement for a polymer becoming conducting polymer. The delocalization of  $\pi$ -bonded electrons over the polymeric backbone, co-existing with unusual low ionization potentials, and high electron affinities lead to special electrical properties of conducting polymers [6]. On the other hand,  $\pi$ -conjugated chain of conducting polymers leads to insoluble and poor mechanical properties of conducting polymers, limiting their application in technology. Thereby continue effort to improve solubility and to enhance mechanic strength of conducting polymers is needed.

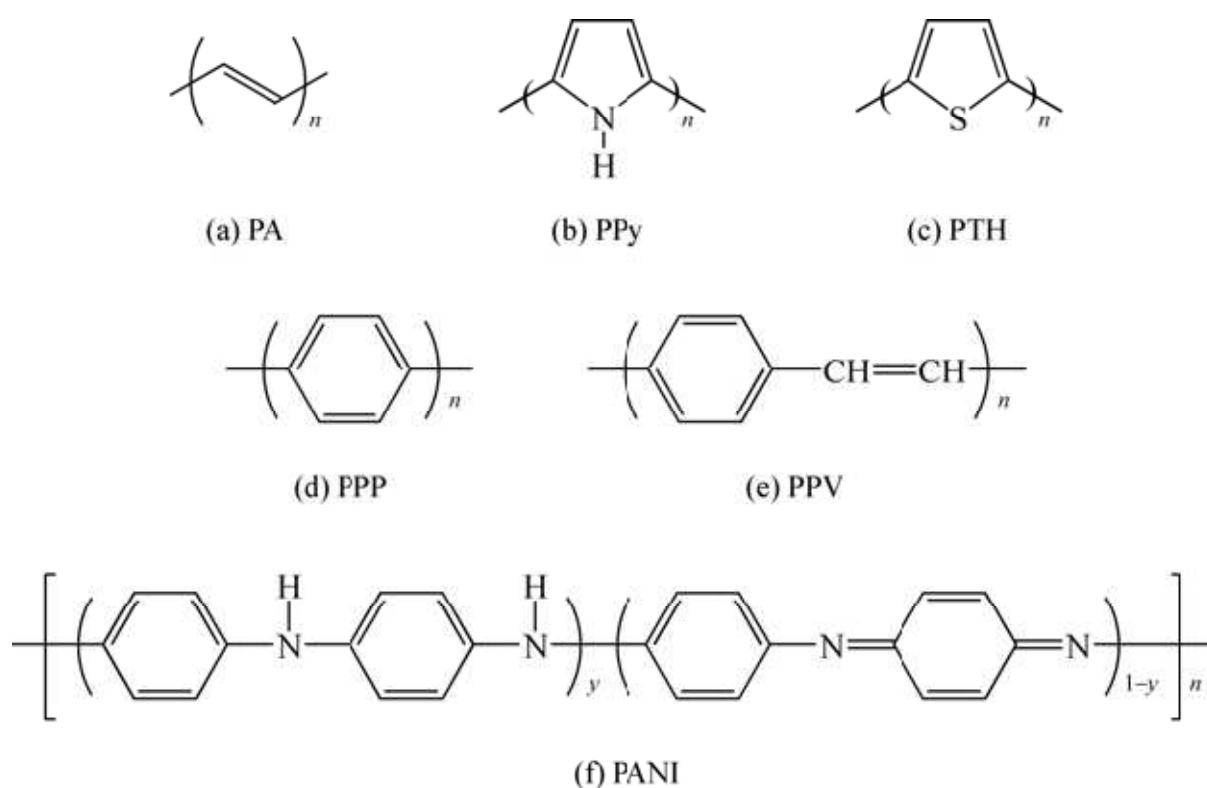
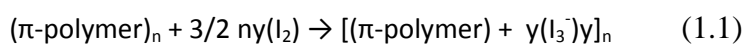


**Figure 1.2 Molecular structure of typical conducting polymers (a) trans-polyacetylene; (b) polypyrrole; (c) Polythiophene; (d) poly(p-phenylene) (e) poly ( p-phenylenevinylene); (f) polyaniline**

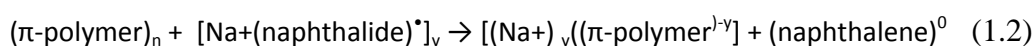
The transition of  $\pi$ -conjugated polymer from insulator to metal is carried out by a “doping” process. However, the “doping” item used in conducting polymers differs significantly from traditional inorganic semiconductor [5]. Differences in “doping” item between inorganic semiconductors and conducting polymers are shown as follows:

(1) Intrinsic of doping item in conducting polymers is an oxidation ( p-type doping) or reduction (n-type doping) process, rather than atom replacement in inorganic semiconductors. Using PA as a sample, for instance, the reaction of p-and n-doping is written as:

Oxidation with halogen ( p-doping):



Reduction with alkali metal (n-doping):

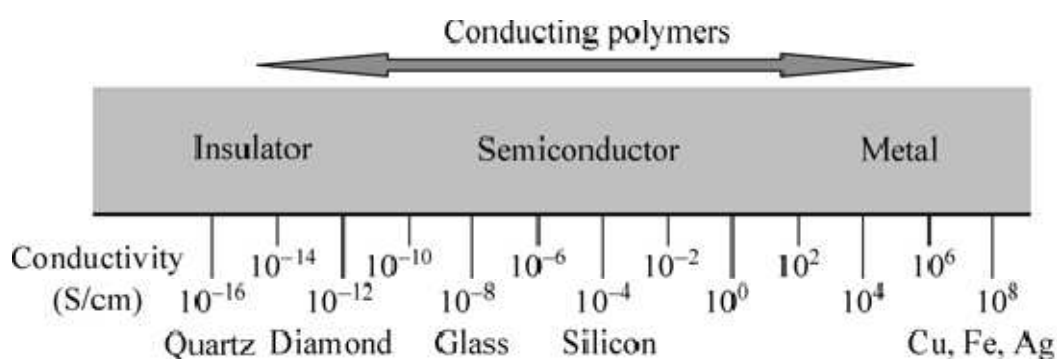


(2) p-doping (withdrawing electron from polymeric chain) or n-doping (adding electron into polymeric chain) in conducting polymers can be acquired and consequently accompanied with incorporation of counterion, such as cation for p-doping or anion for n-doping, into polymer chain to satisfy electrical nature.

In the case of oxidation, taking PA as a sample, the iodine molecule attracts an electron from the PA chain and becomes  $I_3^-$ . The PA molecule, now positively charged, is termed a radical cation [1]. Therefore, conducting polymers not only consist of  $\pi$ -conjugated chain, but also containing counter-ions caused by doping. This differs from conventional inorganic semiconductors, where the counterions are absent. The special chain structure of conducting polymers results in their electrical properties being affected by both structure of polymeric chain (i.e.  $\pi$ -conjugated length) and dopant nature.

Doping process can be completed through chemical or electrochemical method [4]. Except for chemical or electrochemical doping, other doping methods, such as “photodoping” and “charge-injection doping”, are also possible [7]. For instance solar cells is based on “photodoping” whereas light emitting diodes (LEDs) results from “charge-injection doping”, respectively, Besides, “proton doping” discovered in PANI is an unusual and efficient doping method in conducting polymers [8]. The proton doping does not involve a change in the number of electrons associated with the polymer chain [9] that is different from redox doping (e.g. oxidation or reduction doping) where the partial addition ( reduction ) or removal (oxidation ) of electrons to or from the  $\pi$ -system of the polymer backbone took place [4,10].

(3) The insulating  $\pi$ -conjugated polymers can be converted to conducting polymers by a chemical or electrochemical doping and which can be consequently recombined to insulate state by de-doping. This suggests that not only de-doping can take place in conducting polymers, but also reversible doping/de-doping process, which is different from inorganic semiconductor where de-doping can't take place [5]. As a result, conductivity of the conducting polymers at room temperature covers whole insulator-semiconductor-metal region by changing doping degree as shown in Fig. 1.4. On the contrary, those processes are impossible to take place in inorganic semiconductors.

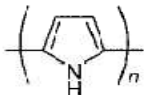
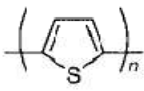
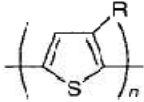
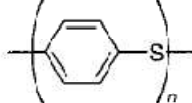
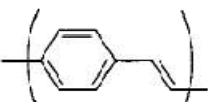
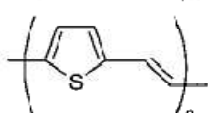
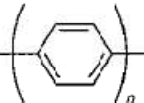
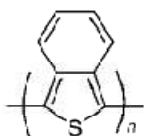
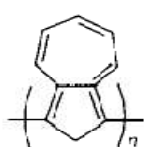
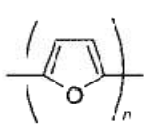
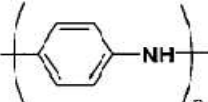


**Figure 1.3 Conductivity of conducting polymers can cover whole insulator-semiconductor-metal region by changing doping degree**

(4) The doping degree in inorganic semiconductor is very low (~ tenth of thousand) whereas doping degree in conducting polymers can be achieved as high as 50% [5]. So electron density in a conducting polymer is higher than that of inorganic semiconductor; however, the mobility of charge carriers is lower than that of inorganic semiconductor due to defects or poor crystalline.

(5) Conducting polymers mostly composed of C, H, O and N elements and their chain structure can be modified by adding substituted groups along the chain or as the side chains that result in conducting polymers reserving light-weight and flexibility of conventional

polymer

Polymer	Structure	Doping Materials	Approximate Conductivity (S/cm)
Polyacetylene	$(\text{CH})_n$	$\text{I}_2$ , $\text{Br}_2$ , Li, Na, $\text{AsF}_5$	$10,000^a$
Polypyrrole		$\text{BF}_4^-$ , $\text{ClO}_4^-$ , tosylate <sup>b</sup>	500–7,500
Polythiophene		$\text{BF}_4^-$ , $\text{ClO}_4^-$ , tosylate <sup>b</sup> , $\text{FeCl}_4$	1,000
Poly(3-alkylthiophene)		$\text{BF}_4^-$ , $\text{ClO}_4^-$ , $\text{FeCl}_4$	$1,000\text{--}10,000^a$
Polyphenylene sulfide		$\text{AsF}_5$	500
Polyphenylenevinylene		$\text{AsF}_5$	$10,000^a$
Polythienylenevinylene		$\text{AsF}_5$	$2,700^a$
Polyphenylene		$\text{AsF}_5$ , Li, K	1,000
Polyisothianaphthene		$\text{BF}_4^-$ , $\text{ClO}_4^-$	50
Polyzulene		$\text{BF}_4^-$ , $\text{ClO}_4^-$	1
Polyfuran		$\text{BF}_4^-$ , $\text{ClO}_4^-$	100
Polyaniline		HCl	$200^a$

<sup>a</sup>Conductivity of oriented polymer.

<sup>b</sup>*p*-Methylphenylsulfonate.

**Table 1 Conductivities of Conducting Polymers**



### 1.1.4: Charge Storage

One early explanation of conducting polymers used band theory as a method of conduction. This said that a half filled valence band would be formed from a continuous delocalized  $\pi$ -system. This would be an ideal condition for conduction of electricity. However, it turns out that the polymer can more efficiently lower its energy by bond alteration (alternating short and long bonds), which, introduces a band width of 1.5 eV making it a high energy gap semiconductor. The polymer is transformed into a conductor by doping it with either an electron donor or an electron acceptor. This is reminiscent of doping of silicon based semiconductors where silicon is doped with either arsenic or boron. However, while the doping of silicon produces a donor energy level close to the conduction band or an acceptor level close to the valence band, this is not the case with conducting polymers. The evidence for this is that the resulting polymers do not have a high enough concentration of free spins, as determined by electron spin spectroscopy. Initially the free spins concentration increases with concentration of dopant. At larger concentrations, however, the concentration of free spins levels off at a maximum.

To understand this it is necessary to examine the way in which charge is stored along the polymer chain and its effect. The polymer may store charge in two ways. In an oxidation process it could either lose an electron from one of the bands or it could localize the charge over a small section of the chain. Localizing the charge causes a local distortion due to a change in geometry, which costs the polymer some energy. However, the generation of this local geometry decreases the ionization energy of the polymer chain and increases its electron affinity making it more able to accommodate the newly formed charges. This method increases the energy of the polymer less than it would if the charge was delocalized and, hence, takes place in preference of charge delocalization. This is consistent with an increase in disorder detected after doping by Raman spectroscopy. A similar scenario occurs for a reductive process.

Typical oxidizing dopants used include iodine, arsenic pentachloride, iron(III) chloride and  $\text{NO}_2^+$ . A typical reductive dopant is sodium naphthalide. The main criteria is its ability to oxidize or reduce the polymer without lowering its stability or whether or not they are capable of initiating side reactions that inhibit the polymer's ability to conduct electricity.

An example of the latter is the doping of a conjugated polymer with bromine. Bromine is too powerful an oxidant and adds across the double bonds to form  $sp^3$  carbons. The same problem may also occur with  $NO_2PF_6$  if left too long.

The oxidative doping of polypyrrole proceeds in the following way. An electron is removed from the p system of the backbone producing free radical and a spinless positive charge. The radical and cation are coupled to each other via local resonance of the charge and the radical. In this case, a sequence of quinoid-like rings is used. The distortion produced by this is of higher energy than the remaining portion of the chain. The creation and separation of these defects costs a considerable amount of energy. This limits the number of quinoid-like rings that can link these two bound species together.

In the case of polypyrrole it is believed that the lattice distortion extends over four pyrrole rings. This combination of a charge site and a radical is called a polaron. This could be either a radical cation or radical anion. This creates a new localized electronic states in the gap, with the lower energy states being occupied by a single unpaired electrons. The polaron state of polypyrrole are symmetrically located about 0.5 eV from the band edges. Upon further oxidation the free radical of the polaron is removed, creating a new spinless defect called a bipolaron.

This is of lower energy than the creation of two distinct polarons. At higher doping levels it become possible that two polarons combine to form a bipolaron. Thus at higher doping levels the polarons are replaced with bipolarons. The bipolarons are located symmetrically with a band gap of 0.75 eV for polypyrrole. This eventually, with continued doping, forms into a continuous bipolaron bands. Their band gap also increases as newly formed bipolarons are made at the expense of the band edges. For a very heavily doped polymer it is conceivable that the upper and the lower bipolaron bands will merge with the conduction and the valence bands respectively to produce partially filled bands and metallic like conductivity. This is shown in next page.

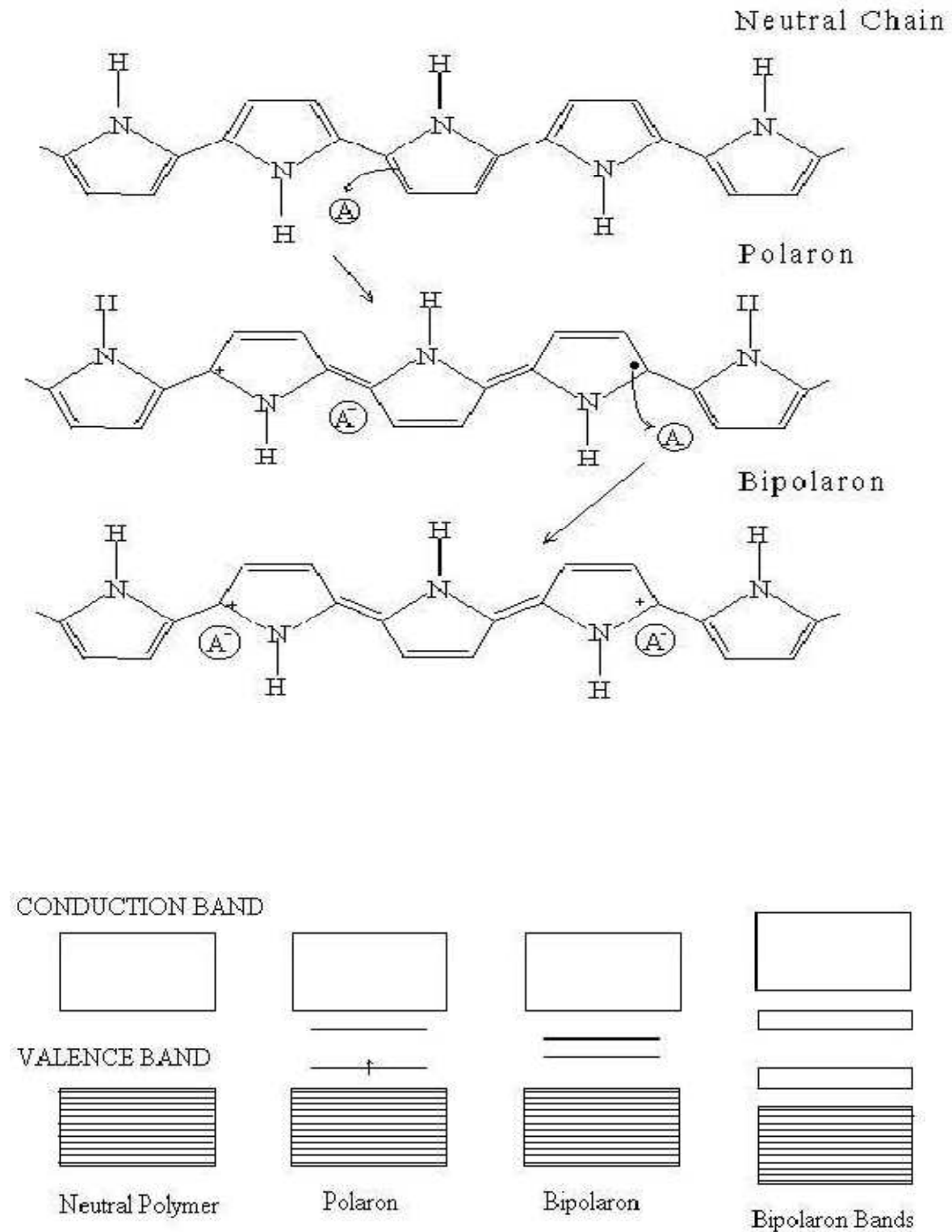


**Figure 1.4** Show conduction mechanism in polypyrrole

Conjugated polymers with a degenerate ground state have a slightly different mechanism. As with polypyrrole, polarons and bipolarons are produced upon oxidation. However, because the ground state structure of such polymers are twofold degenerate, the charged

cation are not bound to each other by a higher energy bonding configuration and can freely separate along the chain. The effect of this is that the charged defects are independent of one another and can form domain walls that separate two phases of opposite orientation and identical energy. These are called solitons and can sometimes be neutral. Solitons produced in polyacetylene are believed to be delocalized over about 12 CH units with the maximum charge density next to the dopant counterion. The bonds closer to the defect show less amount of bond alternation than the bonds away from the centre. Soliton formation results in the creation of new localized electronic states that appear in the middle of the energy gap. At high doping levels, the charged solitons interact with each other to form a soliton band which can eventually merge with the band edges to create true metallic conductivity. This is shown below.

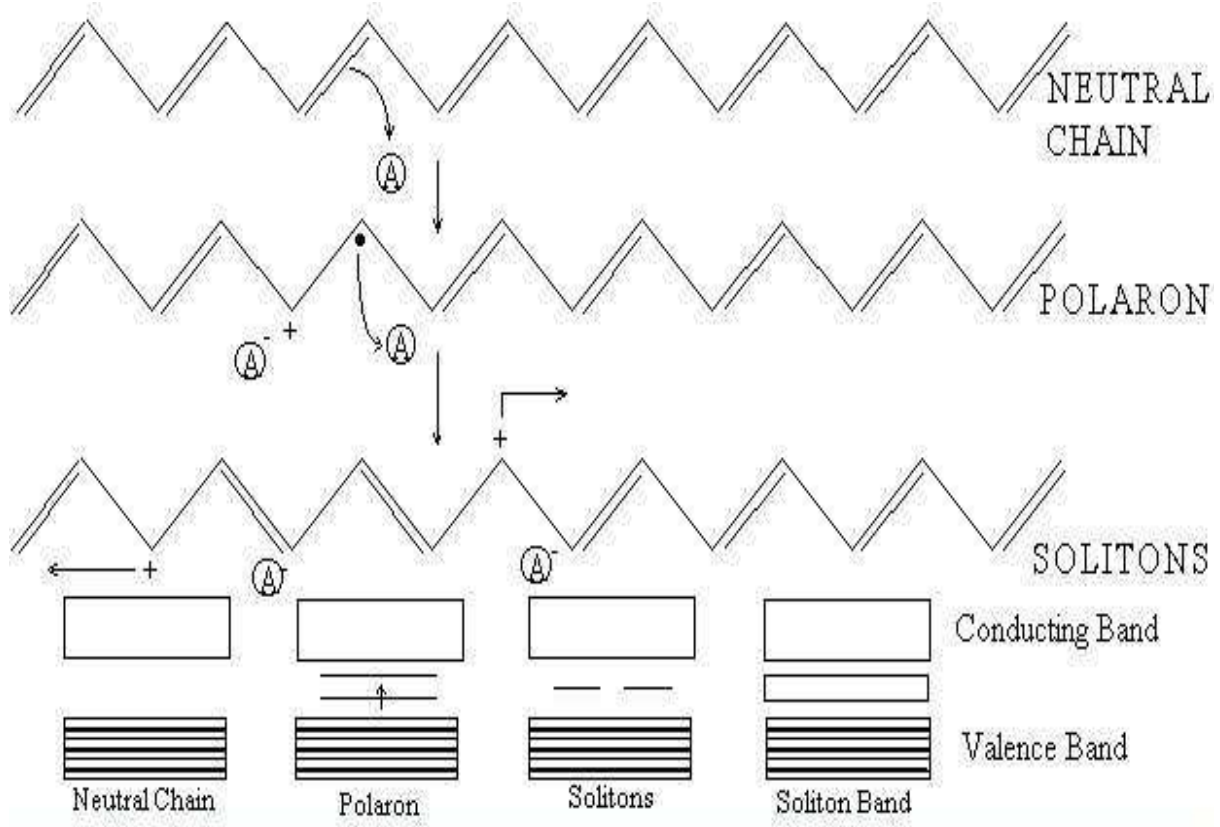


**Figure 1.5 Shows conduction mechanism in polyacetylene**

### 1.1.5: Charge Transport

Although solitons and bipolarons are known to be the main source of charge carriers, the precise mechanism is not yet fully understood. The problem lies in attempting to trace the path of the charge carriers through the polymer. All of these polymers are highly disordered, containing a mixture of crystalline and amorphous regions. It is necessary to consider the transport along and between the polymer chains and also the complex boundaries established by the multiple number of phases. This has been studied by examining the effect of doping, of temperature, of magnetism and the frequency of the current used. These test show that a variety of conduction mechanisms are used. The main mechanism used is by movement of charge carriers between localized sites or between soliton, polaron or bipolaron states.

Alternatively, where inhomogeneous doping produces metallic island dispersed in an insulating matrix, conduction is by movement of charge carriers between highly conducting domains. Charge transfer between these conducting domains also occurs by thermally activated hopping or tunnelling. This is consistent with conductivity being proportional to temperature.

### 1.1.6: Stability

There are two distinct types of stability. Extrinsic stability is related to vulnerability to external environmental agent such as oxygen, water, peroxides. This is determined by the polymers susceptibility of charged sites to attack by nucleophiles, electrophiles and free radicals. If a conducting polymer is extrinsic unstable then it must be protected by a stable coating. Many conducting polymers, however, degrade over time even in dry, oxygen free environment. This intrinsic instability is thermodynamic in origin. It is likely to be cause by irreversible chemical reaction between charged sites of polymer and either the dopant counter ion or the p-system of an adjacent neutral chain, which produces an  $sp^3$  carbon, breaking the conjugation. Intrinsic instability can also come from a thermally driven mechanism which causes the polymer to lose its dopant. This happens when the charge sites become unstable due to conformational changes in the polymer backbone. This has been observed in alkyl substituted polythiophenes.

### 1.1.7: Processibility

Conjugated polymers may be made by a variety of techniques, including cationic, anionic, radical chain growth, co-ordination polymerization, step growth polymerization or electrochemical polymerization.

Electrochemical polymerization occurs by suitable monomers which are electrochemically oxidized to create an active monomeric and dimeric species which react to form a conjugated polymer backbone. The main problem with electrically conductive plastics stems from the very property that gives it its conductivity, namely the conjugated backbone. This causes many such polymers to be intractable, insoluble films or powders that cannot melt. There are two main strategies to overcoming these problems. There are to either modify the polymer so that it may be more easily processed, or to manufacture the polymer in its desired shape and form. There are, at this time, four main methods used to achieve these aims.

The first method is to manufacture a malleable polymer that can be easily converted into a conjugated polymer. This is done when the initial polymer is in the desired form and then, after conversion, is treated so that it becomes a conductor. The treatment used is most often thermal treatment. The precursor polymer used is often made to produce highly aligned polymer chain which are retained upon conversion. These are used for highly orientated thin films and fibres. Such films and fibres are highly anisotropic, with maximum conductivity along the stretch direction.

The second method is the synthesis of copolymers or derivatives of a parent conjugated polymer with more desirable properties. This method is the more traditional one for making improvements to a polymer. What is done is to try to modify the structure of the polymer to increase its processibility without compromising its conductivity or its optical properties.

All attempts to do this on polyacetylene have failed as they always significantly reduced its conductivity. However, such attempts on polythiophenes and polypyrroles proved more fruitful. The hydrogen on carbon 3 on the thiophene or the pyrrole ring was replaced with an alkyl group with at least four carbon atoms in it. The resulting polymer, when doped, has a comparable conductivity to its parent polymer whilst be able to melt and it is soluble.

A water soluble version of these polymers has been produced by placing carboxylic acid group or sulphonic acid group on the alkyl chains. If sulphonic acid group or groups are used along with built-in ionizable groups, then such system can maintain charge neutrality in its oxidized state and so they effectively dope themselves. Such polymers are referred to as "self-doped" polymers. One of the most highly conductive derivative of polythiophene is made by replacing the hydrogen on carbon three with a  $-\text{CH}_2-\text{O}-\text{CH}_2-\text{CH}_2-\text{O}-\text{CH}_2-\text{CH}_2-\text{O}-\text{CH}_3$ . This is soluble and reaches a conductivity of about  $1000 \text{ S cm}^{-1}$  upon doping.

The third method is to grow the polymer into its desired shape and form. An insulating polymer impregnated with a catalyst system is fabricated into its desired form. This is then exposed to the monomer, usually a gas or a vapour. The monomer then polymerizes on the surface of the insulating plastic producing a thin film or a fibre. This is then doped in the usual manner. A variation of this technique is electrochemical polymerization with the conducting polymer being deposited on an electrode either the polymerization stage or before the electrochemical polymerization. This cast may be used for further processing of the conducting polymer. For instance, by stretching aligned bends of polyacetylene/polybutadiene the conductivity increase 10 fold, due to the higher state of order produced by this deformation.

The final method is the use of Langmuir-Blodgett trough to manipulate the surface active molecules into a highly ordered thin films whose structure and thickness which are controllable at the molecular layer. Amphiphilic molecules with hydrophilic and hydrophobic groups produces monolayers at the air-water surface interface of a Langmuir-Blodgett trough. This is then transferred to a substrate creating a multilayer structure comprised of molecular stacks which are normal about 2.5 nm thick. This is a development from the creation of insulating films by the same technique. The main advantage of this technique is its unique ability to allow control over the molecular architecture of the conducting films produced. It can be used to create complex multilayer structures of functionally different molecular layers as determined by the chemist. By producing alternating layers of conductor and insulator it is possible to produce highly anisotropic film which is conducting with in the plane of the film, but insulating across it.

POLYMER	CONDUCTIVITY (S cm <sup>-1</sup> )	STABILITY (doped state)	PROCESSING POSSIBILITIES
Polyacetylene	10 <sup>3</sup> - 10 <sup>5</sup>	Poor	Limited
Polyphenylene	1000	Poor	Limited
PPS	100	Poor	Excellent
PPV	1000	Poor	Limited
Polypyrroles	100	good	Good
Polythiophenes	100	good	Excellent
Polyaniline	10	good	Good

### 1.2.1: Polyaniline

Polyaniline was the first conducting polymer to be prepared, when in 1862 H. Lethe by[11]. of the college of London Hospital in the U.K. anodically oxidized aniline in sulfuric acid but there had been only limited interest in this polymer until the resurgence of interest in conductive polymers driven by the high conductivities found in polyacetylene when doped.

In 1985, MacDiarmid, for the first time, found that aniline monomer in an acid aqueous solution (e.g.1.0 mol/L HCl) can be chemically oxidized by ammonium peroxydisulfate (APS) to obtain green powder of PANI with a conductivity of as high as 3 S/cm, as measured by four-probe method, which results were published in 1986 [12].This was the first sample of the conducting polymers doped by proton, which latterly was called “proton doping”. Compared with other conducting polymers, PANI is advantageous of easy synthesis, low-cost, structure complex and special proton doping mechanism, as well as physical properties controlled by both oxidation and protonation state. These unique properties result in PANI holding an important position in the field of conducting polymers.



## 1.2.2: Molecular Structure and Proton Doping

Compared with other conducting polymers, PANI has a complex molecular structure dominated by its oxidation and protonation state. MacDiarmid et al. [13], for the first time, proposed that the base form of PANI has a general formula [14] as shown Fig. 1.6. They assumed that the base form of PANI consists of alternating reduced and oxidized repeat unit chain and can be divided into three states based on the oxidation state [12, 15] as shown in Fig. 1.6. The completely reduced form and oxidized form are assigned as “leucoemeraldine” base form ( $y = 1$ , LEB) and “pernigraniline” form ( $y = 0$ , PEN), respectively. The “halfoxidized” form is called as “emeraldine base” form ( $y = 0.5$ , EB). The general molecular formula of the base form of PANI proposed by MacDiarmid has been firstly conformed by the analysis of the  $^{13}\text{C}$ -NMR spectra [16].

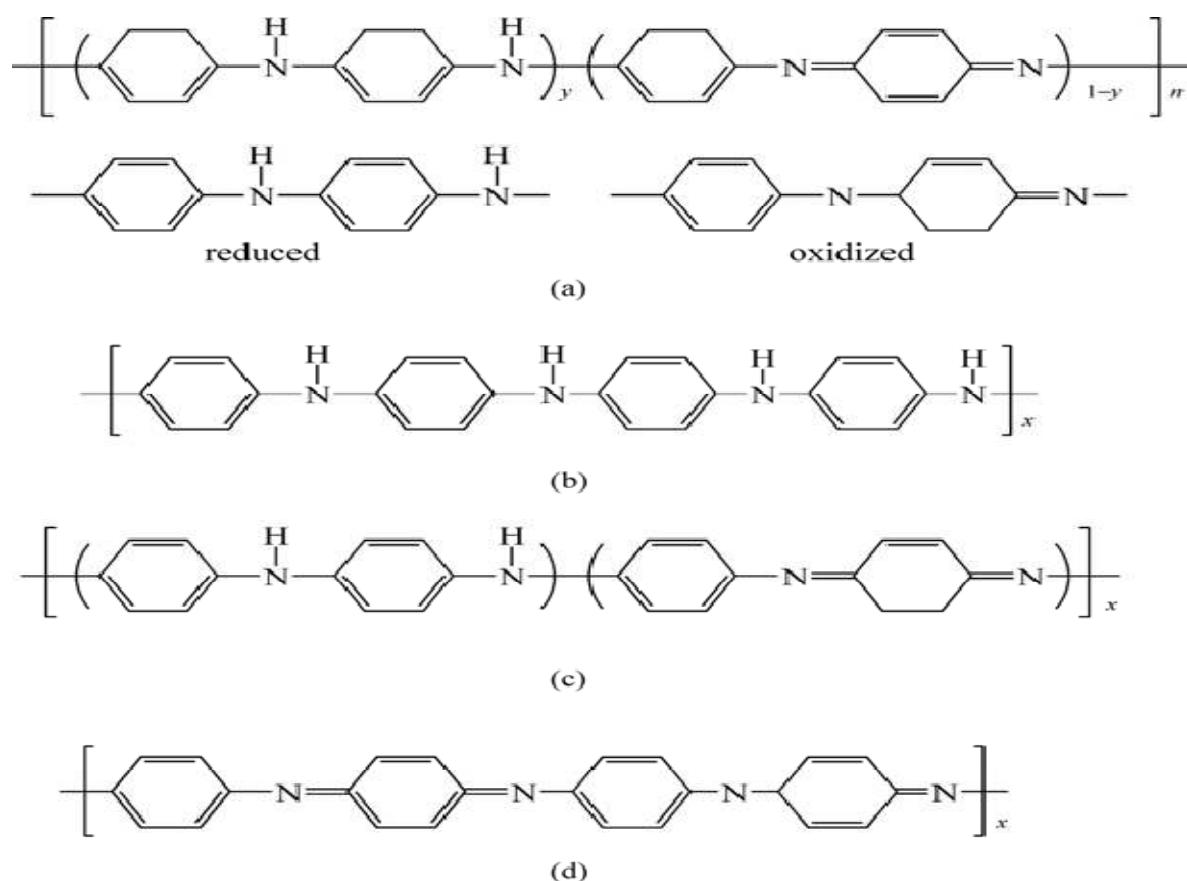


**Figure 1.6 (a) Generalized composition of PANI indicating the reduced and oxidized repeat units; (b) completely reduced polymer; (c) half-oxidized polymer; (d) fully oxidized polymer**

PANI was the first sample of a doping conjugated polymer to a highly conducting regime by a proton doping [12]. Proton doping means that the emeraldine base form (EB,  $y = 0.5$ ) is doped with a protonic acid (e.g. 1.0 mol/L HCl) to produce a protonated emeraldine base form with a high conductivity ( $\sim 3$  S/cm), which is called as the emeraldine salt form (ES) [12, 15b]. As shown in Fig. 1.7, the proton doping does not involve a change of the number of electrons associated with the polymer backbone during the proton doping [12, 15b]. This significantly differs from redox doping (e.g. oxidation or deduction) where involves the partial addition (reduction) or removal (oxidation) of electrons to or from the polymer backbone [17]. Thus proton doping is major characteristics of PANI differing from other conducting polymers.

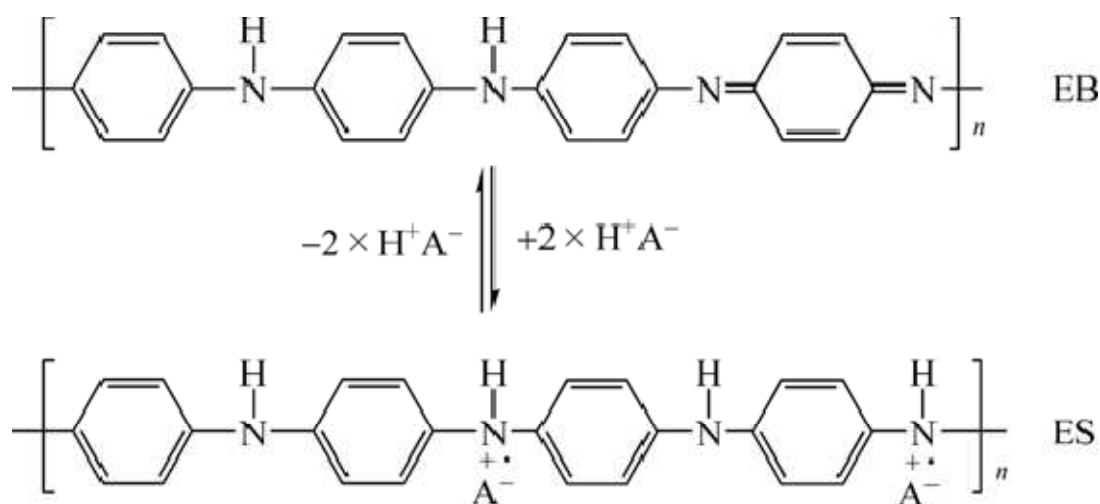


**Figure 1.7 Scheme of proton doping in PANI**

In principle, the imine nitrogen atom on the polymeric chain of PANI can be protonated in whole or in part to obtain the corresponding salts and the protonation degree on the polymeric base, depending on its oxidation state and the pH value of the aqueous acid [12]. MacDiarmid et al. [13], for the first time, proposed that proton doping only took place on the imine segment of the emeraldine base form to form a bipolaron. However, this was contradictory with both theoretical calculation and ESR, because theoretical calculation rules out the presence of a bipolaron lattice (spinless) in the emeraldine salt form [18] and a strong ESR signal rather than spinless was observed [19]. In order to solve above contradictory, Epstein et al. [19, 20] and Wnek [21] suggested that spinless bipolaron can

convert to two spinning protons due to instability of bipolaron. MacDiarmid et al. [15b] also proposed the polaron is of semiquinone form as shown in Fig. 1.7. It means that the complete protonation of the imine nitrogen atom in the emeraldine base by proton doping results in the formation of a delocalized poly-semiquinone radical cation [12, 15b, 17a].

### 1.2.3: Synthesis Method

Like other conducting polymers, PANI is generally synthesized by both chemical and electrochemical methods [17a]. But mechano-chemical route has been recently reported to prepare conducting PANI. These methods to PANI will be briefly discussed below.

#### 1.2.3(a): Chemical Method

In general, the emeraldine salt form of PANI (i.e. its conducting state) is prepared by oxidative polymerization of aniline in a strong acidic medium [12,13]. The scheme of chemical polymerization of aniline can be described as follows:

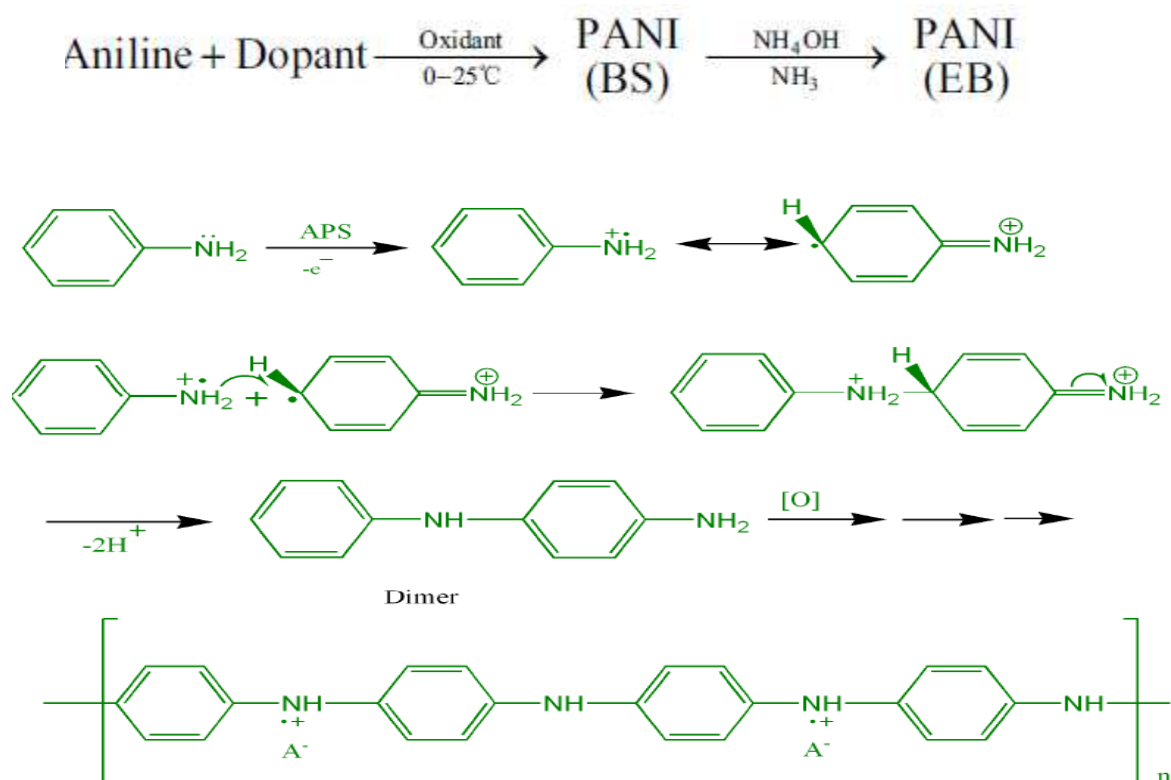


Figure 1.8 Shows mechanism of polymerization of aniline

Typical chemical polymerization of PANI is as follows [17a]: APS of 10 mL (e.g. of 2.5 mol/L) as an oxidant is added with stirring to 100 mL solution of a mixture of aniline monomer (e.g. 0.55 mol/L) and 1.0 mol/L HCl at room temperature or in an ice/water bath (0 - 5°C) and the polymerization is continued for pre-desired time. The precipitate is then filtered, washed with small amounts of 0.5 mol/L HCl solution, then with methanol until colorless, and finally diethyl ether until color-less. It is finally dried at ca. 60 -70°C in air for ca. 24 h. The product so obtained is the emeraldine salt form with conductivity of ~ 10 S/cm, depending preparation conditions. The resultant emeraldine salt form can be converted to its emeraldine base form by NH<sub>4</sub>OH or NH<sub>3</sub>, which process is called as de-doping. From above scheme of polymerization of aniline, one can see, the reaction system of aniline polymerization is very simple, only including monomer, dopant and oxidant and water. Among these reagents, dopant is the most important reagent, because it is mainly attributed to electrical properties of PANI. Speaking generally, inorganic acids (e.g. HCl, H<sub>2</sub>SO<sub>4</sub>, H<sub>3</sub>PO<sub>4</sub> and HF) and organic acids are widely used as dopants for doping PANI. Dopant feature includes molecular structure and acidity, strongly affect the properties of the doped PANI [17a].

Except for dopant, oxidant is another important reagent for chemical polymerization of PANI. Up to date various oxidants such as APS [12], tetrabutylammonium persulfate (TBAP) [22], hydrogen peroxide (H<sub>2</sub>O<sub>2</sub>) [23], benzoyl peroxide [24], ferric chloride (FeCl<sub>3</sub>) [25] and chloroaurate acid (HAuCl<sub>4</sub>) [26], have been used to synthesize PANI. However, most previous reported results mainly emphasized the effect of oxidants on the polymerization yield, and APS was regarded as the optimal oxidant for PANI because of its high yield [27]. Interestingly, author found that the diameter of PANI nanotubes synthesized by template-free method is directly related to the redox potential of oxidant [28].

In addition, reaction temperature, polymerization time as well as stirring fashion and speed also affect the structure and physical properties of the final PANI product. Reaction temperature is more important because it affects the crystallinity of PANI, showing a low reaction temperature is favorable for preparing high crystalline PANI [9a]. A low reaction temperature can be achieved by freezing the reaction bath (e.g. ice/salt bath with T<4°C) or by addition of inorganic salts (e.g. NaCl) in the reaction solution, resulting in the polymerization is proceed in the solid state [29].



**Figure 1.9 Powder of PANI prepared by chemical method**

### **1.2.3(b): Electro-Chemical Method**

Electrochemical polymerization is another major tool to prepare conductive PANI. In an electrochemical method, a PANI film or layer is formed on a work electrode surface in an acidic medium (e.g. 1.0 mol/L HCl) including high concentrations of aniline monomer [9a]. The electrochemical method has some advantages over chemical procedures to prepare PANI as follows:

Electrochemical method is easy to be controlled by changing current quantity passed through between the work and counter electrodes, applied voltage and polymerization time. Moreover, the oxidation and electrically conducting form of PANI is reversibly transformed into the reduced, isolating form by changing its electrochemical potential to negative values. On the other hand, the chemical method is difficult to ensure a same micro-environment for preparing PANI, insulating in disorder of the product.

A small amount reagent is required in an electrochemical method. On the contrary, a large amount of reactive chemical reagents in the chemical method is required, which could cause environment pollution.

The quantum of the product prepared by electrochemical method is limited by size of the work electrode; however, large amount of product is easily synthesized by a chemical method. It has been demonstrated that the electrochemical polymerization of aniline is as a

bimolecular reaction involving a radical cation intermediate and a two-electron-transfer process for each step of polymerization [30]. Based on the assumption that the oxidation of PANI follows Faraday's law, the electrochemical polymerization of aniline can be monitored by PANI deposition on the work electrode and doping charges [31]. In some strong acids such as HCl or H<sub>2</sub>SO<sub>4</sub>, the deposition charge was found to increase proportionally to the second powers of the cycle number [30]. When potentiostatic techniques was used to electrochemically polymerize aniline, moreover, the initial formation (or nucleation) of PANI on the surface of the electrode is slow, but the initially formed PANI accelerated the polymer growth greatly and the current increased proportionally with the second power, which is called as "self-catalyzing" or "auto-acceleration" process in the electrochemical polymerization of aniline [32]. Wei et al. [30] employed the anodic peak current instead of charges to monitor the electrochemical polymerization process of aniline in aqueous HCl solution using cyclic potential sweep techniques. This method was more sensitive to the presence of irreversible side reaction [33]. By using this method, the cyclic voltammograms of aniline polymerization showed three peaks [30], which are associated with three oxidation states suggested by MacDiarmid [14]. Wei et al. [34] also investigated effect of the additives, such as paminodiphenylamine, benzidine, and phenoxyaniline, on the rate of electrochemical polymerization of aniline. They found all of these additives have lower oxidation potentials than the aniline monomers and at least one satirically accessible aromatic amino group incorporated into polymer chains as a part of the structural backbones [34].

### **1.2.3(c): Mechano-Chemical Route**

Since the liquid monomer aniline forms solid salts with doping acids (e.g. HCl, H<sub>2</sub>SO<sub>4</sub> and CSA) through an acid/base reaction, room-temperature solid-state polymerization of aniline is possible using a solid anilinium salt as the precursor. Kaner et al. [35] recently describe a solvent-free mechano-chemical route to PANI in which the reaction is induced by ball-milling an aniline salt and an oxidant under ambient conditions. According to the report of Kaner et al. [35], the typical synthesis procedure of mechano-chemical route to PANI is shown as: firstly a salt of aniline and CSA was prepared by the reaction between aniline and CSA in water followed by evaporation that was served as the precursor. Then a mixture of an anilinium salt (e.g. aniline/CSA) and APS as an oxidant were loaded into a stainless steel grinding bowl and which was then sealed and spun at 600 r/min in a planetary micro-

mill for 1 h [35]. Once the spinning stopped, the product was transferred into a beaker and washed with water for several times. A yield of up to 65% based on aniline can be achieved using a 1:1 molar ratio of anilinium salt to oxidant and typical sample of the PANI powder prepared by this method is shown in Fig. 2.6. Spectroscopic studies indicate that the resultant PANI is identical to the emeraldine salt form of PANI with a conductivity of  $10^{-2}$  S/cm [35]. This method opens a simple and solvent-free method to prepare a large amount of the conducting PANI.

### 1.2.4: Physical Properties

Like other conducting polymers, PANI has unique physical properties including optical, electrical and magnetic properties and corresponding effects (Schottky and thermo-chromic effect and photo-emission effect) which will be briefly discussed below.

#### 1.2.4(a): Nonlinear Optical (NLO)

Nonlinear optical (NLO) effect is defined that when a light passes through a nonlinear optic-active medium, the frequency, phase, amplitude or transmission of the coming out of light are changed [36]. The NLO phenomena therefore are expected to provide key functions necessary for the photonic technology of optical switching, frequency modulation, wave-guiding, and eventually practical all-optical computing [37]. Compared with inorganic or organic NLO materials, NLO polymers are of somewhat advantageous as follows:

The design, synthesis and fabrication of NLO polymers are more flexible, facile and cost-effective than those of inorganics [38].

The lower dielectric constant of polymers make it easier to design traveling wave electro-optic (EO) modulators due to the close match of velocity between the microwave and optic wave. Processing polymers in conjunction with thin films technologies offers the unique opportunity for them to be used in inter-grated optic and EO application. As a result, organic and polymeric NLO materials have been received great attention in NLO materials and their applications in technology.

### 1.2.4(b): Electrical and Charge Transport Properties

Highly conducting form (ES) of PANI is controlled by two completely different processes: protonic acid doping and oxidative doping, while other conducting polymers are affected by their oxidation state alone [39], resulting in it has a special position in the field of conducting polymers. As mentioned before, the insulate state of PANI (the emeraldine base form, EB) can be doped by proton doping (e.g. 1 mol/L HCl) to conducting state of PANI (the emeraldine salt form, ES) [12, 13]. As shown in Fig. 2.7, the protonation is accompanied by a 9 to 10 order of magnitude increase in conductivity achieving about 10 S/cm, showing the conductivity is strongly affected by the protonation state (i.e. pH value of reaction) and undergone a change from insulator to metal through semiconductor [14]. A lot of papers dealing with PANI electrical properties have been reported [12,13,40]. Moreover, the doped PANI can be obtained by chemical oxidation (*p*-doping) of the full-reduced form of PANI (i.e. leucoemeraldine base) [15a].

Charge transport of PANI showed that the localized conductivity of PANI is affected by the localized variations in the thickness, stoichiometry, defects, or even substrates [41]. For intermediate protonation levels (e.g. the emeraldine salt form of PANI), for instance, magnetic and optical experiments supported the phase segregation between highly conducting regions and the insulating background [42]. The charge conduction was proposed via charging energy- limited tunnelling among the small granular polymeric grains [43], assuming the conductivity of the “conducting island” in PANI could be up to  $10^3$  S/cm [19]. Moreover, difference in charge transport between PANI-H<sub>3</sub>PO<sub>4</sub> [44] and PANI-H<sub>2</sub>SO<sub>4</sub> [45] has been also observed, implying that the dopants have a large impact on the charge transport properties of doped PANI in bulk. Furthermore, effect of synthesis conditions on morphology and conductivity of PANI has been also reported due to the difference in formation mechanism in different polymerization media [46].

Sulfonated polyaniline (SPAN) is the first reported self-doped water soluble conducting PANI derivative and a prime model for dopant and secondary dopant induced processability [47]. It has high water solubility and a novel pH-dependent conductivity that is of interest for fundamental science and also for applications in technology such as rechargeable batteries with a higher charge density [48] as compared to that obtainable utilizing the parent PANI [49], hetero-structure light emitting diode devices [50],



electrolyte acidity and enzyme activity [51] resist on a wafer [52]. Epstein and coworkers extensively studied synthesis and physical properties of SPAN with different sulfur-to-nitrogen (S/N) ratios (represented as S/N with 0.5-0.75). The physical properties including the pH dependence of the conductivity and electrochemical properties of SPAN with a high S/N ratio of 0.75 (i.e. LEB-SPAN) were extensively studied [53].

### **1.2.4(c): Magnetic Properties**

Since the magnetic properties can provide important details of charge carrying species and unpaired spins, magnetic properties of PANI have been extensively studied [54]. Usually the total static magnetic susceptibilities of the doped PANI could be separated into three components: atomic core diamagnetism, local moment Curie-law paramagnetic and temperature-independent Pauli paramagnetic. It is generally observed that the magnetic susceptibility changes from a Curie-like to a Pauli-like behavior as the temperature increases [55]. Moreover, the magnetic properties of PANI are affected by doping structure and degree, chain structure as well as synthesis conditions. For instance, Jinder et al. [19] found that the Pauli susceptibility of HCl-doped PANI is approximately linearly proportional to the degree of protonation. In addition, the magnetic properties of PANI and its derivatives (e.g. poly-alkyl-aniline) have a nearly linear ( $T$ ) dependence on  $T$  attributed to disorder-induced localized polaron pairs [56]. Although a lot of efforts have been done on the magnetic properties of PANI through different methods such as static magnetic measurements, electron paramagnetic resonance (EPR) and NMR spectroscopy [57], some of the results are still contradictory possibly, particular focused on the nature of the temperature-independent susceptibility, due to the complexity of polymeric materials caused by synthesis and doping conditions [58].

### **1.2.4(d): Other Properties**

Rannom et al. [59] recently reported diesters of 4-sulfophthalic acid doped PANI exhibits strong thermo-chromic effect in the UV-visible -NIR spectra and improved mechanical properties. It was suggested that the diesters of 4-sulfophthalic acid play a double role: one is sufficiently strong acids rendering PANI conductive; another results in lower glass transition temperature  $T_g$  due to containing strongly plasticizing groups. In addition, the thermo-chromic effect of PANI dissolved in *N*-methyl pyrrolidone (NMP) solution of three

principal forms of neutral (i.e., insulating) PANI, namely, leucoemeraldine, emeraldine, and pernigraniline [60] as well as in films plasticized with NMP [61] has been observed. In addition, it has also been reported for optically active doped PANI, i.e., PANI protonated with (+) camphor-10-sulfonic acid; however, the effect was observed at a relatively elevated temperature of 413 K at which slow decomposition of doped PANI takes place [62]. Since spectral changes in polyconjugated systems are caused by changes in the polymer chain conformation, which are not only thermally induced, but also caused by interactions with solvents used, therefore, thermo-chromic polymers frequently exhibit solvatechromism, which is consistent with observations of solvent-induced conformational changes in protonated PANI with CSA [63]. Solution processing of PANI into fibers is extraordinarily difficult because of following reasons:

- (a) Poor solubility in solvents compared with normal engineering plastics.
- (b) Very rapid polymer gelation times at low total solids content.
- (c) Strong aggregation tendency due to inter-chain attractive forces.

There were a few reports [64] regarding the subject of reproducible fiber spinning of PANI. However, Mattes et al. [65] reported the development of PANI fiber production techniques that have been used to create commercial fibers (PANION).

The techniques hold good promise for further significant advances in the field of solid-state electrochemical devices [66]. It is well known that water present in the PANI matrix affects the conductivity of PANI in its emeraldine salt oxidation state due to de-doping process taking place [67]. Only a few studies have been performed on the mechanism of water adsorption by PANI. The earliest work indicated that there existed two forms of water adsorbed by the materials weakly bonded water molecules that possess activation energy of de-sorption of about 5 kcal/mol and strongly bonded water molecules that are only desorbed during simultaneous decomposition of the polymer backbone [68]. It has been suggested that these water molecules form hydrogen bonds with the acid sites in the emeraldine salt form of PANI [69]. More recent work suggested that reversibly absorbed water consists of two forms, that is, the hydrogen bonded water (as found in previous studies with a de-sorption energy of 5 kcal/mol) and another form with a de-sorption energy of 15 - 18 kcal/mol [70]. This energy for de-sorption of the water molecules exceeds that of a single hydrogen bond and could correspond to the formation of a chemical bond with the polymer backbone. Pellegrino et al. [71] studied the water sorption kinetics and mass

uptake of the PANI with respect to the dopant anion. The PANI-ES solid fibers adsorbed as much water as many hydrophilic polymers and the electronic conductivity of these fibers is proportional to the relative humidity in a reproducible fashion [72]. These attributes can provide the possibility for advanced humidity control and sensing applications [72].

### **1.2.4(e): Solubility and Processability**

PANI is very popular conductive polymer and has great scientific and industrial interest because of its high conductivity, environmental stability, simple and cheap synthesis method as well as technological applications in electrical devices [73]. PANI has also great interest as an organic magnet due to the potentially strong exchange interactions occurring through the conjugated backbone [74]. However, for such applications, PANI must be processability including soluble in common solvents or melt process below the glass transition temperature [75].

### **1.2.4(f): Solubility**

The EB form of PANI is soluble in NMP, which can be used to fabricate a freestanding film of the EB form. However its doped form (i.e. ES form) is insoluble in organic solvent or aqueous solution. Therefore, to synthesize soluble conducting PANI (i.e. the protonated state, ES form) is a key for realizing commissural application of PANI in technology. To solve solubility and processability of PANI therefore is not only necessary for commercial application, but also fundamental research (e.g. structural characterizations). Great effort for improving solubility in solvent and processability of PANI has been reported [76]. For instance, sulfonation or incorporation of *N*-alkyl-sulfonic acid pendant groups [77], dopant-induced [78], self-doping polymer [79], micro-emulsion polymerization [80], and controlled relative molecular mass [81], have been reported for improvement of solubility and processability of PANI.

### **1.2.4(f<sub>1</sub>): Substitution onto Backbone**

Alkyl- and aryl-substitution attached on the polymer chain is a common tool to synthesize soluble PANI dissolved in organic solvent or aqueous solution [82]. Although these derivatives of PANI retain their electrochromic properties, their conductivity decreases dramatically to values between  $10^{-3}$  and  $10^{-7}$  S/cm. Moreover, the alkyl- and alkoxy-ring substituted PANI after acid-doping have a moderate conductivity of  $10^{-1}$  -  $10^{-3}$  S/cm, but

their molecular weights are usually low (on the order of 10<sup>3</sup>). Han et al. [83] reported a method to reduce PANI backbones from the emeraldine base form to the leucoemeraldine form and simultaneously derivative the backbones to form functionalized PANI by various functional alkanethiols. This method provided a novel way to control the degree of substitution of PANI. In fact, the most successful approach to a conductive PANI with solubility in aqueous solutions is introduced by sulfuric acid groups. This can be achieved by treating the polymer with the appropriate reagents after the polymerization or by polymerizing the substituted aniline derivatives. An example of the approach is the sulfonation of the emeraldine base with fuming sulfuric acid to produce a soluble PANI in aqueous alkaline solutions [84].

### **1.2.4(f<sub>2</sub>): Self-Doping PANI (SPAN)**

Another successful approach toward soluble conductive PANI is to introduce sulfuric acid groups on PANI chains. Sulfonated polyaniline (SPAN) is the first reported self-doped water soluble conducting PANI derivative, which molecular structure with different degree of sulfonation defined as the sulfur-to-nitrogen (S/N) ratio is shown in Fig. 2.8 [85]. Usually, EB and PNB forms of PANI have been used as starting materials for the preparation of SPAN, which defined as EB-SPAN and PNB-SPAN, respectively. Fuming sulfuric acid, chlorosulfonic acid, and sulfur trioxide/triethyl phosphate complex were also used as sulfonation agents in the synthesis of SPAN [85]. Although Genies et al. [86] have attempted to synthesize a self-doped SPAN by reaction of the EB form directly with propane- or butanesultone, the product has a very poor solubility and low conductivity (10<sup>-9</sup> S/cm) at room temperature. Usually the doping degree for the SPAN is assigned as the S/N ratio and all of these earlier methods resulted in the

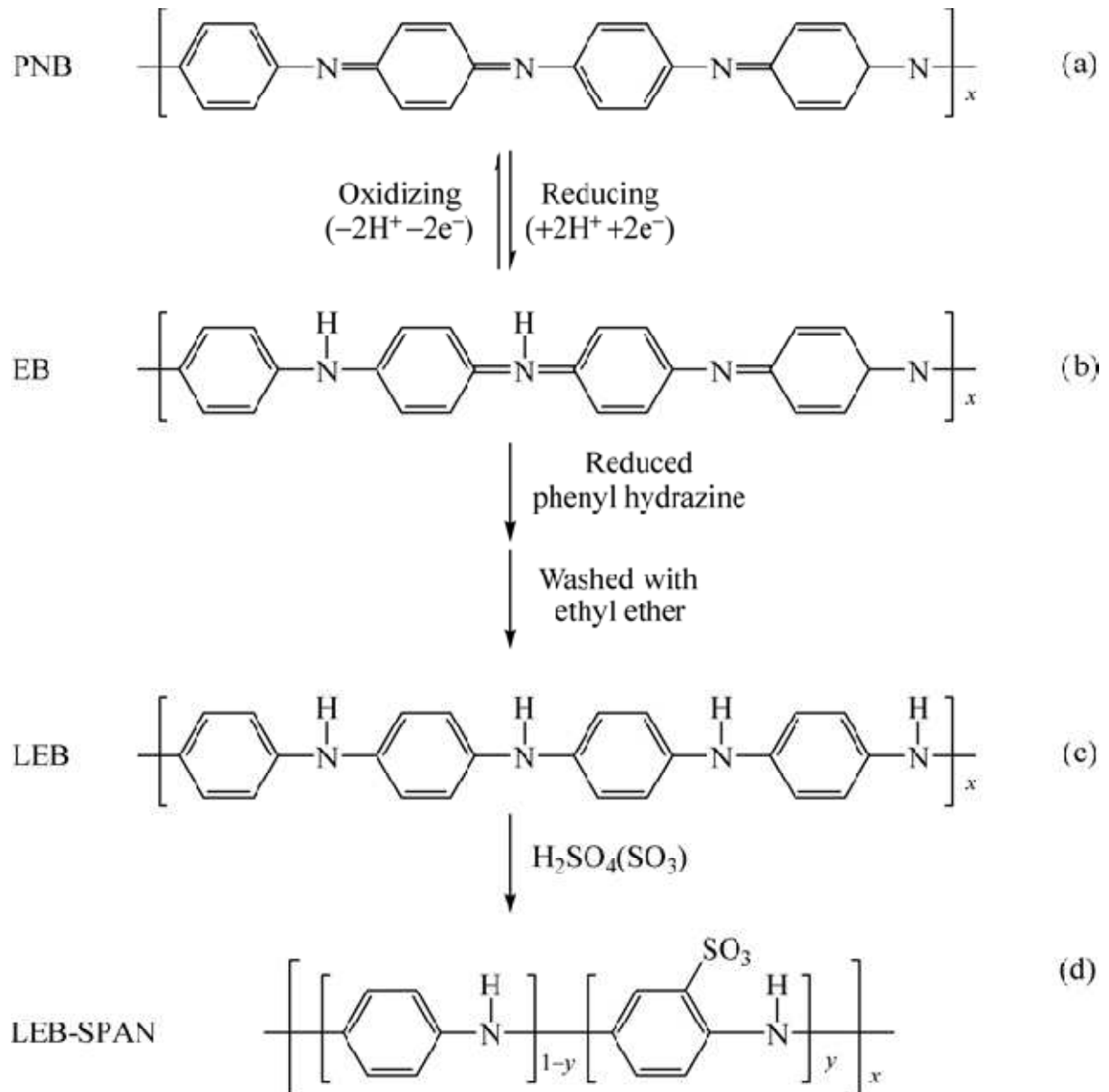


**Figure 1.10 Molecular structure of SPAN**

S/N ratio of 0.5 [85,87]. However, Epstein et al. [79] reported an S/N ratio as high as 0.75 could be synthesized by using the full reduced LEB as the starting material, which final product is termed LEB-SPAN. Bergeron et al. [88] have also synthesized a water-soluble PANI by reaction of LEB with propanesulfonic. The S/N ratio is a key to control the physical properties of the self-doped SPAN.

The conductivity of SPAN with S/N ratio of 0.5 is about  $10^{-1}$  S/cm, for instance, the conductivity of LEB-SPAN (S/N ratio of 0.75) is enhanced by one order of magnitude to be about 1.0 S/cm [79]. Moreover, the conductivity of LEB-SPAN is unaffected by pH over the

range  $0 < \text{pH} < 14$  whereas EB-SPAN becomes insulating at  $\text{pH} > 3$  and  $\text{pH} > 7.5$ , respectively [79]. In addition, the thermal stability of SPAN is better than PANI doped with HCl [89].

### 1.2.4(f<sub>3</sub>): Water soluble PANI

Water soluble PANI is of interesting because of its low cost and environmental friendly. It is noted that the above-mentioned SPAN is only soluble in aqueous alkaline solution ( $\text{NH}_4\text{OH}$ ) and NaOH rather than in pure water. To obtain an aqueous solution of SPAN, it is therefore necessary to follow the treatment with an  $\text{H}^+$  type ion-exchange resin [90]. Thus, an efficient approach toward water soluble conductive PANI is substituted aniline co-monomer to produce copolymers [91].

The copolymers are advantageous of the electrical conductivity and solubility of the copolymer being varied by adjustment of the monomer ratio in the copolymer.

For instance to polymerize protonic-acid moiety containing aniline derivatives, such as amino benzyl phosphoric acid to give poly (o-amino benzyl phosphoric acid) (PABPA) [92] or to copolymerize aniline with similar monomers, such as N-(4-sulfophenyl) aniline and o-anthranilic acid to yield poly (aniline-co-N-(4-sulfophenyl) aniline) (PASPA) [93], and poly(aniline-co-o-anthranilic acid) (PAAA) [94] have been reported. However, the above two copolymers are also partially soluble in water, while the homo-polymer PABPA is only soluble in alkaline aqueous solution. Therefore, a new water-soluble self-doped PANI has been proposed by grafting PANI onto a water-soluble polymer having pendant aniline dimers and sulfonic acid groups to obtain poly(aniline-co-2-acrylamido-2-methyl-1-propanesulfonic acid) (PAMPANI) [95]. Bhavana et al. [96] also reported a novel approach to the creation of a substituted PANI can be controlled via complication between boronic acid groups along the backbone with D-fructose in the presence of fluoride. Nguyen et al. [93] also report copolymers of poly (N-(4-sulfophenyl) aniline) and the poly-(aniline-co-N-(4-sulfophenyl)) aniline.

They found that their conductivities are range between  $3.5 \times 10^{-4}$  S/cm and 5.2 S/cm for homo-polymer of poly (N-(4-sulfophenyl)aniline) and PANI, respectively. Although the conductivity of homo-polymer poly (N-(4-sulfophenyl) aniline) is  $10^3$  times less conductive than PANI, it is still  $10^6$  times more conductive than other PANI polymers with

sulfonated groups. These copolymers are soluble in aqueous  $\text{NH}_4\text{OH}$ , but not in aqueous  $\text{HCl}$  solutions. In addition, poly (aniline-co-N-propanesulfonic acid aniline) (PAPSAH) with a conductivity of  $10^{-2}$  S/cm without external doping could be cast into free-standing film directly from

its aqueous solution [97]. Chan et al. [98] also reported a novel conducting PANI synthesized by persulfate oxidative coupling of o-minobenzyl phosphonic acid in an acidic medium. The resultant PANI is water-soluble in its conducting form.

However, it does not exhibit any conductivity dependence on pH below 6, in marked contrast to the  $\text{HCl}$ -doped PANI. The lower conductivity ( $10^{-3}$  S/cm) obtained is attributed to the decrease in conjugation resulted from a large steric effect of the bulky  $\text{PO}_3\text{H}_2$  and a significant hydrogen bond interaction between  $\text{PO}_2(\text{OH})$  and  $\text{NH}^+$  [98]. In addition, water-soluble copolymers of poly-(aniline-co- N-(4-sulfophenyl) aniline (PAPSA) was synthesized directly from aniline and sodium diphenylamine-4-sulfonate salt by a chemical polymerization [93].

The monomer composition of the copolymers (PAPSA) can be controlled by varying the molar ratio of the monomers in the reaction mixture. The copolymers have a monotonic variation in their molecular weight, solubility in aqueous  $\text{NH}_4\text{OH}$ , and electrical conductivity with the monomer composition. Besides, Liu et al. [99] reported oxidizing aniline in the presence of aniline-formaldehyde condensates (AFC) through a cation radical mechanism to synthesize conductive PANI/AFC copolymer with high molecular weight and solubility. AFC acts as a terminating agent in the polymerization process and by terminating many PANI chains, resulting in branchlike structural copolymers. The conductivity ( $\sim 10$  S/cm), average molecular weight ( $\sim$  of  $10^6$ ), and solubility of the copolymer are controlled by the ratio of AFC to aniline monomer prior to chemical polymerization [99].

As above-mentioned, grafted polymer is one way to produce soluble conducting polymers. Poly (ethylene glycol) (PEG) has many unique physical and biochemical properties, such as non-toxicity, biocompatibility, and miscibility with many solvents [100]. These unique properties lead to their promising application in biomedical and industrial applications [101]. Wang et al. [102] reported that PEG-grafted PANI copolymers were

prepared by incorporating a chlorine end-capped methoxy PEG (mPEGCl) onto the LEB form of PANI via N-alkylation. The graft concentration (degree of N-alkylation) can be controlled by adjusting the molar feed ratio of mPEGCl to the number of repeat units of PANI. The mPEG-g-PANI copolymers enhanced solubility in common organic solvents and water [102]. In addition, the enzyme horseradish peroxidase (HRP) has been also extensively used for the oxidative polymerization of phenols and anilines in the presence of hydrogen peroxide [103].

Aniline monomers containing hydrophilic substituent [104] or photodynamic azobenzene groups [105], and HRP-catalyzed polymerization of aniline [106] have been polymerized to yield a wide range of soluble PANI. In these cases, the polyelectrolyte provides a preferential local environment for coupling of the monomer, the counter-ions for doping the PANI, and imparting water solubility. Recently, Roy et al. [107] reported that the biomimetic polymerization of aniline in the presence of lignosulfonate (LGS) to yield a conducting, water-soluble PANI, where LGS was used as either dopant or polymeric template. The LGS-PANI complex provided a unique combination of properties for the PANI including electrical conductivity, processability, corrosion protection, and biodegradability [108].

### **1.2.5: Processability**

Most applications for electronic devices of conducting polymers, such as transistors [109], and light-emitting diodes (LEDs) [110], require in the formation of thin film or patterned conducting polymers with feature sizes less than 100 nm. Soluble PANI is easy to prepare its thin film by spinning coating. Besides, various other approaches, such as photolithographic techniques based on photo-induced doping/de-doping [111], photochemical reaction [112], chemical implication [113] and non-photolithographic methods [114], ink-jet [115], screen printing [116] and electrochemical dip-pen nanolithography [117] have been used to prepare thin film of conducting polymers. Some typical methods to prepare thin films or patterns of PANI are briefly introduced as follows:



### 1.2.5(a): Adsorption Polymerization

In 1989, MacDiarmid et al. [118] actually noted that “PANI may also be deposited by *in-situ* adsorption polymerization as strongly adhering films on a variety of substrates”. This indicated that PANI film coated on any substrate can be prepared by placing a substrate into reaction solution, indicating it is the simplest approach to prepare PANI films. Based on above concept, aniline oligomers anchored on the surface stimulate the growth of PANI chains in a perpendicular direction to the support has been reported [119, 120]. Similar concepts have been also suggested for electrochemically produced films [121]. The growth of the films prepared by this method undergone three processes [122]:

The oxidation of aniline in an acidic aqueous medium at the initial state of polymerization produces aniline oligomers. Those oligomers have a tendency to separate from the aqueous medium by adsorbing themselves at available surfaces in contact with aqueous reaction mixture because of their hydrophobic than the original anilinium cations.

The adsorbed oligomers on the surface of substrate have a higher reactivity toward initiating the growth of PANI chains followed by growth of PANI film along the substrate via an auto-accelerating polymerization.

### 1.2.5(b): Layer-By-Layer

A layer-by-layer is a common and controlling self-assembly technique to prepare thin and oriented films through anion/cation or electrostatic and hydrogen bonding interactions. The method is advantageous of simple in procedure, easy to control and friendly to environment [123]. The method also introduced into fabrication of PANI fibers and films since 1990s, but ionic self-assembled films are not stable in the high ionic strength of the electrolyte solution because they can be easily scaled off [124]. It therefore is a challenge for chemistry to fabricate a much more stable the assembled PANI film. Chen et al. [125] proposed a novel way to fabricate covalently attached multilayer films by the ionic or hydrogenbonding self-assembly technique associated with the photoreaction. By using this method, ultra-thin film is fabricated with diazoresin as poly-cation and SPAN as poly-anion via self-assembly electrostatic process. And then the resulting films are exposed under UV irradiation to undergo photoreaction between diazonium and sulfonate, and finally convert the ionic bonds between the layers into covalent [125]. Interestingly, the covalent attached

films are very stable toward polar solvents and high ionic strength of the electrolyte solution [126]. In addition, PANI can be self-assembled with a number of different nonionic, water-soluble polymers, such as poly (vinylpyrrolidone), poly (vinyl alcohol), poly (acrylamide) and poly (ethylene oxide) [127]. Each of these polymers contains functional groups that are capable of forming hydrogen bonds with PANI. The ability to fabricate multilayer thin films and thin film hetero-structures containing non-ionic polymers opens up new possibilities for self-assembled films of conjugated polymers. Since poly (ethylene oxide) (PEO) is an ion-conducting polymer, for instance, it is possible to create multilayer thin films that are both electronically and ionically conductive. These films may be of use in thin film devices that are based on electrochemical processes such as the light-emitting devices [128]. Stockton et al. [129] demonstrated that hydrogen-bonding interactions can be used to assemble multilayer thin films of PANI by a layer-by-layer manner. The multi-layers prepared by a layer-by-layer through hydrogen bonding interactions are more thickness than that of films made by electrostatic interaction due to the tendency of the hydrogen-bonding polymers to adsorb with a high segmental density of loops and tails [129]. The PANI films formed via hydrogen-bonding self-assembly also exhibit conductivities about one order of magnitude larger than that of films assembled via electrostatic interactions [129].

### **1.2.5(c): Photolithography Technique Associated with Photo-Acid Generation Processes**

PANI can be doped by photon-acid generators due to proton released under light irradiation. It has been showed that the PANI modified with a thermo-labile and acid-labile *tert*-butoxycarbonyl (t-BOC) group is highly soluble and thermodynamically stable in low-boiling solvents (e.g. THF, dioxane, and  $\text{CHCl}_3$ ) and which is converted to the insoluble and electrically conductive emeraldine salts upon photodoping with photo-acid generators (e.g. *N*-(tosyloxy)- or (camphorsulfonyloxy) norborneneimide or -onium salts [130a].

As a result of this solubility difference, conducting patterns of high resolution were produced by conventional photolithography process. Upon removal of the t-BOC groups in PANI

(t-BOC) by acid doping, no obvious morphology change of the films was observed, and such conversion recovered the original conductivity level of the doped PANI [174b]. Since the

t-BOC protecting groups are easily removed in doping or acid-catalyzed reaction by chemical amplification or thermal bake, the PANI (t-BOC) can be used as conductive matrix polymers for negative type photo-imaging or printing materials or for novel solution-processed applications in various microelectronic devices [130b].

In summary, PANI still holds important position in the field of conducting polymers at the present time because of its unique properties such as easy and low-cost synthesis, high conductivity and stable in air as well as physical and electrochemical properties controlled by both oxidation and protonation state, leading to potential applications in technology. However, large-mass synthesis, high solubility in organic or water and high stability of physical properties of PANI are still required to realize its commercial applications.

### **1.3: Present And Future Potential Application**

Potential applications for conducting polymers are numerous, since metals are toxic and can damage the environment. Below are some potential applications for conducting polymers.

#### **1.3.1: Corrosion Protection**

The recent methods of corrosion protection are not very lasting and are coming under increased scrutiny by the Environmental Protection Agency (EPA). As an example, the use of chromium and cadmium for anti-corrosion will soon be banned. A mechanism for corrosion protection involves the use of a sacrificial electrode, such as zinc coating, which will corrode (oxidize) in safekeeping the substrate. Unfortunately, the coatings do not last very long. The oxidized zinc metal is dissolved by water or moisture. For this reason, there are extreme environmental concerns, since toxic metals are being released into the ecosystem. Barrier coatings, such as epoxy, are employed extensively but are not very durable once a pit or hole in the coating has been formed. The corrosive species then attacks the underlying metal and thereby increases the exposed surface, accelerating the corrosion process.

MacDiarmid first suggested the corrosion inhibiting-property of conducting polymers in 1985. Initial studies on the protection of metal surfaces against corrosion by conducting polymers were reported in the literature that same year. A major type of corrosion occurs by oxidation of a metallic surface by a water medium to produce oxides and hydroxides. As these are formed, soluble species are produced, the surface pits increase their surface area, and the rate of decomposition accelerates.

One way to provide corrosion protection is to coat the metal with a barrier to prevent the reactive species from reaching the surface. Galvanization with zinc (or other metals with low oxidation potential) prevents corrosion via the creation of an interfacial potential at the metal-zinc interface. The zinc will corrode preferentially. While the reactive species may encounter the metal, the increased oxidation causes the metal to be insensitive. Corrosion is therefore inhibited.

### **1.3.2: Sensors and Electromechanical Devices**

Since conducting polymers change properties by incorporation of ions and solvents (the property change easiest to measure is conductivity), it is possible to develop and market ion-specific sensors based upon conducting polymers. Conducting polymers could permit the incorporation of sensors into clothing. There are some challenges involved, such as background noise due to water absorption, lifetime, selectivity, and sensitivity. Conducting polymers also change volume depending on their oxidation state. It is therefore possible for conducting polymers to convert electrical energy into mechanical work. Conducting polymers actuators were proposed by Baughmann et al [131].

An oxidation-induced strain of polyaniline and polypyrrole-based actuators has been reported, and the first 'self-contained' actuators were reported by MacDiarmid. There are many interesting possibilities for conducting polymer actuators, but a great deal of work needs to be done.

This field is the first area where conducting polymers promises to have a big commercial impact. The general design for a battery is shown in Figure 1.11. Batteries have several key components: the electrodes allow for collection of current and transmission of power; the cathode material becomes reduced when the anode material is oxidized and vice versa; the

electrolyte provides a physical separation between the cathode and the anode, and provides a source of cations and anions to balance the redox reactions. Aside from picking the best conducting polymer available, there are many other issues, not related to conducting polymers, that affect battery performance, such as electrolyte stability and stability of the counter half-cell reaction (which is at least as important as the conducting polymer electrode), and compatibility between the electrolyte and the materials

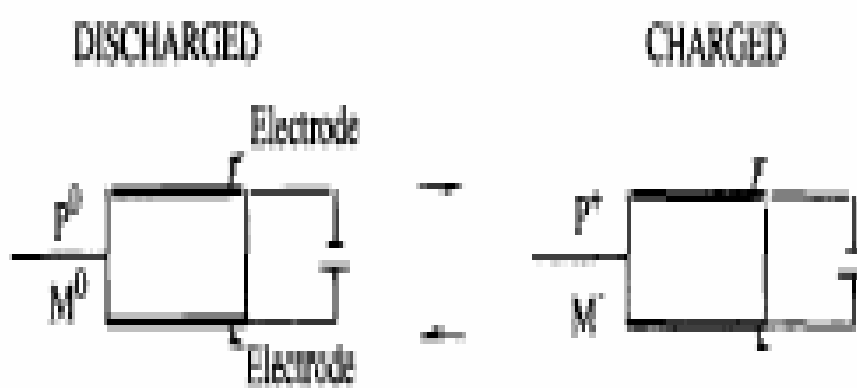


**Figure 1.11 General battery design**

There was a great deal of initial excitement about conducting polymers as active materials in batteries. Owing to their low density, it was thought that battery with power densities much higher than those of the ordinary lead/acid battery could be readily obtained. Since the charge on a polymer backbone is distributed over three or four repeat units, the charge capacity per unit of mass for conducting polymers is marginally better than that of metals. Conducting polymer batteries were investigated by BASF/VARTA and Allied Signal. Bridgestone has marketed a button-sized battery using polyaniline and lithium.

Conducting polymer still has a potential use in lithium-based high-power density batteries, which use the high potential difference between lithium and the polymer to achieve high power densities, although stability and shelf life are still issues. As more and more

individuals utilize cellular phones, laptop computers, and cordless drills, the importance of batteries that will handle many deep cycles (at least 60% depth of discharge) becomes increasingly apparent. Conducting polymer-based batteries show promise, but much work needs to be done.

### 1.3.3: Electrochromic cell

These cells are used to go from opaque to transmissive at selected regions of the electromagnetic spectrum. Batteries and electrochromic cells have many common critical issues for commercial viability. They require cathodic and anodic reactions to be almost perfectly balanced (cyclic voltammetry is a good comparison tool for materials). The operation of an electrochromic cell is shown in Figure 1.12.

The electrochromic window is similar to a battery with some additional requirements: at least one of the electrodes must be transparent to the given electromagnetic spectrum; the cathode material (which colors upon being oxidized) must be electrochemically reversible; the ion-conducting electrolyte must not only provide physical separation between cathode and anode, a source of cations and anions to balance redox reactions, but must also be transparent to the given region of the spectrum; and the anode material (which colors upon being reduced) must also be electrochemically reversible.

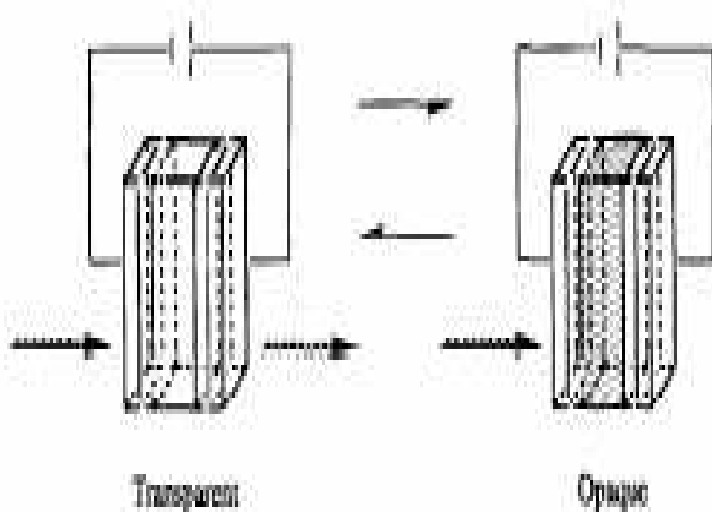


**Figure 1.12 Electrochromic window**

The ion-conducting electrolyte in electrochromic cells is usually an inorganic salt dissolved in a solvent such as propylene carbonate with a polymer such as poly-(methyl methacrylate) added as a stiffener. The ion-conducting electrolyte acts as a source and sink for the ions as the various redox processes take place and maintains ionic contact between the materials. Conducting polymers also have an application in electrochromic cells, attenuating various regions of the electromagnetic spectrum.

Aside from the batteries issues mentioned in the previous section, electrochromic cells have some additional requirements. Although thinner layers (for optical window) are usually sufficient, retention of extinction coefficient and contrast ratios are critical. Many electrochromic cells need to last more than 10,000 cycles, and have switching times of a few minutes. In this case, spectroelectrochemistry is a good evaluation tool for conducting-polymer materials.

Spectroelectrochemistry measures both the electrical and the optical response of the material in question. Again, it must be emphasized that this method is not suitable for devices; spectroelectrochemistry is usually performed in a great excess of electrolyte and, therefore, the counter half-cell reactions are often ill defined.

There is a great deal of data that indicates that conducting polymers are good candidates for materials in electrochromic cells. In particular, polythiophene, polypyrrole and polyaniline have been cycled more than ten thousand times. This data, although good for evaluating differences between polymers, may not accurately reflect the performance of conducting polymers in a sealed, self-contained device. This is because the counter half-cell reaction and those devices often require 'deep cycle' i.e. near complete oxidation/reduction. The device usually starts to degrade at ten to one hundred times fewer cycles than conducting polymers studied by cyclic voltammetry. This does not necessarily mean that polymer is degrading, as either the counter half-cell reaction or the limited amount of electrolyte may control the lifetime of the device.

Furthermore, cyclic voltammetry measures the retention of charge capacity in a polymer film and not the electrochromic contrast ratio. However, whereas a 20% drop in charge capacity might be acceptable in a battery, a 20% decrease in a contrast ratio for

electrochromic cells may be unacceptable. In devices that are based upon retention of surface conductivity, it appears that conductivity is lost long before a significant amount of charge capacity decreases. The evaluation of conducting polymer for battery and electrochromic application should be similar to the actual condition (depth of discharge, cycle time, and transmission of extinction ratio).

### 1.3.4: Controlled-released Application

Another application for conducting polymers is controlled-released devices. Ions can be selectively released, as well as biologically active ions such as adenosine 5'-triphosphate (ATP) and Heparin.

A conducting polymer with a given oxidation potential is electrodeposited onto a substrate with a mobile counter ion. Another polymer layer (polymer B with a higher oxidation potential than polymer A) is electrodeposited (directly on top of polymer A) using an immobile counter ion (polyanion). During complete reduction (a), it is almost impossible for the polymeric anion (Y-) to move into the electrolyte solution and, therefore, cations (M+) from the solution must move into the outer polymer layer, but the mobile anions (X-) from the inner layer move into the electrolyte.

During selective oxidation of polymer A (b), the mobile anions (X-) move from the solution to the inner layer. During oxidation of polymer B (c), the cations (M+) move back into solution. This potential-dependent ion transport is an interesting way to deliver ionic drugs to certain biological systems. Anions can be exclusively delivered by cycling back and forth through step (b), cations can be exclusively delivered by cycling back and forth through step (c), or anions can be delivered and cations can be received by cycling through step (a). Figure 1.13. shows a general schematic diagram showing a selective ion transport of an electroactive bilayer.



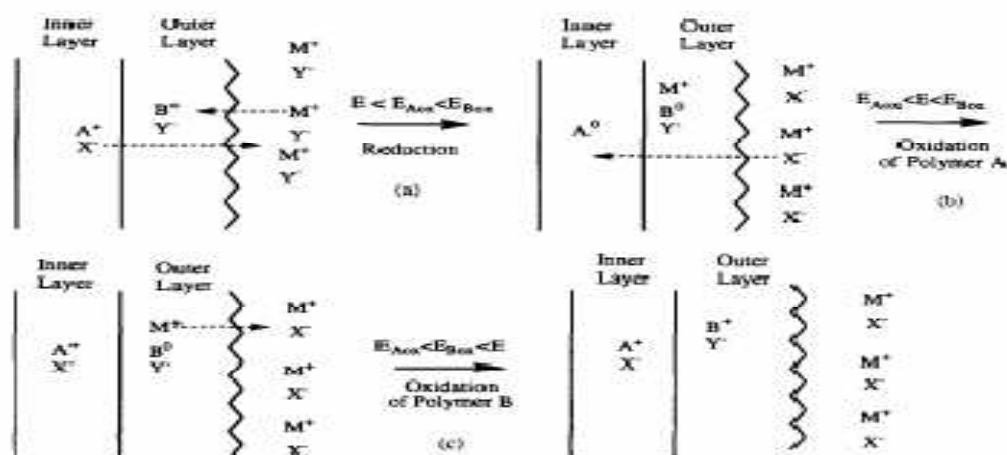


**Figure 1.13. Selective ion transport of an electroactive bilayer**

It is very important for the inner polymer layer to have a lower oxidation potential than the outer layer. If this is not in the case, the inner layer, which is connected to the electrode, will act as an electrical insulator and prevent the oxidation of the outer layer. Once the oxidation potential of the inner layer is reached, a pulse charge will occur, making selective ion transport difficult (rectification). Furthermore, a biologically compatible counter-half cell is necessary for a practical device. This might not present too much of a problem if the drug delivery system is used only once. If repeated uses of the same device are necessary, then issues such as reversibility (like those of batteries and electrochromics) will need to be resolved.

### 1.3.5: Radar Application

Radio Direction and Ranging (RADAR) uses electromagnetic waves that bounce off a particular target and are collected by a receiver, which analyzes the signal and determines the range, direction, and speed of the object in question. Reflections occur whenever there is a sharp impedance difference between the medium (usually air) and the object. Impedance differences are most notable between metals and air. Metals tend to re-radiate (reflect) the incoming signal. Conducting-polymer camouflage works a little differently, in that it reflects back in a way that it has more continuously variable impedance.

A conducting polymer textile used for camouflage has no sharp edges or wings and tends to appear indistinguishable from the surrounding hills and trees and absorbs more than 50% of

incident microwave radiation. Microwave (100 MHz to 12 GHz) properties of conducting polymers have been studied, as have the millimeter wave (24 –40 GHz) properties of polypyrrole-coated fibers. Conducting polymers as radar absorbers in antennas, Salisbury screens, camouflage, and other types of shielding are of interest to the military.

### 1.3.6: LEDs

A significant event occurred when Friend et al [132] published an electroluminescence study on the neutral (non-conducting) form of para-phenylene vinylene. This work has opened up a new avenue of research and, more importantly, a potential market for the material.

A general design for LEDs is shown in Fig. 1.14. The electron injecting electrode is usually a low work function (easily oxidized), metal and the hole-injection electrode is a high work function metal, or indium tin oxide, or a conducting polymer with an oxidation potential higher than that of the active layer. Some general trends have been observed: as a lower work function metal (less stable because it is easily oxidized) is used, the efficiency increases but the lifetime decreases. Studies have been reported in which a layer of neutral conjugated polymer, with a reduction potential closer to zero than that of the active conducting-polymer layer, increases efficiency.

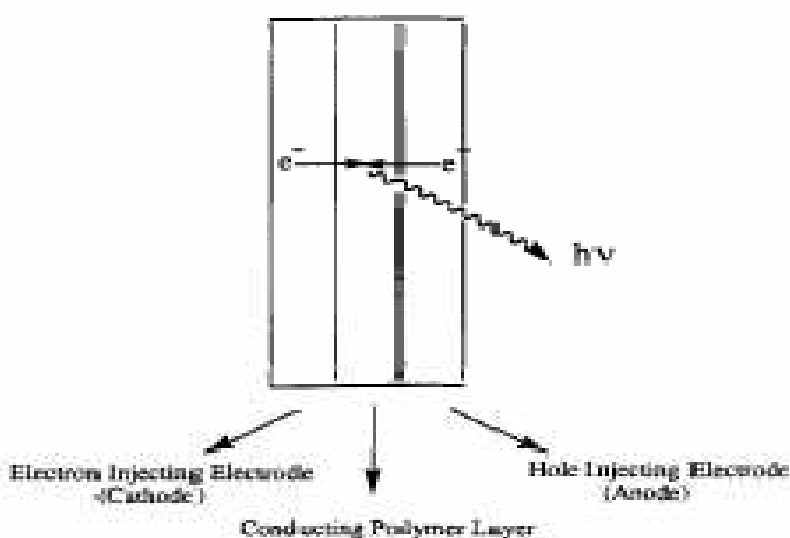


**Figure 1.14** General design for LEDs

A simplistic overview of the function of an LED is as follows: an electron is injected into the polymer from the cathode while a hole is injected from the anode; there is an oxidized polymer on one side of the polymer film and a reduced polymer on the other side. The hole and the electron then migrate towards the center of the film and, when they meet each other, they recombine and give off light. The frequency of the light emitted is roughly equal to the difference between the oxidation and the reduction potential of the polymer (the electrochemical band gap) and, therefore, is related to the electronic band gap.

Polymers with a different band gap have distinct values for the difference between oxidation and reduction potential, and emit different wavelength of light. Several articles on conducting polymer LEDs and the effect of various additives, electrode modifications, tuning emission, the effect of impurities, and discussions of hole tunneling, photo excitation, and unusual symmetric bias, have been published. The efficiency of LEDs is constantly being improved along with novel developments such as flexible LEDs, polarized light-emitting LEDs and light emitting electrochemical cells. The emission of red, green, blue and white light have all been demonstrated, and so has brightness of the order of 400 cdm-1, which is similar in brightness to fluorescent lights or computer displays.

A challenge in the operation of LEDs is the fact that it appears that the mobility of the hole is higher than the mobility of the electron. The barrier height (like a resistance) between the polymer and each of the electrodes must be low and roughly equal, so that the hole and the electron recombine near the center of the conducting-polymer layer, to ensure good operation. Another limit is the competition between radiative and non-radiative decay that, for PPV-type systems, is around 25%, which does not limit device performance at this juncture. Yet another challenge is the fact that the polymers that initially perform well in LEDs contain electron-rich double bonds. These double bonds are fairly easy to oxidize and are most likely one of the major causes for device degradation.

The efficiency, lifetime and brightness depend upon a variety of factors. One major challenge is balancing the electron mobility to that of the hole of mobility. This is done by adding electron transport layers and hole transport layers such as tri substituted amines. These layers reduce the barrier height and encourage the holes and electrons to combine near the center of the film.

Electron and hole transport layers could permit the use of more stable metals without compromising efficiency. Conducting polymers enable a wide variety of structures to be synthesized and therefore many different wavelengths of light are possible. Although conducting polymers will not replace fluorescent light bulbs (which have efficiencies of around 70%), because conducting polymer LEDs are easily patterned, operate at low DC voltages, and have uniform areas of light, there is a potential market for low level backlighting and alphanumeric displays

### **1.3.7: Conducting Polymers for EMI/ESD Shielding**

Shielding of electromagnetic radiation is a more demanding task, placing more stringent conditions on the range of conductivities required. Shielding at low frequencies, requiring metallic levels of conductivity, is not easily met by any of the conducting polymers, but there are applications where conductivity levels may be appropriate. One of these lies in the absorption of microwave radiation to prevent radar detection of sensitive equipment, and polyaniline in its various forms has been extensively investigated in this regard.

Electric cables of various types also offer markets for conductive polymers. Carbon loaded polymers are currently used to provide a field-smoothing layer between the insulating layer and the outer conducting braid in very high tension power cables. The role of this conductive layer is to prevent field inhomogeneities at the insulator layer which might produce corona discharge into the dielectric layer. Several companies have shown interest in the possible use of polyaniline in this role, although the ambient conditions are demanding (operating temperatures up to 100°C) and the reliability requirement stringent (up to 100 years average working life for buried high tension power cables). Another area of application is one in which the conductive polymer is again in contact with the outer metal braid, in a coaxial cable. This can give improved very high frequency shielding, which would become increasingly ineffective at frequencies high enough to allow field leakage through the metal braid.

### **1.3.8: Conducting polymer coated Fabrics for EMI Shielding**

Conducting polymer-coated fabrics can be effectively used for the shielding of electromagnetic waves in the microwave range, W-band, RFI range as well as in UV Vis-

NIR range. In the radio frequency range from 100 MHz to 1 GHz, conducting polyaniline coated fabrics shows a shielding effectiveness in the range of 30-40 dB. Shielding effectiveness of the conducting fabrics in W-band region at 101 GHz shows an attenuation of 35.61 dB.

### **1.4: FLYASH**

Of total power generated in india, about 70% is produced by thermal power plant(TPPs),majorities of TPPs(84%)are run by coal and rest on gas(13%)and oil(3%).About 260 million tonns(MT) of coal (65%) of annual coal production in india is being used by TPPs .Presently about 112 MT of flyash is being generated by TPPs as by product of coal combustion Flyash quality depend on coal, coal particle fineness,percentage of ash in coal,combustion technique used,air/fuel ratio ,burner used and types of boiler.

#### **1.4.1: Composition and Property of Flyash**

Fly ash, a coal combustion residue (CCR) is a complex heterogeneous material. Although, in the strictest sense, fly ash is the finest CCR (0.2–90 Am) formed due to the transformation of mineral matter present in coal particles during combustion [133], it has become a misnomer, particularly in respect of fly ash generated at Thermal Power Plants (TPPs) in India. Because of the poor combustion efficiency of the combustors, lack of proper quality control in maintaining the particle size of the pulverised coal feed etc, the fly ash has a wide distribution of char, semi-coke or coked carbon matters of large dimension (90–300 Am). It is irregularly shaped, containing lacy, vesicular, alumino-siliceous matter of complex composition and fine solid/hollow alumino-siliceous spheres. The chemical composition of fly ash varies depending upon the type of coal used in combustion, combustion conditions and removal efficiency of air pollution control device [134,135]. The lignite and sub-bituminous coals on combustion produce Class C fly ash, while anthracite and bituminous coal under similar process generate Class F fly ash. The sum of  $\text{SiO}_2$ ,  $\text{Al}_2\text{O}_3$  and  $\text{Fe}_2\text{O}_3$  content in fly ash should be greater than 70% for Class F fly ash, whereas the CaO content should be less than 5% [136]. The Class C fly ash is classified as [8] those fly ashes having less than 50% of  $\text{SiO}_2$ ,  $\text{Al}_2\text{O}_3$  and  $\text{Fe}_2\text{O}_3$  combined. The CaO content varies from 20% to 30% for such fly ash.

However, the composition of fly ash may vary to some extent depending upon whether the same is of low/high calcium or low /high iron fly ashes [137]. Class C and Class F fly ashes have significant differences in their properties. Consequently, their utilisation schemes are also different [138]. The mineralogical composition of fly ash is largely dependent upon the geological features related to formation and deposition of coal [139,140], the combustion condition, etc. [141]. The most common and predominant phases are quartz, mullite, hematite, magnetite and lime apart from other minor constituents [142,143]. It also depends upon the type of the coal used. Thus, lignite fly ash has predominantly quartz, anorthite, gehlenite, hematite and mullite as major crystalline phases [144-146]. The low calcium fly ashes contain quartz and mullite as the major crystalline phases, whereas the high calcium fly ashes consist of quartzite, C3A and [140]. Indian fly ashes mostly consist of quartz, mullite, magnetite, hematite, faylite and glass [147].

The morphology of fly ash is an important aspect that requires thorough evaluation. Based on examination using light microscopy, fly ash particles can be classified into eleven morphologic classes [148]. Amongst the carbonaceous particles present in fly ash the most important one is Fchar\_ which is formed due to devolatilisation of the coal particles. Subsequent char burning and intrinsic mineral matter transformation leads to the formation of ash particles [133], which may be in the form of irregular particles, solid and hollow spherical particles. Amongst these, the most important and value added particles are cenospheres, plerospheres and ferrospheres [134,147,149-155].

Fly ash is collected in electrostatic precipitators or baghouses, then transferred to large silos for shipment. When needed, fly ash is classified by precise particle size requirements, thus assuring a uniform, quality product Class F fly ash is available in the largest quantities. Class F is generally low in lime, usually under 15 percent, and contains a greater combination of silica, alumina and iron (greater than 70 percent) than Class C fly ash. Class C fly ash normally comes from coals which may produce an ash with higher lime content — generally more than 15 percent often as high as 30 percent. Elevated CaO may give Class C unique self-hardening characteristics.

Although both types of fly ash impart a wide range of qualities to many types of concrete, they differ chiefly in the following ways:

### Class F

1. Most effectively moderates heat gain during concrete curing and is therefore considered an ideal cementitious material in mass concrete and high strength mixes. For the same reason, Class F is the solution to a wide range of summer concreting problems.
2. Provides sulfide and sulfate resistance equal or superior to Type V cement. Class F is often recommended for use where concrete may be exposed to sulfate ions in soil and ground water.

### Class C

1. Most useful in “performance” mixes, prestressed applications, and other situations where higher early strengths are important.
2. Especially useful in soil stabilization since Class C may not require the addition of lime

Engineering properties of Fly Ash	
Parameter	
Specific gravity	1.90-2.55
Plasticity	Non Plastic
Proctor compaction - Maximum dry density (gm/cc)	0.90-1.60
Optimum moisture content (%)	38.0-18.0
Angle of internal friction ( O)	30 <sup>0</sup> -40 <sup>0</sup>
Cohesion (kg/cm <sup>2</sup> )	Negligible
Compression index	0.05-0.4
Permeability (CM/SEC)	10 <sup>5</sup> -10 <sup>3</sup>
Particle size distribution	
Clay size fraction (%)	1-10
Silt size fraction (%)	8-85
Sand size fraction (%)	7-90
Gravel size fraction (%)	0-10
Coefficient of uniformity	3.1-10.7

## **Table 1.2 Engineering properties of FlyAsh**

### **1.4.2: Application of Fly Ash**

Fly ash can be used for construction of road and embankment.

Fly ash can be used in portland cement concrete to enhance the performance of the concrete.

Large scale use of ash as a fill material can be applied where Fly ash replaces another material and is therefore in direct competition with that material. Fly ash itself is used by the power generating company producing the fly ash to improve the economics of the overall disposal of surplus fly ash.

### **1.5: Corrosion Study:**

#### **1.5.1: Electrochemical Basis of Corrosion**

Most metal corrosion occurs via electrochemical reactions at the interface between the metal and an electrolyte solution. A thin film of moisture on a metal surface forms the electrolyte for atmospheric corrosion. Wet concrete is the electrolyte for reinforcing rod corrosion in bridges. Although most corrosion takes place in water, corrosion in non-aqueous systems is not unknown.

Corrosion normally occurs at a rate determined by equilibrium between opposing electrochemical reactions. The first is the anodic reaction, in which a metal is oxidized, releasing electrons into the metal. The other is the cathodic reaction, in which a solution species (often  $O_2$  or  $H^+$ ) is reduced, removing electrons from the metal. When these two reactions are in equilibrium, the flow of electrons from each reaction is balanced, and no net electron flow (electrical current) occurs. The two reactions can take place on one metal or on two dissimilar metals (or metal sites) that are electrically connected.

Figure 1.15 diagrams this process. The vertical axis is potential and the horizontal axis is the logarithm of absolute current. The theoretical current for the anodic and cathodic reactions are shown as straight lines. The curved line is the total current -- the sum of the anodic and cathodic currents. This is the current that you measure when you sweep the potential of the metal with your potentiostat. The sharp point in the curve is actually the



point where the current changes signs as the reaction changes from anodic to cathodic, or vice versa. The sharp point is due to the use of a logarithmic axis. The use of a log axis is necessary because of the wide range of current values that must be displayed during a corrosion experiment. Because of the phenomenon of passivity, it is not uncommon for the current to change by six orders of magnitude during a corrosion experiment.

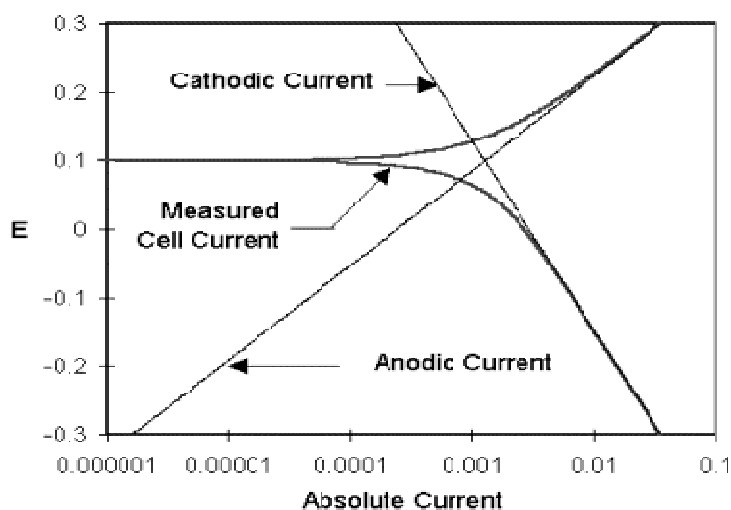


**Figure 1.15 Showing Anodic and Cathodic Current Components.**

The potential of the metal is the means by which the anodic and cathodic reactions are kept in balance. Refer to Figure 1.15. Notice that the current from each half reaction depends on the electrochemical potential of the metal. Suppose the anodic reaction releases too many electrons into the metal. Excess electrons shift the potential of the metal more negative, which slows the anodic reaction and speeds up the cathodic reaction. This counteracts the initial perturbation of the system.

The equilibrium potential assumed by the metal in the absence of electrical connections to the metal is called the Open Circuit Potential,  $E_{oc}$ . In most electrochemical corrosion experiments, the first step is the measurement of  $E_{oc}$ . The terms  $E_{oc}$  (Open Circuit Potential) and  $E_{corr}$  (Corrosion Potential) are usually interchangeable, but  $E_{oc}$  is preferred.

It is very important that the Corrosion Scientist measures the  $E_{oc}$  and allows sufficient time for the  $E_{oc}$  to stabilize before beginning the electrochemical experiment. A stable  $E_{oc}$  is

taken to indicate that the system being studied has reached "steady state", i.e., the various corrosion reactions have assumed a constant rate. Some corrosion reactions reach steady state in a few minutes, while others may need several hours. Regardless of the time required, a computer-controlled system can monitor the Eoc and begin the experiment after it has stabilized.

The value of either the anodic or cathodic current at Eoc is called the Corrosion Current,  $I_{corr}$ . If we could measure  $I_{corr}$ , we could use it to calculate the corrosion rate of the metal. Unfortunately,  $I_{corr}$  cannot be measured directly. However, it can be estimated using electrochemical techniques. In any real system,  $I_{corr}$  and Corrosion Rate are a function of many system variables including type of metal, solution composition, temperature, solution movement, metal history, and many others.

The above description of the corrosion process does not say anything about the state of the metal surface. In practice, many metals form an oxide layer on their surface as they corrode. If the oxide layer inhibits further corrosion, the metal is said to passivate. In some cases, local areas of the passive film break down allowing significant metal corrosion to occur in a small area. This phenomenon is called pitting corrosion or simply pitting.

Because corrosion occurs via electrochemical reactions, electrochemical techniques are ideal for the study of the corrosion processes. In electrochemical studies, a metal sample with a surface area of a few square centimetres is used to model the metal in a corroding system. The metal sample is immersed in a solution typical of the metal's environment in the system being studied. Additional electrodes are immersed in the solution, and all the electrodes are connected to a device called a potentiostat. A potentiostat allows you to change the potential of the metal sample in a controlled manner and measure the current that flows as a function of potential.

Both controlled potential (potentiostatic) and controlled current (galvanostatic) polarization is useful. When the polarization is done potentiostatically, current is measured, and when it is done galvanostatically, potential is measured. This discussion will concentrate on controlled potential methods, which are much more common than galvanostatic methods. With the exception of Open Circuit Potential vs. Time, Electrochemical Noise, Galvanic Corrosion, and a few others, potentiostatic mode is used to perturb the equilibrium corrosion process. When the potential of a metal sample in solution is forced

away from  $E_{oc}$ , it is referred to as polarizing the sample. The response (current) of the metal sample is measured as it is polarized. The response is used to develop a model of the sample's corrosion behaviour.

Suppose we use the potentiostat to force the potential to an anodic region (towards positive potentials from  $E_{oc}$ ). In Figure 17, we are moving towards the top of the graph. This will increase the rate of the anodic reaction (corrosion) and decrease the rate of the cathodic reaction. Since the anodic and cathodic reactions are no longer balanced, a net current will flow from the electronic circuit into the metal sample. The sign of this current is positive by convention. If we take the potential far enough from  $E_{oc}$ , the current from the cathodic reaction will be negligible, and the measured current will be a measure of the anodic reaction alone. In Figure 17, notice that the curves for the cell current and the anodic current lie on top of each other at very positive potentials. Conversely, at strongly negative potentials, cathodic current dominates the cell current.

In certain cases as we vary the potential, we will first passivate the metal, and then cause pitting corrosion to occur. With the astute use of a potentiostat, an experiment in which the current is measured versus potential or time may allow us to determine  $I_{corr}$  at  $E_{corr}$ , the tendency for passivation to occur, or the potential range over which pitting will occur.

Because of the range of corrosion phenomena that can be studied with electrochemistry, the ability to measure very low corrosion rates, and the speed with which these measurements can be conducted, an electrochemical corrosion measurement system has become a standard item in the modern corrosion laboratory.

### **1.5.2: Quantitative Corrosion Theory**

In the previous section we pointed out that  $I_{corr}$  cannot be measured directly. In many cases, you can estimate it from current versus voltage data. You can measure a log current versus potential curve over a range of about one half volt. The voltage scan is centered on  $E_{oc}$ . You then fit the measured data to a theoretical model of the corrosion process.

The model we will use for the corrosion process assumes that the rates of both the anodic and cathodic processes are controlled by the kinetics of the electron transfer reaction at the metal surface. This is generally the case for corrosion reactions. An electrochemical

reaction under kinetic control obeys Equation 1, the **Tafel Equation**.

$$I = I_0 e^{(2.3(E-E_0)/\beta)} \quad (1)$$

In this equation,

$I$ , is the current resulting from the reaction

$I_0$ , is a reaction dependent constant called the Exchange Current

$E$ , is the electrode potential

$E^0$ , is the equilibrium potential (constant for a given reaction)

$\beta$ , is the reaction's Tafel Constant (constant for a given reaction).

Beta has units of volts/decade.

The Tafel equation describes the behaviour of one isolated reaction. In a corrosion system, we have two opposing reactions – anodic and cathodic.

The Tafel equations for both the anodic and cathodic reactions in a corrosion system can be combined to generate the **Butler-Volmer Equation** (2).

$$I = I_a + I_c = I_{\text{corr}}(e^{(2.3(E-E_{\text{oc}})/\beta_a)} - e^{-(2.3(E-E_{\text{oc}})/\beta_c)}) \quad (2)$$

where

$I$  is the measured cell current in amps

$I_{\text{corr}}$  is the corrosion current in amps

$E$  is the electrode potential

$E_{\text{oc}}$  is the corrosion potential in volts

$\beta_a$  is the anodic Beta Tafel Constant in volts/decade

$\beta_c$  is the cathodic Beta Tafel Constant in volts/decade

At  $E_{\text{oc}}$ , each exponential term equals one. The cell current is therefore zero, as you would expect. Near  $E_{\text{oc}}$  both exponential terms contribute to the overall current. Finally, as the potential is driven far from  $E_{\text{oc}}$  by the potentiostat, one exponential term predominates and the other term can be ignored. When this occurs, a plot of log current versus potential becomes a straight line.

A log I versus E plot is called a Tafel Plot. The Tafel Plot in Figure 17 was generated directly from the Butler-Volmer equation. Notice the linear sections of the cell current curve.

Classic Tafel analysis is performed by extrapolating the linear portions of a log current versus potential plot back to their intersection. See Figure 18 (this is Figure 17 reprinted with annotations that demonstrate the analysis). The value of either the anodic or the cathodic current at the intersection is  $I_{corr}$ . Unfortunately, many real world corrosion systems do not provide a sufficient linear region to permit accurate extrapolation. Most modern corrosion test software, such as Gamry Instruments' DC105 DC Corrosion Techniques software, performs a more sophisticated numerical fit to the Butler-Volmer equation. The measured data is fit to Equation 18 by adjusting the values of  $E_{corr}$ ,  $I_{corr}$ ,  $b_a$ , and  $b_c$ . The curve fitting method has the advantage that it does not require a fully developed linear portion of the curve.

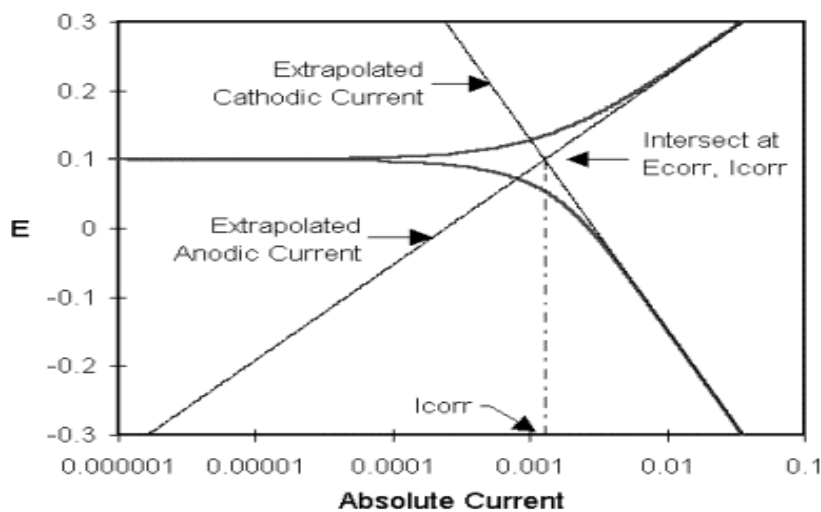


**Figure 1.16 Classic Tafel Analysis**

### 1.5.3: Polarization Resistance

Equation 2 can be further simplified by restricting the potential to be very close to  $E_{oc}$ . Near  $E_{oc}$ , the current versus voltage curve approximates a straight line. The slope of this line has the units of resistance (ohms). The slope is, therefore, called the Polarization

Resistance,  $R_p$ . An  $R_p$  value can be combined with an estimate of the Beta coefficients to yield an estimate of the corrosion current.

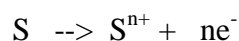
If we approximate the exponential terms in Equation 2 with the first two terms of a power series expansion ( $e^x = 1+x +x^2/2\dots$ ) and simplify, we get one form of the Stern-Geary Equation:

$$I_{corr} = \frac{\beta_a \beta_c}{2.3 R_p (\beta_a + \beta_c)} \quad \text{Equation 1-3}$$

In a Polarization Resistance experiment, you record a current versus voltage curve as the cell voltage is swept over a small range of potential that is very near to  $E_{oc}$  (generally  $\pm 10$  mV). A numerical fit of the curve yields a value for the Polarization Resistance,  $R_p$ . Polarization Resistance data does not provide any information about the values for the Beta coefficients. Therefore, to use Equation 1-3 you must provide Beta values. These can be obtained from a Tafel Plot or estimated from your experience with the system you are testing.

### Calculation of Corrosion Rate from Corrosion Current

The numerical result obtained by fitting corrosion data to a model is generally the corrosion current. We are interested in corrosion rates in the more useful units of rate of penetration, such as millimetres per year. How is corrosion current used to generate a corrosion rate? Assume an electrolytic dissolution reaction involving a chemical species, S:



You can relate current flow to mass via **Faraday's Law**.

$$Q = nFM \quad \text{Equation (4)}$$

where

- Q is the charge in coulombs resulting from the reaction of species S
- n is the number of electrons transferred per molecule or atom of S
- F is Faraday's constant = 96,486.7 coulombs/mole
- M is the number of moles of species S reacting

A more useful form of Equation 4 requires the concept of equivalent weight. The equivalent weight (EW) is the mass of species S that will react with one Faraday of charge. For an atomic species,  $EW = AW/n$  (where AW is the atomic weight of the species).

Recalling that  $M = W/AW$  and substituting into Equation 4 we get:

$$W = \frac{EW \times Q}{F} \quad \text{Equation 1-5}$$

Where W is the mass of species S that has reacted.

In cases where the corrosion occurs uniformly across a metal surface, the corrosion rate can be calculated in units of distance per year. Be careful - this calculation is only valid for uniform corrosion; it dramatically underestimates the problem when localized corrosion occurs!

For a complex alloy that undergoes uniform dissolution, the equivalent weight is a weighted average of the equivalent weights of the alloy components. Mole fraction, not mass fraction, is used as the weighting factor. If the dissolution is not uniform, you may have to measure the corrosion products to calculate EW.

Conversion from a weight loss to a corrosion rate (CR) is straightforward. We need to know the density, d, and the sample area, A. Charge is given by  $Q = I T$ , where T is the time in seconds and I is a current. We can substitute in the value of Faraday's constant. Modifying Equation 1-5:

$$CR = \frac{I_{corr} \cdot K \cdot EW}{dA} \quad \text{Equation 1-6}$$

CR	The corrosion rate. Its units are given by the choice of K
I <sub>corr</sub>	The corrosion current in amps
K	A constant that defines the units for the corrosion rate
EW	The equivalent weight in grams/equivalent
d	Density in grams/cm <sup>3</sup>
A	Sample area in cm <sup>2</sup>

## References

- [1] H. Shirakawa, E. J. Louis, A. G. MacDiarmid, C. K. Chiang, A. J. Heeger. *J. Chem. Soc. Chem. Commun.*, 1977, 578
- [2] [www.nobel.se/chemistry/laureates/2000/index.html](http://www.nobel.se/chemistry/laureates/2000/index.html)
- [3] a) V. V. Walatka, M. M. Labes and J. H. Perlstein. *Phys. Rev. Lett.*, 1973, 31: 1139; b) C.
- M. Mikulsk, P. J. Russo, M. S. Saran, A. G. MacDiarmid, A. F. Garito, A. J. Heeger. *J. Am. Chem. Soc.*, 1975, 97: 6358
- [4] *Handbook of Conducting Polymers* (Ed. T. A. Skotheim). Marcel Dekker, New York, 1986 and 1998
- [5] *Encyclopedia of Nanoscience and Nanotechnology* (Ed. H. S. Nalwa). 2004, 2: 153 169
- [6] J. D. Stenger-Smith. *Progr. Polym. Sci.*, 1998, 23: 57
- [7] A. G. MacDiarmid. *Angew. Chem. Int. Ed.*, 2001, 40: 2581
- [8] J. C. Chiang, A. G. MacDiarmid. *Synth. Met.*, 1986, 13: 193
- [9] A. G. MacDiarmid, A. J. Epstein. *Faraday Discuss. Chem. Soc.*, 1989, 88: 317
- [10] *Conductive Polymers* (Ed. R.B. Seymour). New York: Plenum Press, 1981, 23 47
- [11] Moulton SE, Innis PC, Kane-Maguire LAP, Ngamna O, Wallace GG. *Curr Appl Phys* (2004);4:402–6.
- [12] J. C. Chiang, A. G. MacDiarmid. *Synth. Met.*, 1986, 13: 193
- [13] W. S. Huang, B. D. Humphrey, and A. G. MacDiarmid. *J. Chem. Soc. Commun. Faraday Trans.*, 1986, 82: 2385
- [14] A. G. MacDiarmid. *Angew. Chem. Int. Ed.*, 2001, 40: 2581 Chapter 2 Polyaniline as A Promising Conducting Polymer 39
- [15] a) A. G. MacDiarmid, A. J. Epstein. *Faraday Discuss. Chem. Soc.*, 1989, 88: 317; b) A. G. MacDiarmid, J. C. Chiang, A. F. Richter, A. J. Epstein. *Synth. Met.*, 1987, 18: 285



- [16] T. Hagiwara, M. Yamaura, and K. Iwata. *Synth. Met.*, 1988, 26: 185
- [17] a) A. G. MacDiarmid, A. J. Heeger. *Synth. Met.*, 1879/80, 1: 101; *Handbook of Conducting Polymers*, Vol.1 &2 (Ed. T. A. Skotheim), Marcel Dekker, New York, 1986; b) M. G. Kanatzidis. *Chem. Eng. News*, 1990, 68: 36
- [18] S. Stafström, J. L. Bredas, A. J. Epstein, et al. *Phys. Rev. Lett.*, 1987, 59: 1464
- [19] J. M. Ginder, A. F. Richter, A. G. MacDiarmid and A. J. Epstein. *Solid State Commun.*, 1987, 63: 97
- [20] A. J. Epstein, J. M. Ginder, F. Zuo et al. *Synth. Met.*, 1987, 18: 303
- [21] G. Wnek. *Synth. Met.*, 1986, 16: 213
- [22] I. Kogan, L. Fokeeva, I. Shunina, Y. Estrin, L. Kasumova, M. Kaplunov, G. Davidova, E. Knerelman. *Synth. Met.*, 1999, 100: 303
- [23] a) Z. Sun, Y. Geng, J. Li, X. Wang, X. Jing, F. Wang. *J. Appl. Polym. Sci.*, 1999, 72: 1077;
- b) B. K. Kim, Y. H. Kim, K. Won, H. Chang, Y. Choi, K. Kong, B. W. Rhyu, J. J. Kim, J. O. Lee. *Nanotechnology*, 2005, 16: 1177 *Conducting Polymers with Micro or Nanometer Structure* 40
- [24] a) S. Palaniappan. *Polym. Adv. Technol.*, 2004, 15: 111; b) P. S. Rao, D. N. Sathyanarayana, S. Palaniappan. *Macromolecules*, 2002, 35: 4988
- [25] A. Yasuda, T. Shimidzu. *Polym. J.*, 1993, 4: 329
- [26] Y. Wang, Z. Liu, B. Han, Z. Sun, Y. Huang, G. Yang. *Langmuir*, 2005, 21: 833
- [27] a) A. Pron, F. Genoud, C. Menardo, M. Nechtschein. *Synth. Met.*, 1988, 24: 193; b) Y. Cao, A. Andreatta, A. J. Heeger, P. Smith. *Polymer*, 1989, 30: 2305; c) S. Tan, J. H. Tieu,

D. Belanger. *J. Phys. Chem. B*, 2005, 109: 14085; d) E. Erdem, M. Karakisla, M. Sacak.

*Europ. Polym. J.*, 2004, 40: 785

[28] H. J. Ding, M. X. Wan, Y. Wei. *Adv. Mater.*, 2007, 19: 465

[29] a) H. Gong, X. J. Cui, Z. W. Xie, S. G. Wang, L. Y. Qu. *Synth. Met.*, 2002, 129: 187;

b) J. Stejskal, A. Riede, D. Hlavata, J. Prokes, M. Helmstedt, P. Holler. *Synth. Met.*, 1998, 96: 55

[30] Y. Wei, Y. Sun, and X. Tang. *J. Phys. Chem.*, 1989, 93: 4878

[31] a) A. Kitani, J. Izumi, J. Yano, Y. Hiromoto, K. Sasaki. *Bull. Chem. SOC. Jpn.*, 1984, 57:

2254; b) G. Zotti, S Cattarin, N. Comisso. *J. Electroanal. Chem.*, 1987, 235: 259; c) G. Zotti,

S Cattarin, N. Comisso. *J. Electroanal. Chem.*, 1988, 239: 387

[32] a) K. Sasaki, M. Kaya, J. Yano, A. Kitani, A. Kunai. *J. Electroanal. Chem.*, 1986, 215:

401; b) A. Thyssen, A. Borgerding, J. W. Schultze. *Makromol. Chem., Macromol. Symp.*, 1987, 8: 143

[33] U. Kenig, J. W. Schultze. *J. Electroanal. Chem.*, 1988, 242: 243

[34] Y. Wei, G. W. Jaag, C. C. Chan, K. F. Hsueh, R. Hariharan, S. A. Patel, and C. K.

Whitecar. *J. Phys. Chem.*, 1990, 94, 7716

[35] J. Huang, J. A. Moore, J. H. Acquaye, and R. B. Kaner. *Macromolecules*, 2005, 38: 317

[36] M. Thakur and S. Tripathy. in *Encycloedia of Polymer Science and Engineering (J. I. Kroschwitz Ed., 2nd ed.)*. New York: John Wiley and Sons Ltd., 1986, Vol.5, p.756 771

[37] D. F. Eaton. *Science*, 1991, 253: 281; D. F. Eaton. *Chemtech.*, 1992, 22: 308

[38] *Nonlinear Optics: Fundamentals, Materials and Devices* (Ed. S. Miyata). New York:

Elsevier, 1992

[39] Handbook of Organic Conductive Molecules and Polymers (Ed. H. S. Nalwa).  
Chichester: John Wiley & Sons Ltd., England, 1997, Vol.2

[40] a) D.E. Stilwell, S. M. Park. *J. Electrochem. Soc.*, 1988, 135: 2254; b) G. Zotti, S. Cattarin. *J. Electroanal. Chem.*, 1988, 239: 387; c) A. F. Diaz, J. A. Logan. *J. Electroanal. Chem.*, 1980, 111: 111; d) E. M. Genies, E. Vieil. *Synth. Met.*, 1987, 20: 97; e) H. Pingsheng, Q. Xiaohua, L. Chune. *Synth. Met.*, 1993, 57: 5008

[41] a) S. B. Basame, H. S. White. *J. Phys. Chem.*, 1995, 99: 16430; b) S. B. Basame, H. S. White. *J. Phys. Chem. B*, 1998, 102: 9812; c) C. J. Boxley, H. S. White, C. E. Gardner, J. V. Macpherson. *J. Phys. Chem. B*, 2003, 107: 9677

[42] H. Y. Choi, E. Mele. *J. Phys. Rev. Lett.*, 1987, 59: 2188

[43] B. Abeles, P. Sheng, M. D. Coutts, Y. Arie. *Adv. Phys.*, 1975, 24: 407

[44] A. M. Elamin, Z. L. Liu, K. I. Yao. *Acta Phys. Sin (Overseas ed.)*, 1997, 7: 458

[45] V. Luthra, R. Singh, S. K. Gupta, A. Mansingh. *Curr. Appl. Phys.*, 2003, 3: 219

[46] a) Z. M. Zhang, Z. X. Wei, M. X. Wan. *Macromolecules*, 2002, 35: 5937; b) R. Cordova, M. A. Valle, A. Arratia, H. Gomez, R. Schrebler. *J. Electroanal. Chem.*, 1994, 377: 75; c) S. J. Choi, S. M. Park. *J. Electrochem. Soc.*, 2002, 149: E26

[47] a) A.G. MacDiarmid, A. J. Epstein. *Synth. Met.*, 1994, 65: 103; b) A. G. MacDiarmid, A. J. Epstein. *Trans. 2nd Congresso Brasileiro de Polimeros*, 1993, 5 8: 544; c) Y. Min, A. G. MacDiarmid, A. J. Epstein. *Polym. Prepr.*, 1993, 231 2; d) A. G. MacDiarmid, A. J. Epstein. *Conducting Polymers with Micro or Nanometer Structure* 42Epstein. *Synth. Met.*, 1995, 69: 85; e) Y. Cao, P. Smith, A. J. Heeger. *Synth. Met.*, 1992, 48: 91; f) Y. Cao, A. J. Heeger. *Synth. Met.*, 1993, 52: 193; g) Y. Cao, G. M. Treacy, P. Smith, A. J. Heeger. *Appl. Phys. Lett.*, 1992, 60: 2711; h) Y. Cao, P. Smith. *Polymer*, 1993, 34: 3139

[48] a) C. Barbero, M. C. Miras, B. Schnyder, O. Haas, R. Koetz. *J. Mat. Chem.*, 1994, 4: 1775; b) C. Barbero, M. C. Miras, R. Kotz, O.Haas. *Lithium Batteries. In Proc.*

Electrochem. Soc., 1994, 94-4: 281; c) C. Barbero, M.C. Miras, R. Koetz, O. Haas. Synth. Met., 1993, 55: 1539

[49] a) H. Tsutsumi, S. Fukuzawa, M. Ishikawa, Y. Morita. J. Electrochem. Soc., 1995, 142: L168; b) K. Hwang, J.S. Kim, M. Kong. Synth. Met., 1995, 71: 2201; c) N. Oyama, T. Tatsuma, T. Sato, T. Sotomura. Nature, 1995, 373: 598; d) M. Morita, S. Miyazaki, M.

Ishikawa, Y. Matsuda, H. Tajima, K. Adachi, F. Anan. J. Electrochem. Soc., 1995, 142: L3

[50] a) M. Onoda, K. Yoshino. J. Appl. Phys., 1995, 78: 4456; b) M. Onoda, K. Yoshino. Jpn. J. Appl. Phys., Part 2, 1995, 34: L260; c) M. Ferreira, M. F. Rubner. Macromolecules, 1995, 28: 7107

[51] J. Yue, A. J. Epstein. J. Chem. Soc., Chem. Commun., 1992, 21: 1540

[52] a) T. Namiki, E. Yano, K. Watabe, Y. Igarashi, Y. Kuramitsu, T. Maruyama, K. Yano, T. Nakamura, S. Shimizu, T. Saito. Patent, JP 07179754 A2 950718; b) K. Watable, Y.

Yoneda, T. Maruyama, K. Yano, T. Nakamura, S. Shimizu, T. Saito. Patent, JP 06003813 A2 940114

[53] X. L. Wei, Y. Z. Wang, S. M. Long, C. Bobeczko and A. J. Epstein. J. Am. Chem. Soc., 1996, 118: 2545

[54] a) Y. Long, J. Luo, J. Xu, Z. Chen, L. Zhang, J. Li, M. Wan. J. Phys.: Condens. Matter, 2004, 16: 1123; b) Y. Cao, A. J. Heeger. Synth. Met., 1992, 52: 193; N. S. Sariciftci, A. J. Heeger, Y. Cao. Phys. Rev. B, 1994, 49: 5988; c) A. Raghunathan, T. S. Natarajan, G. Rangarajan, S. K. Dhawan, D. C. Trivedi. Phys. Rev. B, 1993, 47: 13189; d) P. K. Kahol, J. C. Ho, Y. Y. Chen, C. R. Wang, S. Neeleshwar, C. B. Tsai, B. Wessling. Synth. Met., 2005, 151: 65; e) A. Raghunathan, P. K. Kahol, J. C. Ho, Y. Y. Chen, Y. D. Yao, Y. S. Lin, B. Wessling. Phys. Rev. B, 1998, 58: R15955; f) P. K. Kahol, B. McCormick. J. Phys. Rev. B, 1993, 47: 14588; J. Fan, M. Wan, D. Zhu. Solid State Commun., 1999, 110: 57

[55] B. R. Weinberger, J. Kaufer, A. J. Heeger, A. Pron, A. G. MacDiarmid. Phys. Rev. B, 1979, 20: 223

[56] a) P. K. Kahol, A. Raghunathan, B. J. McCormick. *Synth. Met.*, 2004, 140: 261; b) P. K. Kahol, J. C. Ho, Y. Y. Chen, C. R. Wang, S. Neeleshwar, C. B. Tsai, B. Wessling. *Synth. Met.*, 2005, 151: 65; c) A. Raghunathan, P. K. Kahol, J. C. Ho, Y. Y. Chen, Y. D. Yao, Y. S. Lin, B. Wessling. *Phys. Rev. B*, 1998, 58: R15955; d) P. K. Kahol, B. J. McCormick. *Phys. Rev. B*, 1993, 47: 14588; e) P. K. Kahol, A. Raghunathan, B. J. McCormick, A. J. Epstein. *Synth. Met.*, 1999, 101: 815; f) N. J. Pinto, P. K. Kahol. *Synth. Met.*, 2001, 119: 317

[57] Y. Z. Long, Z. J. Chen, J. Y. Shen, Z. M. Zhang, L. J. Zhang, H. M. Xiao, M. X. Wan, and J. L. Duvail. *J. Phys. Chem. B*, 2006, 110: 23228

[58] a) D. C. Trivedi. *Phys. Rev. B*, 1993, 47: 13189; b) S. M. Yang, C. P. Li. *Synth. Met.*, 1993, 55: 636; c) F. Genoud, M. Nechtschein, C. Santier. *Synth. Met.*, 1993, 55: 642; d) P. K. Kahol, A. Raghunathan, B. J. McCormick. *Synth. Met.*, 2004, 140: 261 Chapter 2 Polyaniline as A Promising Conducting Polymer 43

[59] P. Rannou, B. Dufour, J. P. Travers, and A. Pron. *J. Phys. Chem. B*, 2002, 106: 10553

[60] J. G. Masters, J. M. Ginder, A. G. MacDiarmid, A. J. Epstein. *J. Chem. Phys.*, 1992, 96: 4768

[61] H. T. Lee, K. R. Chuang, S. A. Chen, P. K. Wei, J. H. Hsu, W. Fann. *Macromolecules*, 1995, 28: 7645

[62] I. D. Norris, L. A. P. Kane-Maguire, G. G. Wallace. *Macromolecules*, 1998, 31: 6529

[63] Y. Xia, J. M. Wiesinger, A. G. MacDiarmid. *Chem. Mater.*, 1995, 7: 443

[64] a) A. Andreatta, A. J. Heeger, P. J. Smith. *Polym. Commun.*, 1990, 31: 275; b) E. M. Sherr, A. G. MacDiarmid, S. K. Manohar, J. G. Masters, J. G. Sun, Y. X. Tang, M. A. Druy, P. J. Glatkowski, V. P. Cajipe, J. E. Fisher, K. R. Cromack, M. E. Ginder, R. P. Macall, A. J. Epstein. *Synth. Met.*, 1991, 41: 735; c) C. H. Hsu, J. D. Cohen, R. F. Tietz. *Synth. Met.*, 1993, 59: 37; d) J. Rajiv, R. V. Gregory. *Synth. Met.*, 1995, 74: 263; e) C. H. Hsu, A. J. Epstein. *Synth. Met.*, 1997, 84: 51; f) S. J. Pomfret, P. N. Adams, N. P. Comfort, A. P. Monkman. *Adv. Mater.*, 1998, 10: 1351; g) K. Eaiprasersak, R. V. Gregory. *ANTEC '98*. 1998, 2: 1263; h) S. J. Pomfret, P. N. Adams, A. P. Monkman, N. P. Comfort. *Synth.*

Met., 1999, 101: 24; i) S. J. Pomfret, P. N. Adams, N. P. Comfort, A. P. Monkman.

Polymer, 2000, 41: 2265

[65] B. R. Mattes, P. N. Adams, D. Yang, L. A. Brown, A. G. Fadeev, I. D. Norris, Spinning, PCT WO 2004/042743, 2004

[66] W. Lu, A. G. Fadeev, B. Qi, E. Smela, B. R. Mattes, J. Ding, G. M. Spinks, J. Mazurkiewicz, D. Zhou, G. G. Wallace, D. R. MacFarlane, S. A. Forsyth, M. Forsyth. Science, 2002, 287: 983

[67] a) M. Nechtschein, C. Santier, J. P. Travers, J. Chroboczek, A. Alix, M. Ripert. Synth.

Met., 1987, 18: 311; b) T. Taka. Synth. Met., 1993, 55 57: 5014

[68] B. Lubentsov, O. Timofeeva, S. Saratovskikh, V. Krinichnyi, A. Pelekh, V. Dmitrenko, M. Khidekel. Synth. Met., 1992, 47: 187

[69] A. Alix, V. Lemoine, M. Nechtschein, J. P. Travers, C. Menardo. Synth. Met., 1989, 29: 457

[70] E. S. Matveeva, R. Diaz Calleja, V. P. Parkhutik. Synth. Met., 1995, 72: 105

[71] M. M. Ostwal, J. Pellegrino, I. Norris, T. T. Tsotsis, M. Sahimi, B. R. Mattes. Ind. Eng. Chem. Res., 2005, 44: 7860

[72] B. Qi, B. R. Mattes. U.S. Patent Application 2005/0062486, 2005

[73] a) V. George, D. Young. J. Polym. Commun., 2002, 43: 4073; b) M. G. Mikheal, A. B. Padias, H. K. Hall. J. Polym. Sci. Polym. Chem., 1997, 35: 1673

[74] N. A. Zaidi, S. R. Giblin, I. Terry, A. P. Monkman. Polymer, 2004, 45: 5683

[75] a) H. Goto, M. Okuda, T. Oohazama, K. Akagi. Synth. Met., 1999, 102: 1293; b) A. Gök, B. Sarl, M. Talu. Synth. Met., 2004, 142: 41

[76] a) M. Leclerc, J. Guay, L. H. Dao, Macromolecules, 1982, 22: 649; b) Y. Wei, W. W. Focke, G. E. Wnek, A. Ray, A. G. MacDiarmid. J. Phys. Chem., 1989, 93: 495; c) D. Jr.

MaCinnes, B. L. Funt. Synth. Met., 1989, 25: 235; d) L. H. C. Mattoso, S. V. Mello, A.

Jr. Riul, O. N. Jr. Oliverira, R. M. Faria. Thin Solid Film, 1994, 244: 714

- [77] a) J. Yue, A. J. Epstein. *J. Am. Chem. Soc.*, 1990, 112: 2800; b) J. Yue, Z. F. Wang, K. R. Cromack, A. J. Epstein, A. G. MacDiarmid. *J. Am. Chem. Soc.*, 1991, 113: 2665; c) S. A. Chen, G. W. Hwang. *J. Am. Chem. Soc.*, 1994, 116: 7939 Conducting Polymers with Micro or Nanometer Structure 44
- [78] Y. Cao, P. Smith, A. J. Heeger. *Synth. Met.*, 1992, 48: 91
- [79] J. Yue, G. Gordon, A. J. Epstein. *Polymer*, 1992, 33: 4409
- [80] H. S. O. Chan, L. M. Gan, C. H. Chew, L. Ma, S. H. Seow. *J. Mater. Chem.*, 1993, 3: 1109
- [81] R. E. Cameron, S. K. Clement. U.S. Patent 5,008,041, 1991
- [82] A. F. Dim, A. Logan. *J. Electroanal. Chem.*, 1980, 111: 111
- [83] C. C. Han, W. D. Hsieh, J. Y. Yeh, S. P. Hong. *Chem. Mater.*, 1999, 11: 480
- [84] a) J. Yue, H. Wang, K. R. Cromack, A. J. Epstein, A. G. MacDiarmid. *J. Am. Chem. Soc.*, 1991, 113: 2665; b) E.T. Kang, K. G. Neoh, K. L. Tan, H. K. Wong. *Synth. Met.*, 1992, 48: 231
- [85] X. L. Wei, Y. Z. Wang, S. M. Long, C. Bobeczko, and A. J. Epstein. *J. Am. Chem. Soc.*, 1996, 118: 2545
- [86] P. Hany, E. M. Genies, C. Santier. *Synth. Met.*, 1989, 31: 369
- [87] a) J. Yue, A. J. Epstein. *J. Am. Chem. Soc.*, 1990, 112: 2800; b) J. Yue, Z. H. Wang, K. R. Cromack, A. J. Epstein, A. G. MacDiarmid. *J. Am. Chem. Soc.*, 1991, 113: 2665; c) J. Yue, A. J. Epstein. *J. Chem. Soc., Chem. Commun.*, 1992, 1540
- [88] J. Y. Bergeron, J. W. Chevalier, L. H. Dao. *J. Chem. Soc., Chem. Commun.*, 1990, 180
- [89] a) J. Yue, A. J. Epstein, Z. Zhong, P. K. Gallagher, A. G. MacDiarmid. *Synth. Met.*, 1991, 41: 765; b) T. C. Tsai, D. A. Tree, M. S. High. *Ind. Eng. Chem. Res.*, 1994, 33: 2600
- [90] S. A. Chen, G. W. Hwang. *Macromolecules*, 1996, 29: 3950

- [91] a) L. H. Dao, M. T. Nguyen, T. D. Do. *Polym. Prep. (Am. Chem. Soc., Div. Polym. Chem.)*, 1992, 33: 408; b) J. Y. Bergeron, L. D. Dao. *Macromolecules*, 1992, 25: 3332; c) Y. Wei, R. Harihara, S. A. Patel. *Macromolecules*, 1990, 23: 758
- [92] H. S. O. Chan, P. K. H. Ho, S. C. Ng, K. L. Tan. *J. Am. Chem. Soc.*, 1995, 117: 8517
- [93] M. T. Nguyen, P. Kasai, J. L. Miller, A. F. Diaz. *Macromolecules*, 1994, 27: 3625
- [94] M. T. Nguyen, A. F. Diaz. *Macromolecules*, 1995, 28: 3411
- [95] W. Yin, E. Ruckenstein. *Macromolecules*, 2000, 33: 1129
- [96] B. A. Deore, I. Yu, and M. S. Freund. *J. Am. Chem. Soc.*, 2004, 126: 52
- [97] S. A. Chen, G. W. Hwang. *J. Am. Chem. Soc.*, 1994, 116: 7939
- [98] H. S. O. Chan, P. K. H. Ho, S. C. Ng, B. T. G. Tan, K. L. Tan. *J. Am. Chem. Soc.*, 1995, 117: 8517
- [99] G. Liu, M. S. Freund. *Macromolecules*, 1997, 30: 5660
- [100] J. H. Lee, H. B. Lee, J. D. Andrade. *Prog. Polym. Sci.*, 1995, 20: 1043
- [101] a) J. M. Harris. *J. Macromol. Sci. RMCP*, 1983, C25: 325; b) P. Novak, K. Muller, K. S. V. Santhanam, O. Haas. *Chem. Rev.*, 1997, 97: 207
- [102] P. Wang and K. L. Tan. *Chem. Mater.*, 2001, 13: 581
- [103] J. A. Akkara, K. J. Senecal, D. L. Kaplan. *J. Polym. Sci., Polym. Chem.*, 1991, 29: 1561
- [104] a) K. S. Alva, J. Kumar, K. A. Marx, S. K. Tripathy. *Macromol. Rapid Commun.*, 1996, 17: 859; b) K. S. Alva, J. Kumar, K. A. Marx, S. K. Tripathy. *Macromolecules*, 1997, 30: 4024 Chapter 2 Polyaniline as A Promising Conducting Polymer 45
- [105] K. S. Alva, T. S. Lee, J. Kumar, S. Tripathy. *Chem. Mater.*, 1998, 10: 1270
- [106] a) L. Samuelson, A. Anagnostopoulos, K. S. Alva, J. Kumar, S. K. Tripathy. *Macromolecules*, 1998, 31: 4376; b) W. Liu, A. Cholli, R. Nagarajan, J. Kumar, S.



Tripathy, F. F. Bruno, L. Samuelson. *J. Am. Chem. Soc.*, 1999, 121: 11345; c) W. Liu, J.

Kumar, S. Tripathy, K. Senecal, L. Samuelson. *J. Am. Chem. Soc.*, 1999, 121: 71

[107] S. Roy; J. M. Fortier, R. Nagarajan, S. Tripathy, J. Kumar, L. A. Samuelson, and F. F. Bruno; *Biomacromolecules* 2002, 3, 937

[108] a) K. Underhill-Shanks, T. Viswanathan. *Polym. Prep. (Am. Chem. Soc; Div. Polym. Chem.)*, 1996, 37: 508; b) M. Sudhakar, A. D. Toland, T. Viswanathan. *Polym. Prep. (Am. Chem. Soc.; Div. Polym. Chem.)*, 1998, 39: 125; c) B. Berry, A. Shaikh, T. Viswanathan, *Polym. Prep. (Am. Chem. Soc.; Div. Polym. Chem.)*, 2000, 41: 327; d) B. Berry, D. Lindquist, J. P. Smith, T. Viswanathan. *Polym. Prep. (Am. Chem. Soc.; Div. Polym. Chem.)*, 2000, 41: 1110

[109] a) Y. Yang, A. J. Heeger. *Nature*, 1994, 372: 344; b) A. R. Brown, A. Pomp, C. M. Hart, D. M. Leeuw. *Science*, 1995, 270: 972 Conducting Polymers with Micro or Nanometer Structure 46

[110] a) H. Sirringhaus, N. Ztessler, R. H. Friend. *Science*, 1998, 280: 1741; b) M. Berggren, A. Dodabalapur, R. E. Slusher, Z. Bao. *Nature*, 1997, 389: 466; c) F. Hide, M. A. Diaz-Garcia, B. L. Schwartz, A. J. Heeger. *Acc. Chem. Res.*, 1997, 30: 430 435; d) M. Granstrom, M. Berggren, O. Inganas. *Science*, 1995, 267: 1479

[111] M. Angelopoulos, J. M. Shaw. *Polym. Eng. Sci.*, 1992, 32: 153

[112] *Handbook of Organic Conductive Molecules and Polymers* (Ed. H. S. Nalwa). Chichester: John Wiley & Sons, 1997, Vol. 4

[113] a) J. Yu, M. Abley, C. Yang, S. Holdcroft. *Chem. Commun.*, 1998, 1503 1504; b) J. Lowe, S. Holdcroft. *Synth. Met.*, 1997, 85: 1427 1431; c) J. Yu, S. Holdcroft. *Chem. Commun.*, 2001, 1274 1275

[114] W. S. Beh, I. T. Kim. D. In Xia, G. M. Whitesides. *Adv. Mater.*, 1999, 11: 1038

[115] a) L. F. Rozsnyi, M. S. Wrighton. *J. Am. Chem. Soc.*, 1994, 116: 5993; b) T. R. Hebner, J. C. Sturm. *Appl. Phys. Lett.*, 1998, 73: 1775

- [116] Z. Bao, Y. Feng, A. Dodabalapur, A. Lovinger. *Chem. Mater.*, 1997, 9: 1299
- [117] R. D. Piner, J. Zhu, F. Xu, S. H. Hong, C. A. Mirkin. *Science*, 1999, 283: 661
- [118] A. G. MacDiarmid and A. J. Epstein. *Faraday Discuss. Chem. Soc.*, 1989, 88: 317
- [119] a) A. G. MacDiarmid. *Synth. Met.*, 1997, 84: 27; b) R. V. Gregory, W. C. Kimbrell, H. H. Kuhn. *Synth. Met.*, 1989, 28: C823
- [120] a) I. Sapurina, A. Riede, J. Stejskal. *Synth. Met.*, 2001, 123: 503; b) I. Sapurina, A. Yu. Osadchev, B. Z. Volchek, M. Trchová, A. Riede, J. Stejskal. *Synth. Met.*, 2002, 129: 29
- [121] H. Okamoto, M. Okamoto, T. Kotaka. *Polymer*, 1998, 39: 4359; G. Láng, M. Ujvári; G. Inzelt. *Electrochim. Acta*, 2001, 46: 4159
- [122] J. Stejskal, I. Sapurina. *Pure Appl. Chem.*, 2005, 77: 815
- [123] a) G. Decher. *Science*, 1997, 277: 1232; b) N. Sarkar, M. K. Ram, A. Sarkar, R. Narizzano, S. Paddeu, C. Nicolini. *Nanotechnology*, 2000, 11: 30
- [124] G. Mao, Y. Tsao, M. Tirrell, H. T. Davis, V. Hessel, H. Ringsdorf. *Langmuir*, 1995, 11: 942
- [125] a) J. Y. Chen, L. Huang, L. M. Ying, G. B. Luo, X. S. Zhao, W. X. Cao. *Langmuir*, 1999, 15: 7208; b) T. B. Cao, S. M. Yang, Y. L. Yang, C. H. Huang, W. X. Cao. *Langmuir*, 2001, 17: 6034; c) T. B. Cao, J. Y. Chen, C. H. Yang, W. X. Cao. *Macromol. Rapid Commun.*, 2001, 22: 181
- [126] T. B. Cao, L. H. Wei, S. M. Yang, M. F. Zhang, C. H. Huang, W. X. Cao. *Langmuir*, 2002, 18: 750
- [127] W. B. Stockton, M. F. Rubner. *Mater. Res. Soc. Symp. Proc.*, 1994, 369: 587
- [128] Q. Pei, G. Yu, C. Zhang, Y. Yang, A. J. Heeger. *Science*, 1995, 269: 1086
- [129] G. F. Li, C. Martinez, and S. Semancik. *J. Am. Chem. Soc.*, 2005, 127: 4903

- [130] a) C. W. Lee, Y. H. Seo, S. H. Lee. *Macromolecules*, 2004, 37: 4070; b) X. Zhang, J. P. Sadighi, T. W. Mackewitz, S. L. Buchwald. *J. Am. Chem. Soc.*, 2000, 122: 7606
- [131] Stenger-Smith, J. D. 1998. *Intrinsically Electrically Conducting Polymers. Synthesis, Characterization and Their Application. Progress in Polymer Science. 23: 57-79*
- [132] Kinlen, P. J., D.C. Silverman and C.R. Jeffreys. 1997. *Corrosion Protection Using Polyaniline Coating Formulations. Synthetic Metals. 85: 1327-1332*
- [133] J. Tomeczek, H. Palugnoik, *Fuel* 81 (2002) 1251–1258.
- [134] S. Torrey, *Coal Ash Utilisation: Fly ash, Bottom ash and Slag*, Noyes Data, Park Ridge, NJ, USA, 1978.
- [135] A.F. Jimenez, A. Palomo, *Fuel* 82 (2003) 2259– 2265.
- [136] ASTM C 618 94, *Specification for coal fly ash and raw calcined natural pozzolan for use as a mineral admixture in Portland cement concrete*, Annual Book of ASTM Standards, vol. 4.02, 1994, pp. 296–298.
- [137] Flyash in soil stabilization and as an engineered construction material. [www.Geocities.SoilStab.htm](http://www.Geocities.SoilStab.htm).
- [138] Typical chemistry of coal fly ash (in wt.%). [www.Geocities.Chemistry.htm](http://www.Geocities.Chemistry.htm).
- [139] S.V. Vassilev, C.G. Vassileva, *Fuel Processing Technology* 47 (1996) 261– 280.
- [140] D.N. Singh, P.K. Kolay, *Progress in Energy and Combustion Science* 28 (2002) 267–299.
- [141] R.P Gupta, T.F. Wall, I. Kajigaya, S. Miyamae, Y. Tsumita, *Progress in Energy and Combustion Science* 24 (1998) 523– 543.
- [142] A.H. Miguel, PhD Thesis (1976), Univ. of Illinois, Urbana.
- [143] D.F.S. Natush, C.F. Bauer, H. Matusiewicz, C.A. Evans Jr., J. Baker, A. Loh, R.W. Linto, P.K. Hopke, *Int. Conf. Heavy Met. Environ.*, Toronto, 1975, pp. 553– 576.
- [144] M. Ilic, C. Cheeseman, C. Sollars, J. Knight, *Fuel* 82 (2003) 331– 336.
- [145] O. Bayat, *Characterisation of Turkish fly ash*, *Fuel* 77 (1998) 1059– 1066.
- [146] V. Sakorafa, F. Burragato, K. Michailidis, *Fuel* 75 (1996) 416– 423.
- [147] P.S.M. Tripathy, S.N. Mukherjee, *Perspectives on Bulk use of fly ash*, CFRI Golden Jubilee Monograph, Allied Publishers Limited, 1997, p. 123.

- [148] G.L. Fisher, B.A. Prentic, D. Silberman, J.M. Ondov, R.C. Ragaini, A.H. Biermann, A.R. McFarland, *Environmental Science & Technology* 12 (1978) 447–451.
- [149] D.M. Roy, K. Luke, S. Diamond, Characterisation of fly ash and its reaction in concrete, in: J.G. McCarthy, R.J. Lauf (Eds.), *Fly ash and Coal Combustion By-Products: Characterisation Utilisation and Disposal I*, Material Research Society Symposium Proceedings, vol. 43, Material Research Society, Pittsburgh, PA, USA, 1985, pp. 3 – 20.
- [150] E.V. Sokol, V.M. Kalugin, E.N. Nigmatulina, N.I. Volkava, A.E. Frenkel, N.V. Maksimova, *Fuel* 81 (2002) 867– 876.
- [151] E.V. Fomenko, Magnetic microspheres of constant composition and their catalytic properties in reactions of methane oxidative transformation, PhD thesis, Krasnoyursk (1998) 22.
- [152] A.G. Anshits, E.N. Voskresenskaya, E.V. Kondratenko, E.V. Fomenko, E.V. Sokol, *Catalysis Today* 42 (1998) 197.
- [153] A.G. Anshits, V.A. Nizov, E.V. Kondratenko, E.V. Fomenko, N.N. Anshits, A.M. Kovalov, O.A. Bajnkov, O.M. Sharonova, A.A. Salanor, *Chemistry for Sustainable Development* 7 (1999) 105.
- [154] A.G. Anshits, E.V. Kondratenko, E.V. Fomenko, A.M. Kovalov, O.A. Bajnkov, N.N. Anshits, E.V. Sokol, D.I. Kochubey, A.I. Boronin, A.N. Salanov, S.V. Koshcheev, *Journal of Molecular Catalysis* 158 (2000) 209.
- [155] F. Blanco, P. Garcia, P. Mateos, J. Ayalar, *Cement and Concrete Research* 30 (2000) 1715– 1722.

# **CHAPTER 2**

## **CHARACTERIZATION TECHNIQUES**

In material characterization basically we try to characterize the synthesized material by variety of techniques to assure that the appropriate material with suitable properties is synthesized. Some of the instruments utilized for the characterization of the PANI composites are given below:

### **2.1: Ultraviolet-visible (UV-Vis.) Spectrometer**

Absorption in the ultraviolet (UV) and visible (Vis) region of the spectrum is an important technique of analysis and is dependent on the electronic structure of the molecule [1,2]. This is an excellent tool for detection and for determining the concentration of a compound which absorbs the energy in the UV-vis region (Fig.1). A UV-vis absorption spectrum obeys the Beer-Lambert Law

$$A = -\log I/I_0 = \epsilon lc$$

Where, I is intensity of light, A is defined as absorbance and it is found to be directly proportional to the path length, l, and the concentration of the sample, c. The extinction coefficient ( $\epsilon$ ) is characteristic of the substance under study and is a function of the wavelength.

UV/Vis involves the spectroscopy of photons in the UV-visible region. This means it uses light in the visible and adjacent (near ultraviolet (UV) and near infrared (NIR)) ranges. The absorption in the visible ranges directly affects the color of the chemicals involved. In this region of the electromagnetic spectrum, molecules undergo electronic transitions. This technique is complementary to fluorescence spectroscopy, in that fluorescence deals with transitions from the excited state to the ground state, while absorption measures transitions from the ground state to the excited state. In sunlight (or white light) as uniform or homogeneous in color, it is actually composed of a broad range of radiation wavelengths in the ultraviolet (UV), visible and infrared (IR) portions of the spectrum. Electromagnetic radiation such as visible light is commonly treated as a wave phenomenon, characterized by a wavelength or frequency.

The wavelengths of what we perceive as particular colors in the visible portion of the spectrum are displayed and listed below :

- Violet: 400 - 420 nm
- Indigo: 420 - 440 nm
- Blue: 440 - 490 nm
- Green: 490 - 570 nm
- Yellow: 570 - 585 nm
- Orange: 585 - 620 nm
- Red: 620 - 780 nm

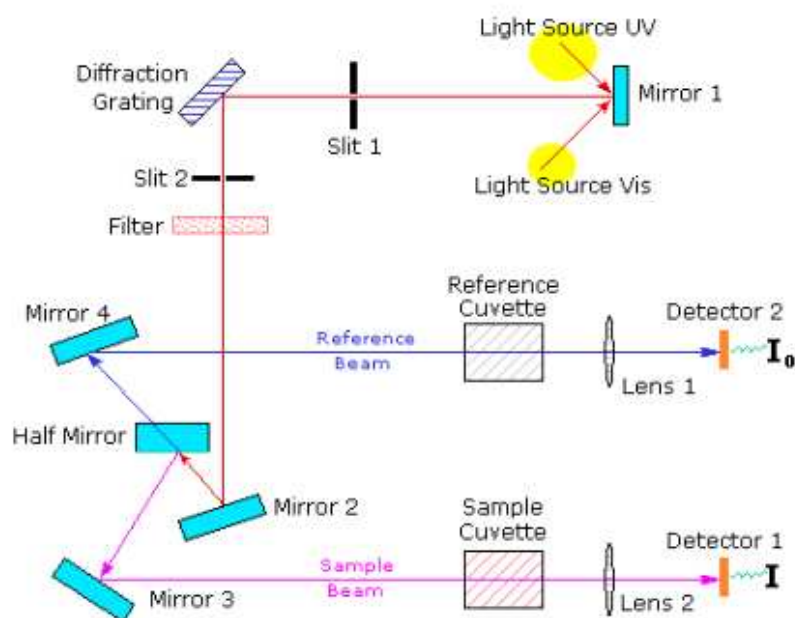


**Figure 2.1: Schematic of UV/Visible Spectrometer**

When sample molecules are exposed to light having an energy that matches a possible electronic transition within the molecule, some of the light energy will be absorbed as the electron is promoted to a higher energy orbital. An optical spectrometer records the wavelengths at which absorption occurs, together with the degree of absorption at each wavelength. The resulting spectrum is presented as a graph of absorbance ( $A$ ) versus wavelength.

## 2.2: Fourier Transform Infrared (FTIR) Spectrometer

FTIR is one of the most valuable spectroscopic probes to illustrate structural features of a molecule/macromolecule on the basis of its response to infra-red (IR) radiation ( $3 \times 10^{12}$  -  $3 \times 10^{14}$  Hz) [3,4]. It helps to understand new bond formation, nature and types of bonds between two atoms in molecule on the basis of (i) strength of bonds to its various vibration modes under IR radiation, and (ii) effective masses of two atoms forming a particular bond under investigation. The IR behavior of a system under investigation is a two dimensional plot of vibrational energy in wave number ( $\text{cm}^{-1}$ ) against absorption/transmission/reflection intensity of radiation.

$$v = \frac{1}{2\pi c} \sqrt{\left(\frac{k}{\mu}\right)} \text{ Hz} \quad (2.1)$$

where, k is bond strength, and  $\mu$  is the effective mass of the two bonded atoms.

The absorption versus frequency characteristics of light transmitted through a specimen irradiated with a beam of infrared radiation provide a fingerprint of molecular structure. Infrared radiation is absorbed when a dipole vibrates naturally at the same frequency in the absorber. The pattern of vibrations is unique for a given molecule, and the intensity of absorption is related to the quantity of absorber.



**Fig2.2: Set up for FT-IR Model 5700**



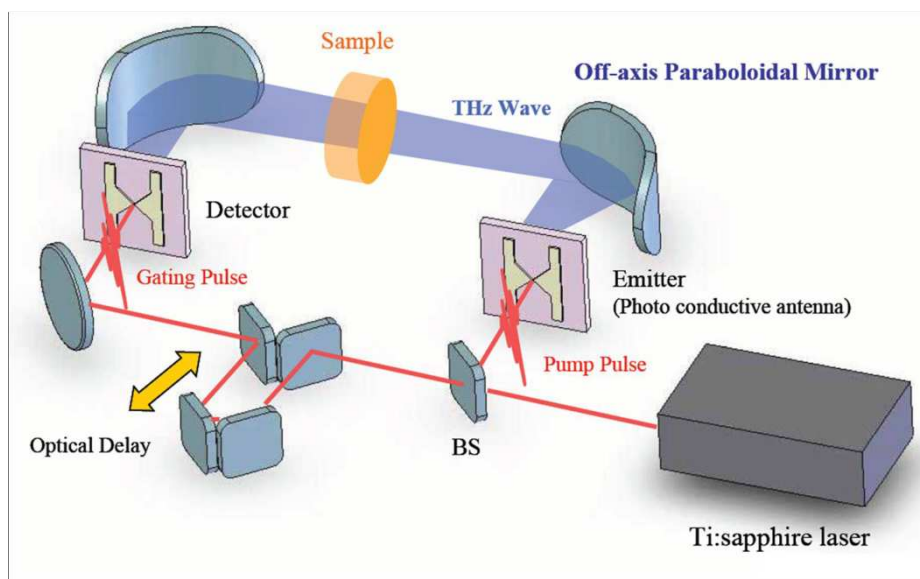


**Figure 2.3: Schematic diagram of the operation of FTIR**

Thus, infrared spectroscopy permits the determination of components or groups of atoms that absorb in the infrared at specific frequencies, permitting identification of the molecular structure [5-8]. With instruments of high spectral resolution, crystallinity and molecular strain can also be measured. Copolymer dispersions can be determined as block copolymers absorb additively and alternating copolymers deviate from this additivity due to interaction of neighboring groups. The conventional spectrometer with a dispersive prism or grating has been largely superseded by the Fourier transform infrared (FTIR) technique. This uses a moving mirror in an interferometer to produce an optical transform of the infrared signal. Numerical Fourier analysis gives the relation of intensity and frequency, that is, the IR spectrum. The FTIR technique can be used to analyze gases, liquids and solids with minimal preparation in short time. The FTIR technique has been applied to the study of many system, including adsorption on polymer surfaces, chemical modification and irradiation of polymers and oxidation of rubbers [9]. The application of infrared spectroscopy to the study of polymers has been reviewed by Bower and Maddams [5].

In particular,  $\pi$ -conjugated delocalized electron system shows an interesting class of long molecules (macromolecule / polymer) where the extent of delocalization of  $\pi$ -electron cloud affects positions of bands for a particular bond and helps in distinguishing two

different types of bonds even for polymeric chains having same constituents. By knowing the absorption position ( $\text{cm}^{-1}$ ) of a particular bond attached to  $\pi$ -conjugated chain, an idea about extent of effective  $\pi$ - electron delocalization can be drawn which ultimately shows the quality of electronic polymer. In the present work, FTIR spectra were recorded on Nicolet 5700 in transmission mode in the wave number range  $400\text{-}4000\text{ cm}^{-1}$ .

The spectroscopic grade KBr disks have been used for collecting the spectra with a resolution of  $4\text{cm}^{-1}$  performing 32 scans. It gave an idea about different functional groups and their arrangements (symmetrical or asymmetrical) in the polymeric chain and showed very sharp changes when the nature and conformation of inherent polymeric chains changed.

### 2.3: X-ray Diffractometer (XRD)

X-ray diffraction (XRD) is the most commonly used technique [10] for identification of crystalline phases present in materials and to measure the structural properties (strain state, grain size, epitaxy, phase composition, preferred orientation and defect structure) of these phases. XRD is also used to determine the thickness of thin films and multilayers, atomic arrangements in amorphous materials (including polymers) and at interfaces. Monochromatic X-rays of wavelength  $\lambda$ , incident upon the sample at an angle ' $\theta$ ', are diffracted by planes of atoms in the crystal separated by a distance ' $d$ '. The diffracted beams interfere constructively only when Bragg's Law is satisfied, giving rises to peaks (or spots) in the measured diffraction pattern. By using X-rays of known wavelength,  $\lambda$  and measuring the different angles  $\theta$ , the d-spacing of various planes of a crystal can be determined. According to Bragg's law

$$2d\sin\theta = n\lambda, \quad (2.2)$$

where,  $d$  is the spacing between atomic planes in the crystalline phase and  $\lambda$  is the x-ray wavelength, intensity of the diffracted X-ray is measured as a function of the diffraction angle  $2\theta$  and the specimen's orientation. This diffraction pattern is used to identify the specimen's crystalline phases and to measure its structural properties.

A diffraction pattern from a material typically contains many distinct peaks, each corresponding to a different interplanar spacing,  $d$ . There are often many individual crystals of random orientation in the sample, so all possible Bragg diffractions can be observed in the “powder pattern.” There is a convention for labeling or indexing, the different Bragg peaks in a powder diffraction pattern using the numbers ( $h$ ,  $k$ , and  $l$ ). One important use of x-ray powder diffractometry is for identifying unknown crystals in a sample. The idea is to match the positions and the intensities of the peaks in the observed diffraction pattern to a known pattern of peaks from a standard sample or from a calculation. For this, the International Centre for Diffraction Data (ICDD, formerly the Joint Committee on Powder Diffraction Standards, JCPDS) maintains a database of diffraction patterns for more than one hundred thousand inorganic and organic materials. For each material, the data fields include the observed interplanar spacing for all observed diffraction peaks, their relative intensities, and their  $hkl$  indexing. Software packages identify peaks in the experimental diffraction pattern and then search the ICDD database to find materials. Computerized fingerprint searches are particularly valuable when the sample contains a mixture of phases, and their chemical compositions are uncertain. When the chemical compositions of the crystallographic phases are known with some accuracy, however, the indexing of diffraction patterns is considerably easier.

XRD is nondestructive technique and does not require elaborate sample preparation which partly explains the wide usage of this technique in materials characterization. In conducting polymer, due to their semi-crystalline nature, only wide and low intensity peaks have been observed for indexing. Whereas, in case of polymer nanocomposites, due to the crystalline nature of the incorporated nanoparticles, polymeric diffraction peaks have been suppressed and only crystalline phase appeared.

### **2.4: Scanning Electron Microscope (SEM)**

In order to study the surface structure and morphology of the PANI composites a high performance scanning electron microscope LEO-440 has been used. It is a software Controlled SEM.



**Figure 2.4 LEO-440 Scanning Electron Microscope**

The electron gun has ionic emitter, as source of source electrons. The normal source is a tungsten hairpin filament, although the LEO-440 may have the lanthanum hexboride LaB<sub>6</sub> option fitted. Three electromagnetic lenses beneath the gun, focus and shape the electron beam before it strikes the specimen in a scanned or rastered, fashion. The energy of the beam is adjustable from 300 volts to 40 kilovolts in 10 volt steps and the electron beam current is continuously adjustable from 1 pico-amp to micro-amp to suit the type of examination in progress. The specimen chamber of the LEO-440 holds the specimen to be viewed in such a way that it may be freely maneuvered during examination. The specimen stage that holds the specimen is attached to the door of the chamber and may be of the normal cartesian type. The cartesian stage permits movement of 120 mm in the y direction, 100 mm in x direction, 58 mm in z direction, 0 to 90° tilt and 360° rotation. Control of the motorized stage movements may be achieved either by a joystick controller or via the LEO software. The stage may be opened for examination once the vacuum within the chamber is released. The instrument has a resolution 3.5 nm SEI mode and 5.5 nm BEI mode at variable working distances. The magnification on the computer screen can be

varied from 5x to 300000x. Specimen with 10 cm x 10 cm x 5 cm or 10 cm diameter and 5 cm thickness distances. It is complete software controlled instrument and operates like a desktop computer i.e. all operations are controlled through the mouse and the keyboard. In the present work the SEM was operated at 25 kV (unless otherwise mentioned) in the secondary electron imaged mode. In the case of conducting sample the surface morphology and surface structure were examined directly. However, in the specimen was coated with a very thin layer (10 nm).

### **2.5: Thermo Gravimetric Analysis (TGA)**

Thermo gravimetry (TG) is the branch of thermal analysis which examines the mass change of a sample as a function of temperature in the scanning mode or as a function of time in the isothermal mode. Not all thermal events bring about a change in the mass of the sample (for example, melting, crystallization or glass transition), but there are some very important exceptions which include desorption, absorption, sublimation, vaporization, oxidation, reduction and decomposition.[10]

TGA is used to characterize the decomposition and thermal stability of materials under a variety of conditions and to examine the kinetics of the physicochemical processes occurring in the sample. The mass change characteristics of a material are strongly dependent on the experimental condition employed. Factors such as samples mass, volume and physical form, the shape and nature of sample holder, the nature and pressure of atmosphere in the sample chamber and the scanning rate, all have important influences on the characteristics of the recorded TGA curve. TGA curves are recorded using a thermo balance. The principal elements of a thermo balance are - an electronic microbalance, a furnace, a temperature programmer and an instrument for simultaneously recording the outputs from these devices. Thermo gravimetric analysis operates on a null balancing principle with a sensitive balance maintaining a reference position for comparison with the weight of the sample. A current flow is produced to balance variations in weight between the reference and the sample, and this current is proportional to the change in sample weight. The relative thermal stability of polymers is quite important in end use properties. In case of conducting polymers, it is a useful technique to study the thermal stability of the polymer and the quantitative analysis of the amount of different substituents present in the

polymer. The quantitative analysis of the polymer is carried out by subtracting the final residual product of the doped form from the residual product in undoped form of polyaniline at 700°C. TGA along with the mass spectrometry gives the important information about the gases evolved from the samples. In the present work, Thermo gravimetric analysis of Polyaniline has been carried out using Mettler Toledo TGA 851e in nitrogen atmosphere with a flow rate of 60 mL/min. To study the complete thermal behavior, samples have been heated from 25-700°C with heating rate 10°C/min so that every volatile material could get detached from the samples.

### 2.6: Four Probe Method

Conductivity measurements are one of the main factor in the study of conducting polymer because all potential applications depend on the charge transport phenomenon in the conjugated polymers. The conductivity is usually measured by using a two-probe or four-probe method. Selection of a particular method depends upon the range of conductivity to be measured. If resistivity of the sample is very high, contact resistance becomes negligible and the two-point probe method is the simplest method for the determination of conductivity of undoped conducting polymer. The conductivity refers to the net charge which traverses (flow) the entire conducting polymer pellet. Four-points-probe method is advantageous over two-points-probe method because it overcomes the problem of contact or lead resistance. This technique is used for the determination of conductivity of doped conducting polymer films or pressed pellets. In this method, powder samples are compressed in the form of rectangular pellet of 13x7mm<sup>2</sup> by applying a pressure of 5 tons in a hydraulic press. A constant current source is used to pass a steady current through the two outermost probes and the voltage drop across the inner two probes is measured using conducting silver paste contacts. The conductivity of the samples was then measured from Ohm's law

$$\sigma = \frac{1}{\rho} = \frac{1}{R} \cdot \frac{l}{A} \text{ (S/cm)} \quad (2.4)$$

where, R is the volume resistance of the measured sample ( $\Omega$ ), A is the cross-section area of the sample (cm<sup>2</sup>) and L the effective length of the sample (cm).

The contacts were connected to the Keithley programmable current source (model 6221) and nanovoltmeter (model 2182A) attached to a digital temperature controller (Lakeshore 331) and closed cycle helium cryostat in the 0K.

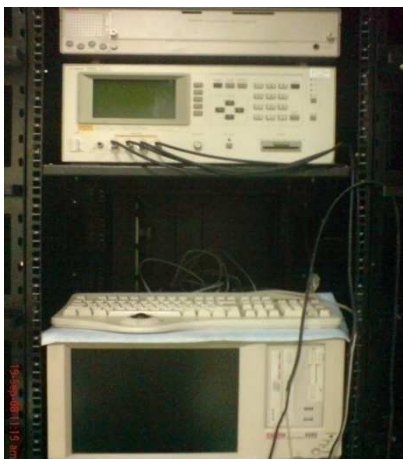
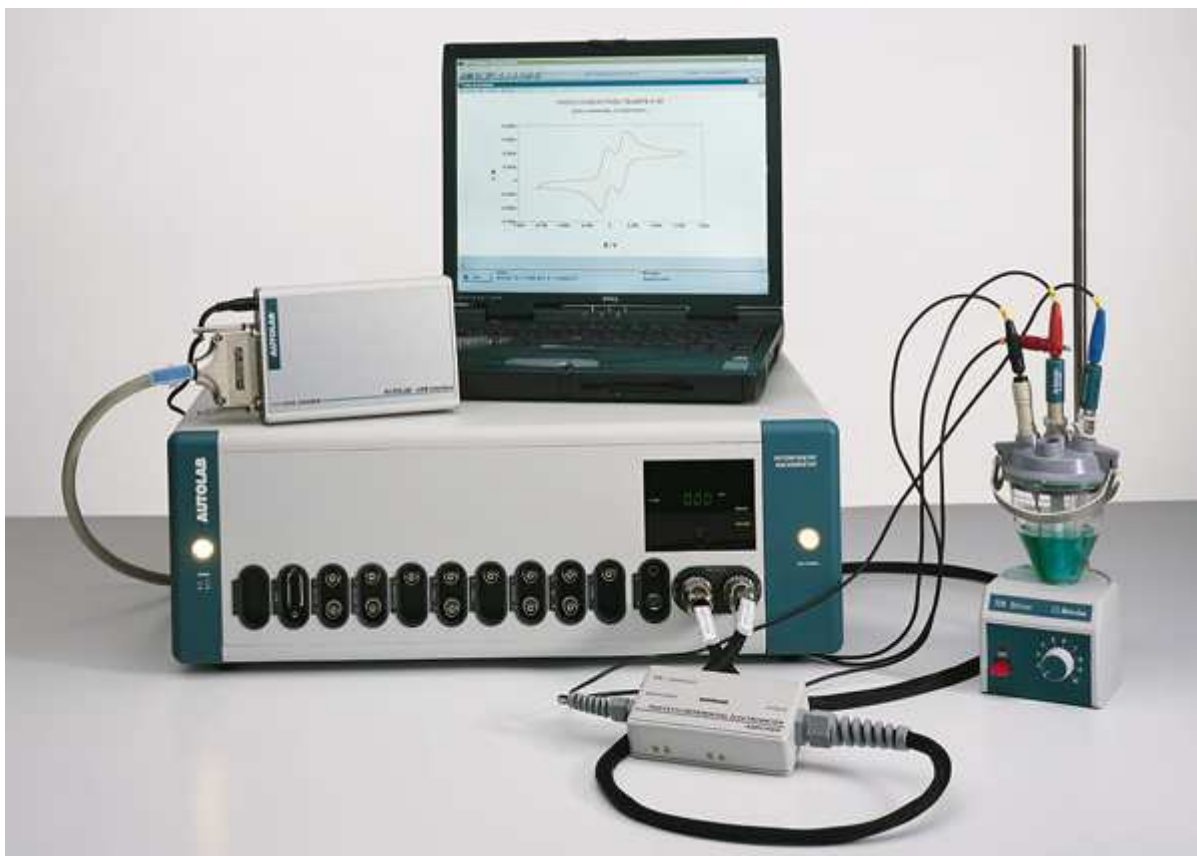


**Figure 2.5** 4200 Keithley Semi Characterization system for conductivity measurement.

### **2.7: Cyclic Voltammetry:**

Cyclic voltammetry or CV is a type of potentiodynamic electrochemical measurement. In a cyclic voltammetry experiment the working electrode potential is ramped linearly versus time like linear sweep voltammetry. Cyclic voltammetry takes the experiment a step further than linear sweep voltammetry which ends when it reaches a set potential. When cyclic voltammetry reaches a set potential, the working electrode's potential ramp is inverted. This inversion can happen multiple times during a single experiment. The current at the working electrode is plotted versus the applied voltage to give the cyclic voltammogram trace. Cyclic voltammetry is generally used to study the electrochemical properties of an analyte in solution [11-13].



**Figur2.6. Setup of Autolab Cyclic Voltmeter**



### References

- [1] P. Atkins, J. de Paula, *Physical Chemistry*, (Oxford University Press), 7<sup>th</sup> Edition, (2002) 291.
- [2] C. N. Banwell, E. M. McCash, “*Fundamentals of Molecular Spectroscopy*”, (Tata McGraw-Hill Publishing Company Limited, New Delhi), 4th Edition, (1994).
- [3] H. W. Siesler, K. H. Moritz, *Infrared and Raman Spectroscopy of Polymers* (Marcel Dekker , New York, 1980).
- [4] P. C. Painter, M. M. Coleman, J. L. Koenig, *The Theory of Vibrational Spectroscopy and its Application to Polymers* (John Wiley, New York, 1982).
- [5] D. L. Bower, W. F. Maddams, *The Vibrational Spectroscopy of Polymers* (Cambridge University Press, Cambridge, 1989).
- [6] E. C. Faulques, D. L. Perry and A. V. Yeremenko, *Eds. Spectroscopy of Emerging Materials* (Springer, Sudak, Crimea , Ukraine , 2004).
- [7] J. L. Koenig, *Infrared and Raman Spectroscopy of Polymers* (Rapra Technology, Shropshire UK, 2001).
- [8] P. R. Griffith, *Chemical Infrared Fourier Transform Spectroscopy* (Wiley, New York , 1975).
- [9] L. H. Lee, Ed. *Characterization of Metal and Polymer Surfaces: Polymer Surfaces* (Academic Press, New York , 1977).
- [10] Elton N. Kaufmann, (ed) *Characterization Of Materials Vol.1*, John Wiley & Sons Inc., Hoboken, New Jersey, 2003.
- [11] Bard, Allen J.; Larry R. Faulkner, *Electrochemical Methods: Fundamentals and Applications* (2 ed.). Wiley. (2000-12-18).
- [12] Nicholson, R. S.; Irving. Shain "Theory of Stationary Electrode Polarography. Single Scan and Cyclic Methods Applied to Reversible, Irreversible, and Kinetic Systems." *Analytical Chemistry* (1964)36 (4): 706–723.
- [13] Heinze, Jurgen "Cyclic Voltammetry-"Electrochemical Spectroscopy". *New Analytical Methods* (25) *Angewandte Chemie International Edition in English* (1984). 23 (11): 831–847

# **CHAPTER 3**

## **EXPERIMENTS**

## Experiments

### 3.1: Synthesis of Polyaniline (PANI)

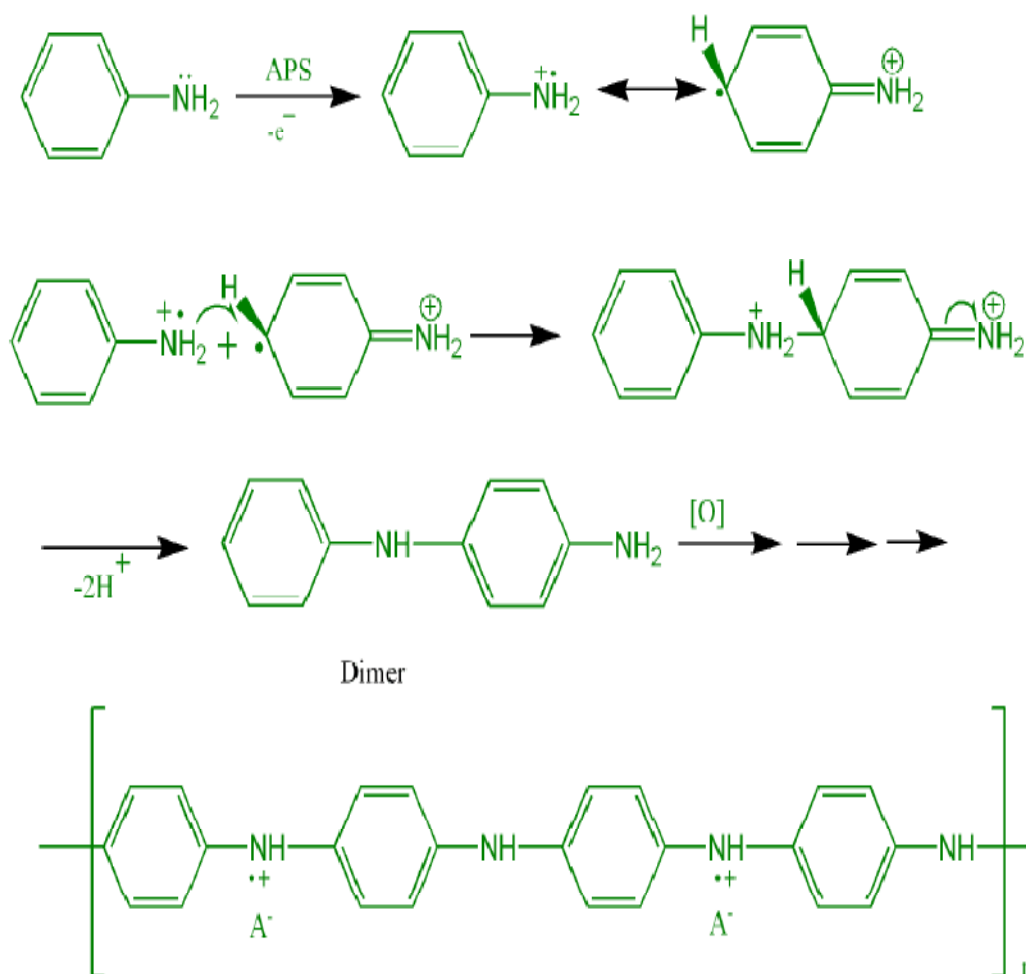
- Take 0.1 mole aniline monomer, 0.2 mole  $H_3PO_4$ , Add distilled water in calculated amount.
- Mix these solution properly after that add APS solution drop wise, polymerisation takes place at 2-5° C, continuous stirring takes place for 3-4 hrs.
- Filter the reaction mixture and wash with distil water properly, after that dry it in oven below 55°C

### 3.2: Cleaning of Flyash

- Take crude fly ash which obtain from coal power plant, distil water and add HCl to make solution acidic
- Heat this solution for 6-7 hrs to remove impurities and unburned carbon incorporated, after that wash properly with distil water and dry it in oven.

### 3.3: Synthesis of Polyaniline/ Flyash Composite(1:1) (PANI+FA1)

- Take 9.3 gm of fly ash and adsorbed it on one mole(9.3gm)of aniline for this heat mixture for 10-20 minutes at 60°C, add 0.2 mole  $H_3PO_4$  after that add appropriate amount of water and mix the solution properly
- Stirring the mixture at 2-5°C, Add APS solution drop wise, stirring the mixture for 3-4 hrs.
- Filter the reaction mixture and wash with distil water properly, after that dry it in oven below 55°C. The schematic representation of the polymerization mechanism is shown



***Polymerization mechanism of aniline using ammonium peroxy disulfate as oxidant***

### 3.4: Synthesis of Polyaniline/ Flyash Composite (1:2) PANI+FA2

- Take 18.6 gm of fly ash and adsorbed it on one mole (9.3 gm) of aniline for this heat mixture for 10-20 minutes at  $60^\circ\text{C}$ , add 0.2 mole  $\text{H}_3\text{PO}_4$  after that add appropriate amount of water and mix the solution properly
- Stirring the mixture at  $2-5^\circ\text{C}$ , Add APS solution drop wise, stirring the mixture for 3-4 hrs.
- Filter the reaction mixture and wash with distil water properly, after that dry it in oven below  $55^\circ\text{C}$

### **3.5: Undoping of Polyaniline/Flyash Composites PANI+FA1, PANI+FA2**

- Take 10 gm polyaniline/flyash composite, add it in 1000 ml water ,add about 60 ml ammonia solution to make solution basic about 10 pH
- stirring the mixture for 4-5 hrs.
- Filter the reaction mixture and wash it properly till neutral,drying in oven at 50°C

# **CHAPTER 4**

## **RESULT AND DISCUSSION**

## Results and Discussion

### 4.1: UV-Visible Spectral Analysis

UV-VIS Spectra of PANI and its composite with Fly ash doped with  $H_3PO_4$  was recorded on a Shimadzu UV-1601 spectrophotometer. PANI doped with  $H_3PO_4$  was dissolved in DMSO, which gives light green colour solution. Spectra were recorded in the wavelength range of 270-1100 nm and maximum absorbance was recorded.

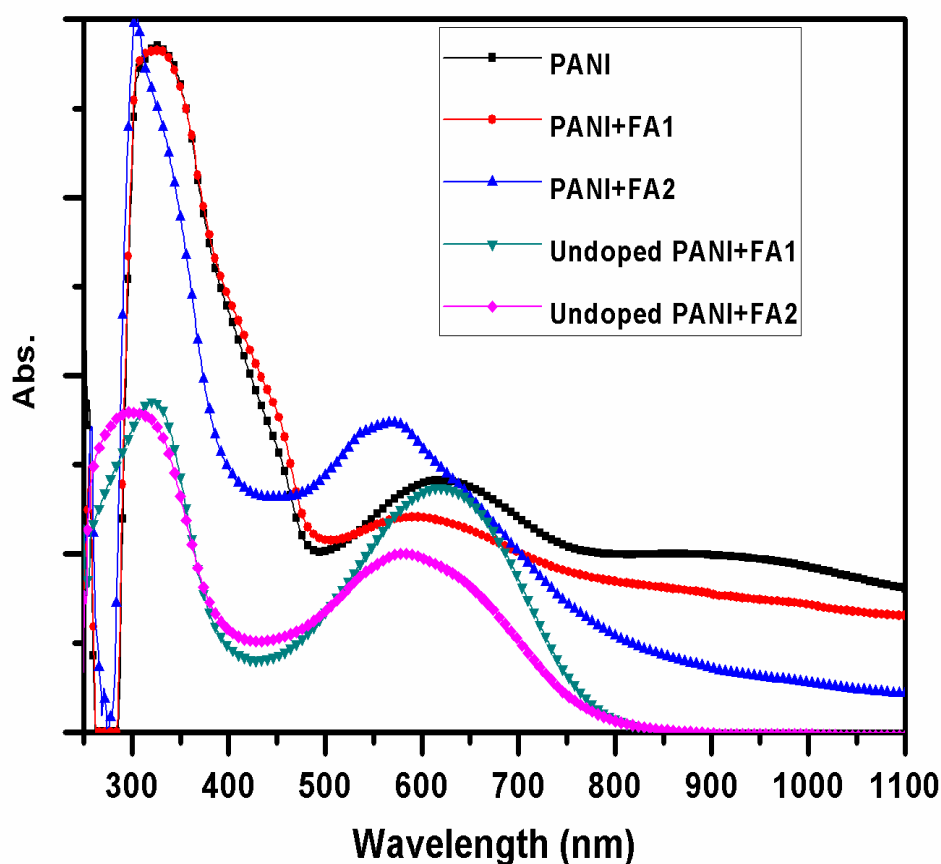


**Fig.4.1: UV/Visible spectra of polyaniline and polyaniline/flyash composite doped with  $H_3PO_4$**

Two bands are observed; band at 350–355 nm has been ascribed to the  $\pi$ - $\pi^*$  transition of the benzenoid ring, whereas, 428-435nm and 550-650 nm have been assigned to the

polaronic transitions. Intensity of the peaks varies due to different concentration of polymer solvent solution. The peaks at 428-435 is not found in undoped polymer due to absence of polaronic transition.

### 4.2: Conductivity Measurement of PANI and its composites

The samples: PANI doped with  $H_3PO_4$  and PANI composite, were pressed into pellets by applying a pressure between 7 to 10 tonnes by using a manual hydraulic press. These pellets were used for measuring the conductivities by four probe method. The values of conductivity of the synthesized polymer polyaniline and polyaniline/flyash composites is given in table.

S.N.	Sample Name	Conductivity
1	PANI	$1.02 \times 10^{-1} S \text{ cm}^{-1}$
2	PANI+FA1	$2.05 \times 10^{-3} S \text{ cm}^{-1}$
3	PANI+FA2	$6.35 \times 10^{-5} S \text{ cm}^{-1}$
4	Undoped PANI+FA1	$1.27 \times 10^{-8} S \text{ cm}^{-1}$
5	Undoped PANI+FA2	$2.87 \times 10^{-10} S \text{ cm}^{-1}$

**Table 4.1: Conductivity data of polyaniline and polyaniline/Flyash composites**

As see in the above table conductivity of polyaniline doped with  $H_3PO_4$  is highest and as we added fly ash conductivity decreases and with increasing concentration of fly ash conductivity



further decreases because fly ash act as insulator. When we undoped polyaniline fly ash composites with ammonia conductivity of composites further decreases and goes to insulator range of conductivity

### 4.3: Scanning Electron Microscope (SEM)

In order to study the surface structure and morphology of the composites a high performance scanning electron microscope LEO-440 has been used. It is a software controlled SEM.

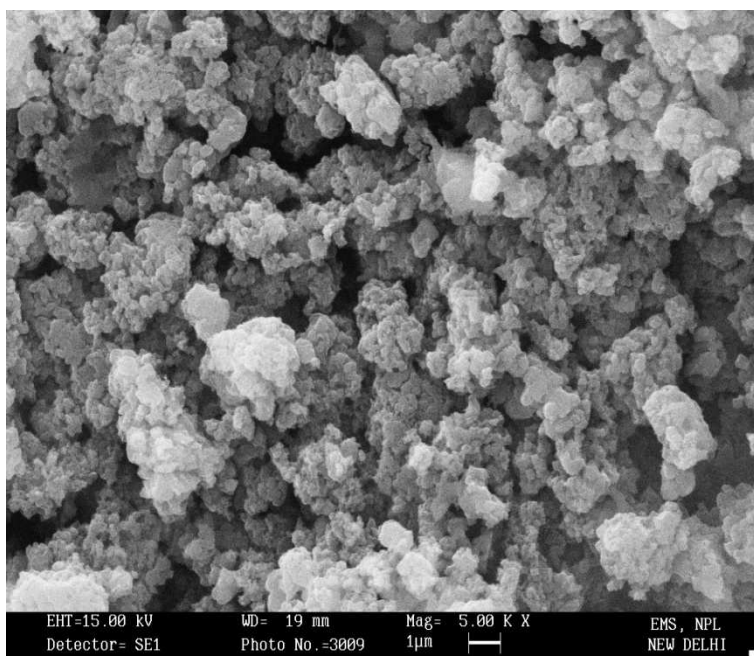


**Fig.4.3a: SEM image of polyaniline(PANI)**

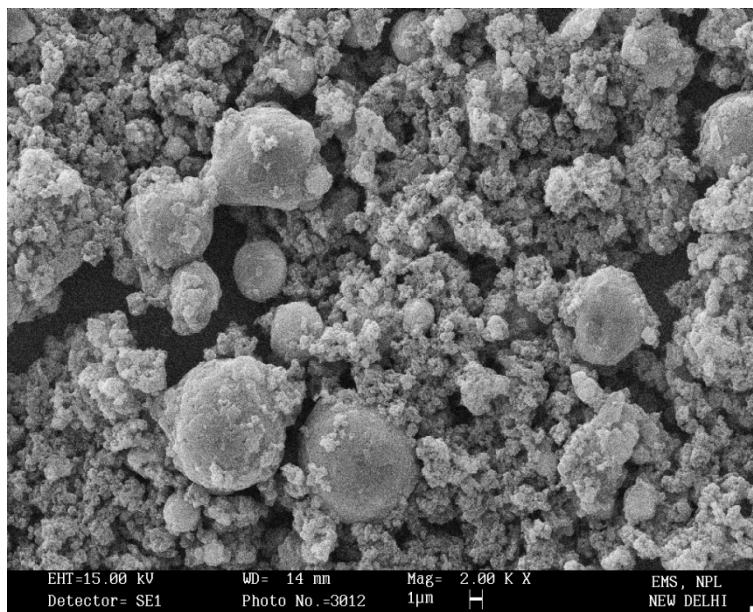


**Fig.4.3b: SEM image of polyaniline/fly ash (1:1)  
Composite (PANI+FA1)**

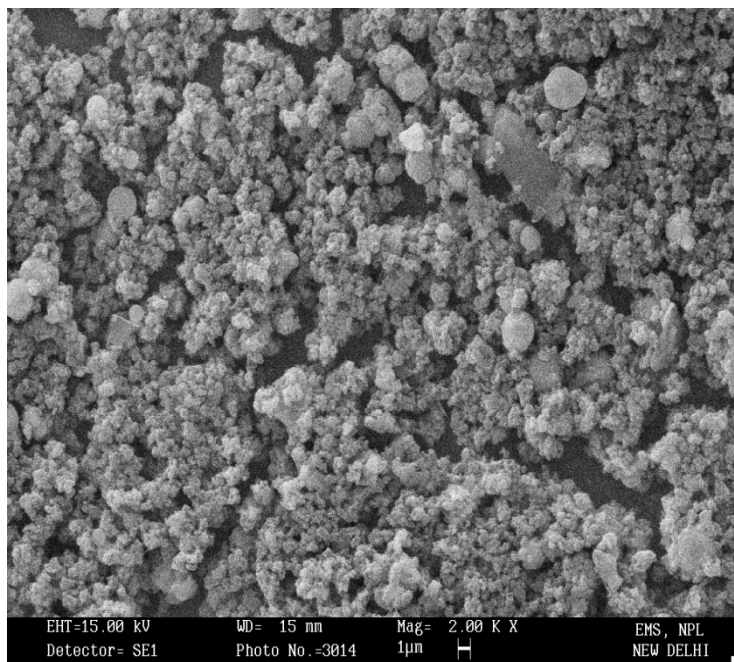


**Fig.4.3c: SEM image of polyaniline/fly ash(1:2)  
Composite (PANI+FA2)**

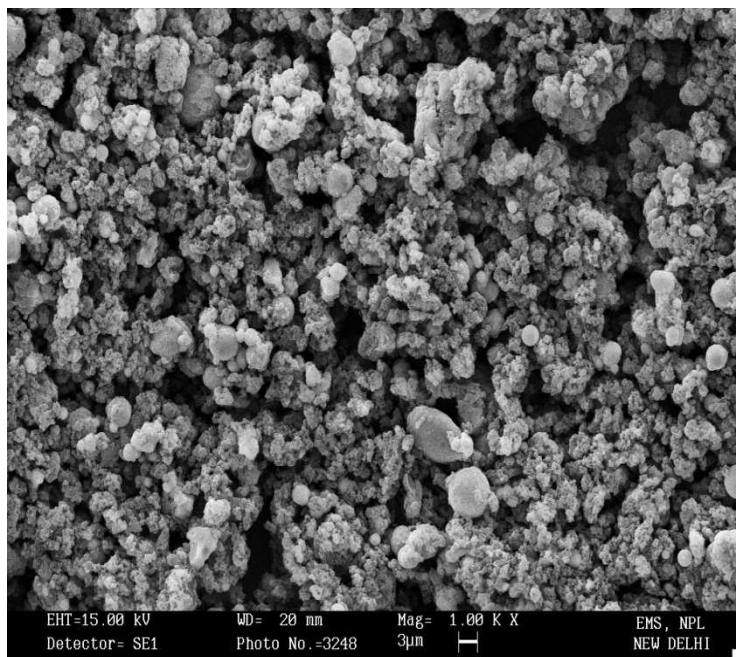


**Fig.4.3d: SEM image of undoped polyaniline/flyash(1:1) Composite (PANI+FA1)**

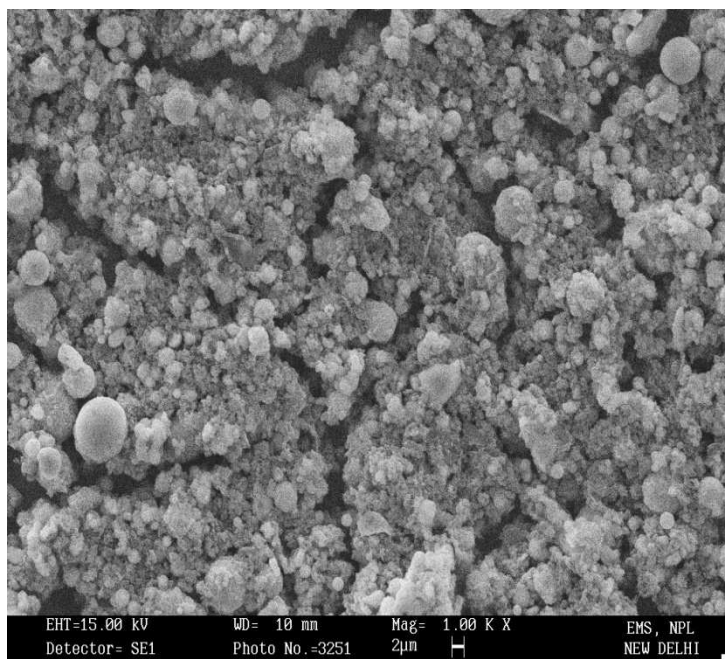


**Fig.4.3e: SEM image of undoped polyaniline/flyash (1:2) Composite**

Figure 4.3 a,b,c,d,e shows different morphology of polyaniline doped with with  $H_3PO_4$ , Polyaniline/Flyash composites doped with  $H_3PO_4$ , Undoped Polyaniline/Flyash composite.

In fig.3.3 a Shows a typical scanning electron micrograph of pure PANI at 10000 $\times$  magnification. It is apparent from the picture that the material is homogeneous with the particle size ranging from 4  $\mu m$  to 10  $\mu m$ , with most of the particles around 5–6  $\mu m$  size. It may also be noted from the SEM that the bigger particles are agglomerations of smaller, well-connected grains. The good connectivity among grains is expected to facilitate good electrical conductivity in this sample.

The SEM of the PANI–FA composites with (1:1) and(1:2) of FA at the same magnification of 10000 $\times$  are shown in Fig. 3.3 (b),(c) respectively. From the SEM pictures, it is evident that granularity increases with addition of FA in PANI, although the pure PANI appears to be more

granular (at 10000 $\times$ ) than the composites. The spherical FA particles (cenospheres) [3] of 1–2  $\mu m$  size may also be seen clearly in Fig. 3.3(b). Moreover, the grain size seems to decrease as the FA concentration increases. Again, the bigger particles seem to be agglomerates of smaller grains. This may also be looked upon as the decreasing grain-connectivity with increasing FA concentration in these composites. Effectively, it should be expected that the electrical conductivity decreases with increasing FA concentration

#### 4.4: X-ray diffraction

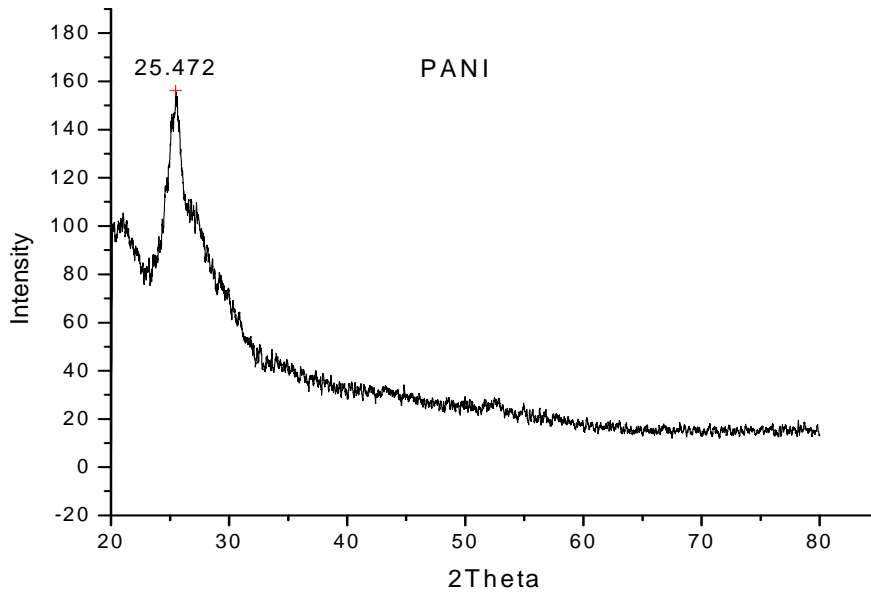


**Figure 4.4 a: XRD plot of Polyaniline(PANI)**

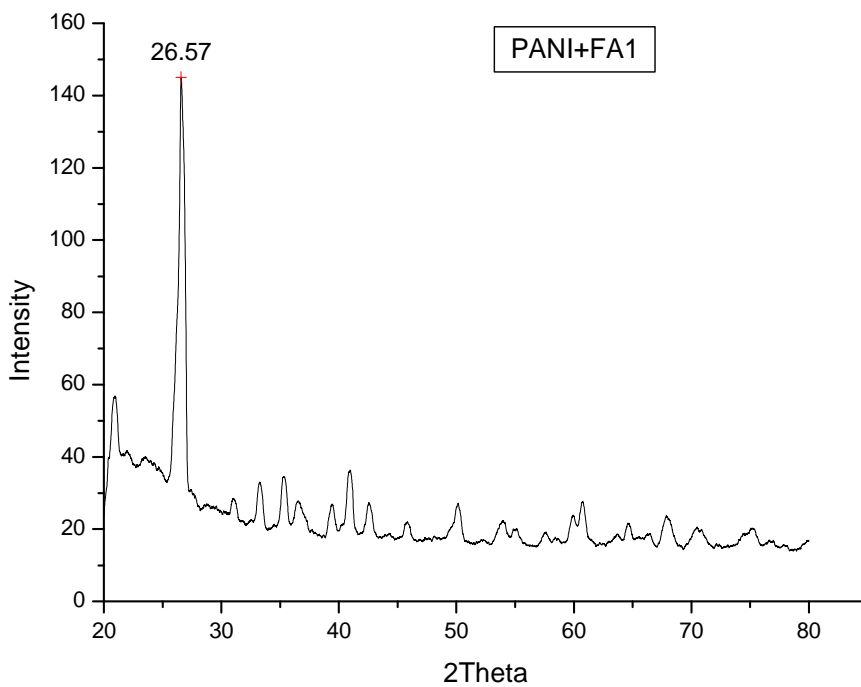


**Figure 4.4 b: XRD plot of polyaniline/Flyash (1:1) composite (PANI+FA1)**

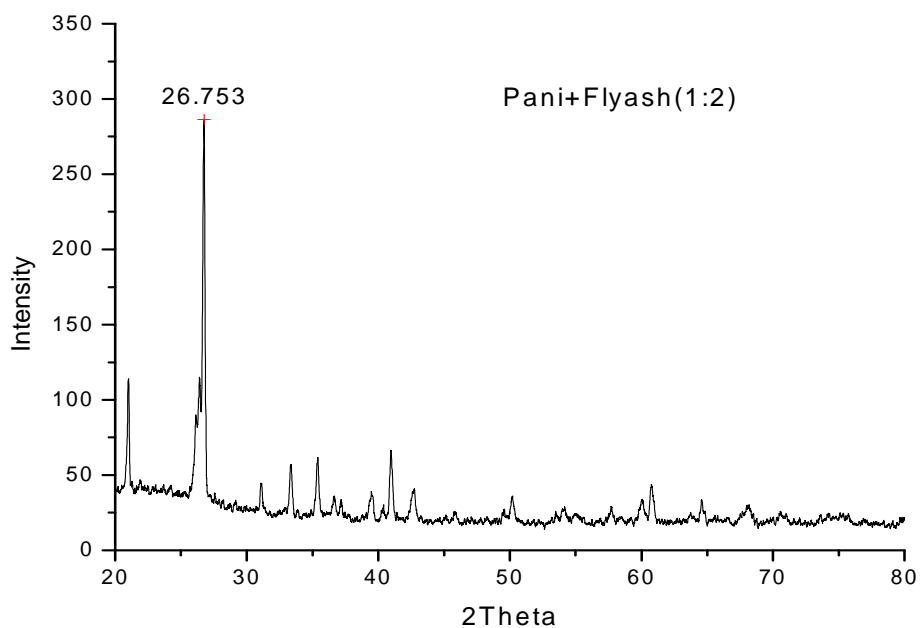


**Figure 4.4 c: XRD plot of polyaniline/Flyash (1:2) composite (PANI+FA2)**

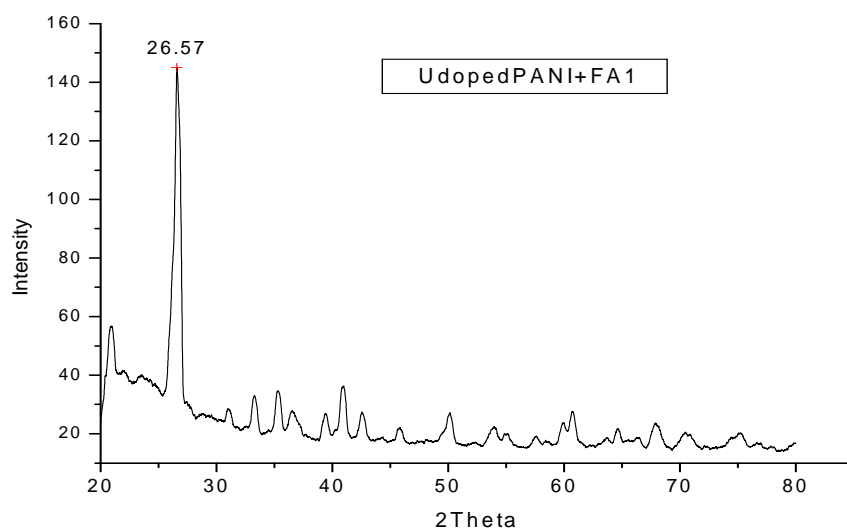


**Figure4.4d: XRD plot of Undoped polyaniline/Flyash (1:1) composite (PANI+FA1)**

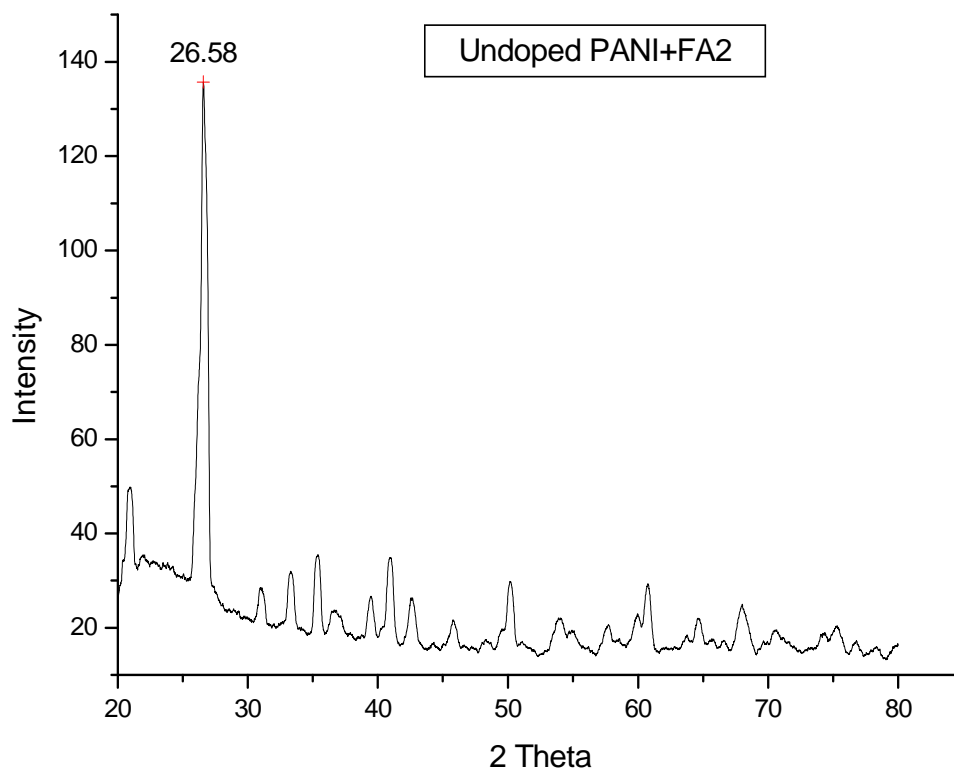


**Figure 4.4 e: XRD plot of Undoped polyaniline/Flyash (1:2) composite (PANI+FA1)**

Pure PANI shows a characteristic XRD peak at  $2\theta = 25.5$  that corresponds to the emeraldine salt (ES-I) phase of the polymer [3,4]. Crystalline phases of quartz ( $\text{SiO}_2$ ), alumina oxide ( $\text{Al}_2\text{O}_3$ ) and mullite ( $3\text{Al}_2\text{O}_3 \cdot 2\text{SiO}_2$ ) are three main constituents of FA, which also contains amorphous phases of these materials along with some other oxides. Therefore, the XRD pattern of PANI-FA composites shows the semi-crystalline nature of the material. As reported earlier by Raghavendra et al. [5], the PANI-FA composites show a sharp peak at  $2\theta = 26.6$ , which is evident in our XRD results. As the FA concentration increases, the height of 25.9 PANI peak gradually diminishes and a peak around  $2\theta = 26.1$  increases and becomes more prominent. This new peak is essentially a combination of the PANI peak ( $2\theta = 25.5^\circ$ ) and the peaks due to the constituents of FA around the same  $2\theta$

value. For example, two main constituents of FA, namely, quartz and alumina oxide peak at  $26.6^\circ$  and  $25.6^\circ$ , respectively. Therefore, as the FA concentration increases, the PANI peak gradually disappears. In the XRD plots, this occurs as a gradual shift of peaks near  $2\theta = 25.9^\circ$  towards slightly higher  $2\theta$  values.

### 4.5: FTIR Spectra

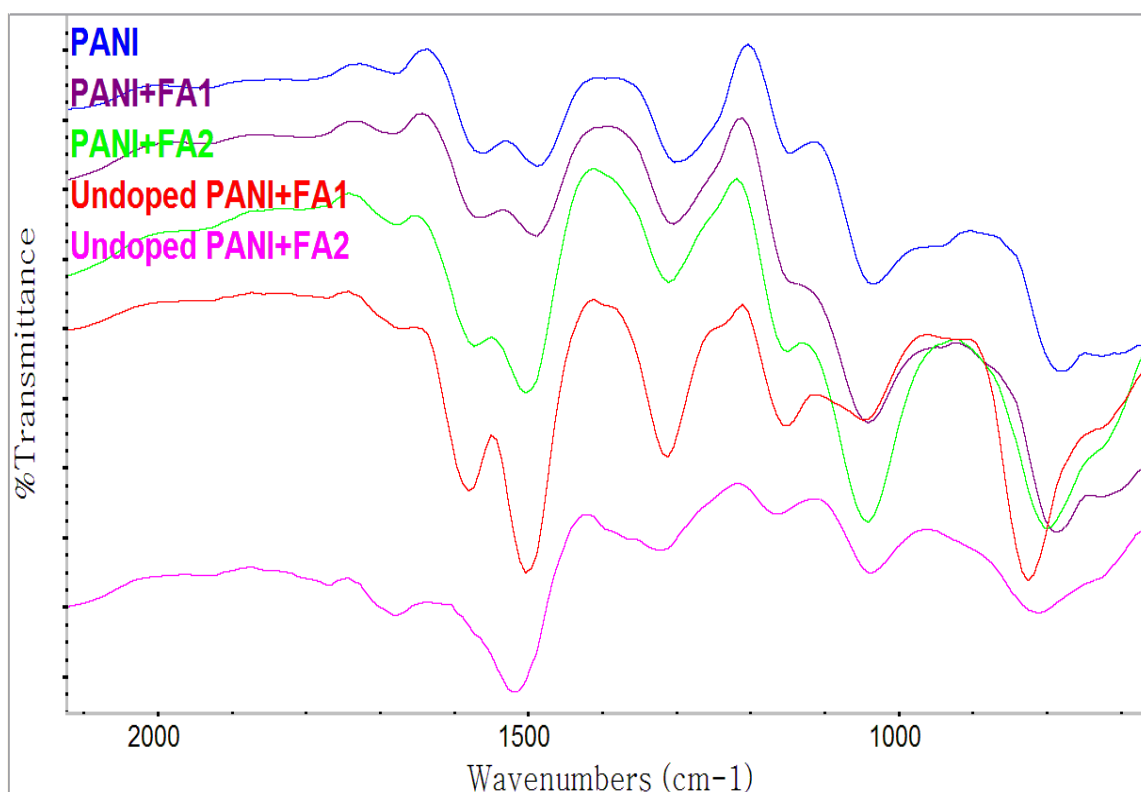


**Figure 4.5 FTIR Spectra of Polyaniline and Polyaniline/Flyash composites**

The characteristic peaks observed at the spectrum of PANI are due to the quinoid ring absorption at  $1630$  and  $1150$  cm<sup>-1</sup> absorption of benzoquinone at  $885$  cm<sup>-1</sup> the absorption due to benzenoid at  $1375$  and  $1500$  cm<sup>-1</sup>. These absorption bands are clear indications of the existence of the quinoid and benzenoid rings in the polymer chain. The bands at  $1630$  and  $1150$  cm<sup>-1</sup> are characteristic of the emeraldine salt (ES-I) form of PANI (as observed from the XRD also). The presence of these peaks also indicates that the emeraldine salt is composed of quinoid and benzenoid moieties [6-9]. The intense and sharp band at  $1630$



$\text{cm}^{-1}$  further indicates the relative abundance of the quinoid ring in the polymer structure. The IR spectrum of the FA/PANI composite in most of the cases resembles that of PANI indicating the existence of PANI in the emeraldine salt form. Slight shifts and additional peaks are observed in the range  $2500\text{--}3000\text{ cm}^{-1}$ ;  $1300\text{--}1500\text{ cm}^{-1}$  and  $1100\text{--}1300\text{ cm}^{-1}$ . The shifts and the additional characteristic peaks may be attributed to the presence of silica and metal oxides present in FA. The IR spectrum of FA (spectrum not shown) gave a very broad peak in the range  $1500\text{--}400\text{ cm}^{-1}$ . The broadening of the peak could be due to the merging of the IR peaks that arise from the absorption of the various metal oxides present in FA [10]. The IR spectra of (1:1)FA in PANI and (1:2)FA in PANI do not exhibit much variation in the characteristic peaks. In case of undoped Polyaniline/Flyash composites characteristic peak at  $1630\text{ cm}^{-1}$  does not appear.

### 4.6: Thermogravimetric analysis

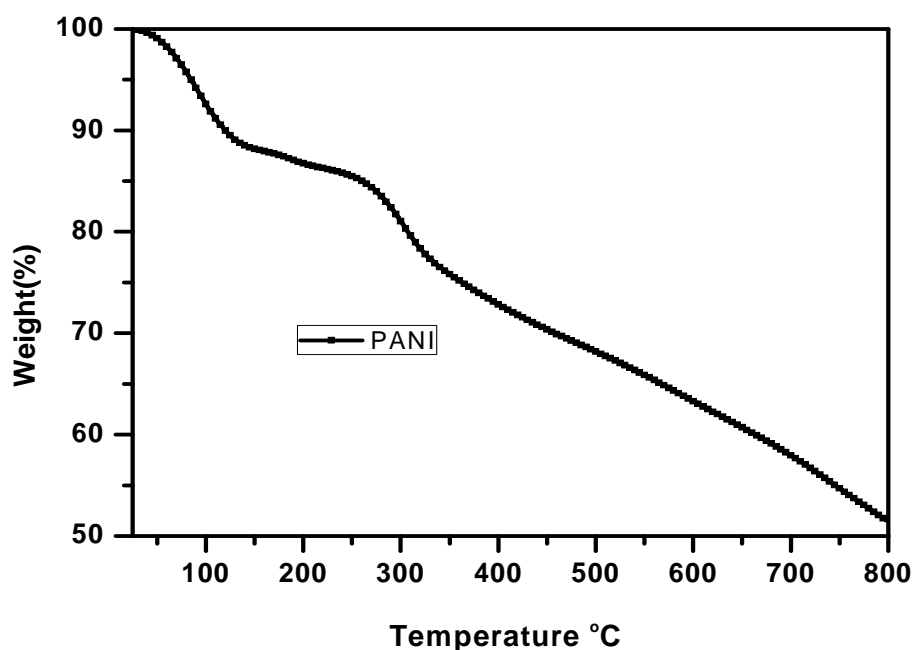


**Figure 4.6 a Thermogravimetric curve of Polyaniline**

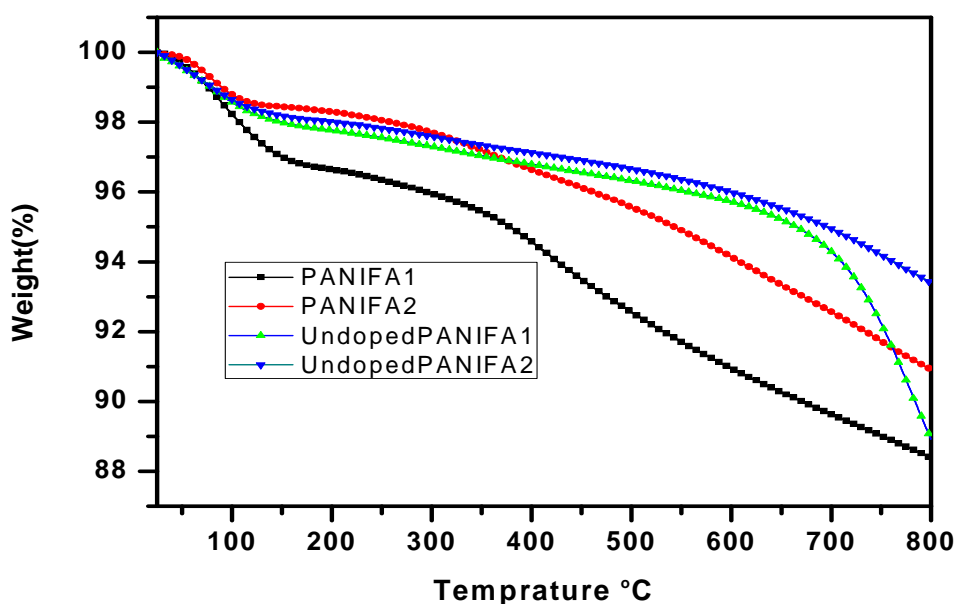


**Figure 4.6 b: Thermogravimetric curve of Polyaniline/Flyash composites**

The thermal behaviour of the PANI and the different PANI/FA samples was investigated by thermogravimetry (TG) and the results are shown in Fig. 4.6. The steady weight loss observed for the PANI/FA samples in the temperature range 80–450 °C is attributed to the elimination of adsorbed water (up to 30%) from both the oxide and polymer surface and acid dopant [11–13]. In this temperature range. In addition to this, a well-differentiated behaviour marked by a strong weight loss in the temperature range 470–600 °C are observed for PANI and PANI/FA composites. This attributes to the degradation of the skeletal polyaniline chain structure [11–13]. Undoped polyaniline /flyash composites are more thermally stable than doped composites due to removal of doping agent.

#### 4.7: Study of the corrosion- inhibition performance of inhibitors

The corrosion inhibition performance study was carried out at room temperature in aqueous solution of 1.0 M HCl by using potentiodynamic polarization technique. Experiments were carried in a conventional three electrode cell assembly using Autolab Potentiostat/Galvanostat, PGSTAT100 (Nova Software) with pure epoxy & polymer-epoxy coated iron of dimension 1 cm x 1 cm as working electrode, Pt as counter electrode and

saturated calomel electrode (SCE) as reference electrode. The cleaning of the working iron electrode was carried out by 1/0, 2/0, 3/0 and 4/0 grade emery papers. The electrodes were then thoroughly cleaned with acetone and trichloroethylene to remove any impurities on the surface. The linear Tafel segments to the anodic and cathodic curves (-0.2 to + 0.2 V versus corrosion potential) were extrapolated to corrosion potential to obtain the corrosion current densities. The corrosion current density [  $i_{corr}$  (A/cm<sup>2</sup>) ] was calculated with the Stern-Geary equation [14].

The corrosion inhibition efficiency (% I.E.) was determined from the measured  $i_{corr}$  (corrosion current densities without addition of inhibitor ( $i_{corr}^0$ ) and corrosion current densities with the addition of various concentrations of inhibitor ( $i_{corr}^i$ ) values by using the following relationship;

$$I.E.(%) = \frac{i_{corr}^0 - i_{corr}^i}{i_{corr}^0} \times 100$$

**Dipole™ Sampling Booth with Powder Recovery System**





GUN-103 N801-Extreme

**Figure 4.7 Set up of Powder coating unit**

Sample was prepared by make blends with 5% loading of Polyaniline and Polyaniline/Flyash composites with epoxy resin, after that these powder is coated on iron electrode of dimension of 1 cm x1 cm by powder coating instrument.

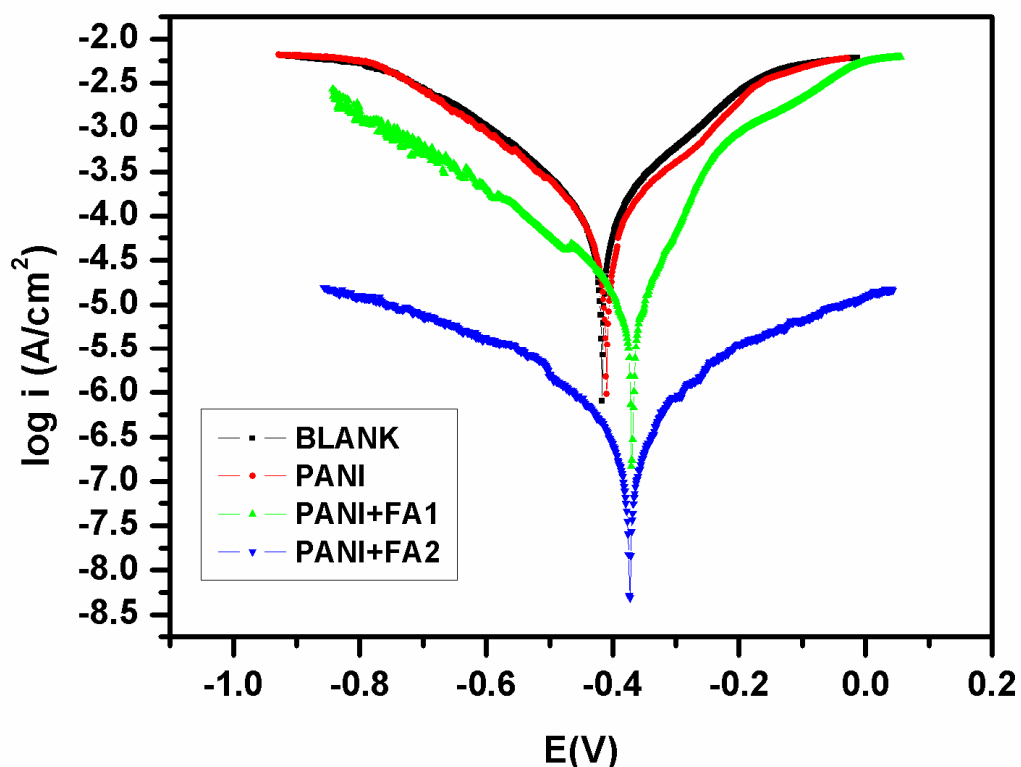


**Figure 4.7 Tafel plots of mild steel samples coated with different inhibitors**

Inhibitor	$i_{corr}(\mu A/cm^2)$	$R_p(\Omega cm^2)$	$E_{corr}(V)$	Corrosion rate (mm/year)	Inhibition Efficiency(%)
BLANK	132.3	246	-0.4135	1.5373	----
PANI	58.8	405	-0.4157	1.1478	25.3%
PANI+FA1	10.9	92143	-0.3643	0.1265	91%
PANI+FA2	5.3	97133	-0.3671	0.006125	96%

**Table 4.2 Corrosion inhibition efficiency polyaniline and polyaniline/flyash composites**

From above table it shows that when PANI and its composites (5%) loaded with epoxy and check corrosion inhibition performance at room temperature in aqueous solution of 1.0 M HCl by using potentiodynamic polarization technique. Corrosion efficiency increases as flyash concentration increases

## References:

- [1] J. P. Pouget, M. E. Jdzefowicz, A. J. Epstein, X. Tang, and A. G. MacDiarmid, *Macromolecules* 24, 779 (1991).
- [2] A. Wolter, P. Rannou, J. P. Travers, B. Gilles, and D. Djurado, *Phys. Rev. B* 58, 7637 (1998)
- [3] J. P. Pouget, M. E. Jdzefowicz, A. J. Epstein, X. Tang, and A. G. MacDiarmid, *Macromolecules* 24, 779 (1991).
- [4] A. Wolter, P. Rannou, J. P. Travers, B. Gilles, and D. Djurado, *Phys. Rev. B* 58, 7637 (1998).
- [5] S. C. Raghavendra, S. Khasim, M. Revanasiddappa, M. Prasad, and A. B. Kulkarni, *Bull. Mater. Sci.* 26, 733(2003)
- [6] S. H. Nalwa (Ed.), *Handbook of Organic Conductive Molecules and Polymers*, Vol. 2 (John Wiley and Sons, New York, USA, 1997), pp. 506–537.
- [7] I. Hazada, Y. Furukawa, and F. Ueda, *Synth. Met.* 29,03 (1989).
- [8] Y. Cao, *Synth. Met.* 35, 319 (1990).
- [9] Y. Cao, P. Smith, and A. J. Heeger, *Synth. Met.* 32, 263 (1989).
- [10] S.C.Raghavendra, S. Khasim, M. Revanasiddappa, M. Prasad, and A. B. Kulkarni, [11] K. Pielichowski, *Solid State Ion.* 104, 123 (1997).
- [12] E. S. Matveeva, R. D. Calleja, and V. P. Parkhutik, *Synth. Met.* 72, 105 (1995).
- [13] M. G. Han, Y. J. Lee, S. W. Byun, and S. S. Im, *Synth. Met.* 124, 337 (2001).
- [14] M. Stern, A. Geary, *Electrochemical polarization*, *J. Electrochem Soc.* 104 (1957) 56.

### **Conclusion:**

Conducting Polyaniline and Polyaniline/Flyash composites were synthesised by insitu polymerization and characterized by X-diffraction, thermogravimetric, infrared, SEM and conductivity techniques. The XRD pattern of pure PANI showed the presence of emeraldine salt phase of polymer and that of PANI/FA composites showed the semi-crystalline nature of the material. As the concentration of FA increases in the composites, a small gradual shift of peak around  $2\theta = 25.9^\circ$  towards higher  $2\theta$  values was also observed. This may be attributed to merging of emeraldine salt peak with those due to FA constituent.

The thermogravimetry curves showed a clear and marked difference between PANI and PANI/FA composites, where the major weight losses were associated with the degradation of the skeletal polyaniline chain structure. Infrared spectra of PANI and PANI/FA composites indicate the existence of the quinoid and benzenoid ring in the polymeric chain of PANI. These spectra also support the XRD result that the polyaniline used in this work is emeraldine salt form of PANI. The SEM pictures of PANI/FA composites showed with increase in granularity with addition of FA in PANI and the existence of the spherical FA particles (cenospheres).

Conductivity data showed that with increase FA concentration conductivity of polymer composites decreases and it undoped with ammonia its conductivity ranges to insulator.

In corrosion inhibition, 5% of polyaniline and polyaniline /flyash composites loaded with epoxy. Corrosion inhibition efficiency increases as flyash concentration increases.